SPRINGER BRIEFS IN MOLECULAR SCIENCE

Xin-Long Ni
Xin Xiao
Hang Cong
Zhu Tao

Supramolecular Assemblies of Cucurbit[*n*]urils with Metal Ions

Coordination, Structures and Properties

Springer

SpringerBriefs in Molecular Science

More information about this series at http://www.springer.com/series/8898

Xin-Long Ni · Xin Xiao · Hang Cong · Zhu Tao

Supramolecular Assemblies of Cucurbit[*n*]urils with Metal Ions

Coordination, Structures and Properties

Springer

Xin-Long Ni
Key Laboratory of Macrocyclic
and Supramolecular Chemistry
of Guizhou Province
Guizhou University
Guiyang
China

Xin Xiao
Key Laboratory of Macrocyclic
and Supramolecular Chemistry
of Guizhou Province
Guizhou University
Guiyang
China

Hang Cong
Key Laboratory of Macrocyclic
and Supramolecular Chemistry
of Guizhou Province
Guizhou University
Guiyang
China

Zhu Tao
Key Laboratory of Macrocyclic
and Supramolecular Chemistry
of Guizhou Province
Guizhou University
Guiyang
China

ISSN 2191-5407 ISSN 2191-5415 (electronic)
SpringerBriefs in Molecular Science
ISBN 978-3-662-46628-5 ISBN 978-3-662-46629-2 (eBook)
DOI 10.1007/978-3-662-46629-2

Library of Congress Control Number: 2015934949

Springer Heidelberg New York Dordrecht London

Printed on acid-free paper

Springer-Verlag GmbH Berlin Heidelberg is part of Springer Science+Business Media
(www.springer.com)

Preface

Over the past two decades, porous coordination polymers (PCPs) and metal organic frameworks (MOFs) have been highlighted as a family of crystalline solids. They are constructed from metal ions and organic ligands via coordination bonds, and self-assembly to provide open structures. In this field, scientists with inorganic, organic, and theoretical backgrounds have produced novel complexes that show remarkably selective chemical behavior including ion and molecular separations, transport and catalysis, and so on. Cucurbit[*n*]urils are a family of molecular container hosts bearing a rigid hydrophobic cavity and two identical carbonyl-fringed portals. Because of their superior molecular recognition properties in aqueous media, they have attracted much attention in supramolecular chemistry. Recent studies reveal that weak noncovalent interactions such as hydrogen bonding, $\pi\cdots\pi$ stacking, C–H$\cdots\pi$, as well as ion–dipole interactions play an important role in the formation of cucurbit[*n*]urils/metal-based coordination architectures. In particular, a number of examples in which the use of a ‘structure inducer’ (often an anionic species or an organic molecule) is employed to make the coordination structures of cucurbit[*n*]urils with metal ions from simple complex to complicated poly-dimensional polymers and even further promote the isolation of new Ln^{3+}–Q[*n*] species. All these processes and phenomena imply a particular property, i.e., ‘cucurbit[*n*]urils-based coordination’—the key word and leading idea of the present book.

This short communication book starts with the first chapter discussing the development of cucurbit[*n*]urils and their derivatives-general properties and the concept of outer-surface interactions. Chapter 2, on the combinatorial development of the host–guest coordination fashions, describes the details of simple coordination complexes of cucurbit[*n*]urils with metal ions. Chapter 3 discusses particular types of complicated coordination polymers derived from supramolecular assemblies of cucurbit[*n*]urils with metal ions and the significant importance of the third ‘structure inducer’ species. Finally, Chap. 4 concerns the potential applications of Q[*n*]-based coordination complexes and polymers.

We hope that this book will be useful for scientists and graduate students working in the fields of coordination and supramolecular chemistry, and in material science.

Xin-Long Ni
Xin Xiao
Hang Cong
Zhu Tao

Contents

Chapter 1
Cucurbit[*n*]uril Chemistry

Abstract Because of their superior molecular recognition properties in aqueous media, cucurbit[*n*]urils (Q[*n*]s or CB[*n*]s), which bear a rigid hydrophobic cavity and two identical carbonyl fringed portals, have attracted much attention in supramolecular chemistry. Till date, the homologs of unfunctionalized cucurbit[*n*]urils include 5, 6, 7, 8, 10, and 14. Meanwhile, a number of substituted cucurbit[*n*]urils (SQ[*n*]s) and their derivates were reported during the last decade. Therefore, in this chapter the development of cucurbit[*n*]urils and their derivates is first briefly reviewed. Importantly, the general properties of out surface-interactions of Q[*n*]s proposed by us recently and their roles in Q[*n*]-based coordination chemistry or Q[*n*]-based host-guest/coordination chemistry are also highlighted in this chapter.

Keywords Substituted cucurbit[*n*]urils · Homologs · Outer-surface interactions · Supramolecular assemblies · Host-guest chemistry · Coordination chemistry

1.1 Development of Cucurbit[*n*]urils and Their Derivates

Cucurbit[*n*]urils (commonly abbreviated as Q[*n*]s or CB[*n*]s) are among the macrocyclic receptors known to date besides, crown ethers, cryptands, cyclodextrins, and calixarenes. As the first reported family member, cucurbit[6]uril (Q[6]) was originally synthesized in 1905 by Behrend and coworkers from the condensation of glycoluril and formaldehyde under strongly acidic conditions [1]. However, it was not until 1981 that Mock structurally characterized Q[6] as a structure comprising six pumpkin-shaped glycoluril units linked with 12 methylene bridges (Fig. 1.1) [2]. Later, the supramolecular chemistry of Q[6] continued to develop in the 1980s and 1990s as a result of the pioneering work by Mock, Buschmann, Kim, and their coworkers [3–6].

In 2000, the research groups of Kim and Day performed the successful isolation and X-ray characterization of Q[5], Q[7], and Q[8] (Fig. 1.2) [7–9].

X.-L. Ni et al., *Supramolecular Assemblies of Cucurbit[*n*]urils with Metal Ions*,
SpringerBriefs in Molecular Science, DOI 10.1007/978-3-662-46629-2_1

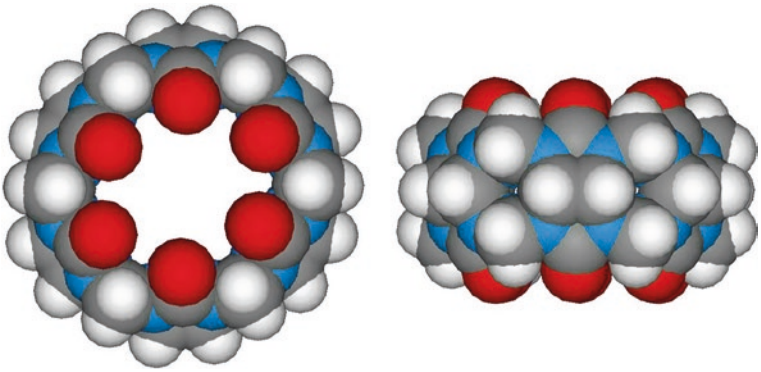

Fig. 1.1 X-ray crystal structure of Q[6]

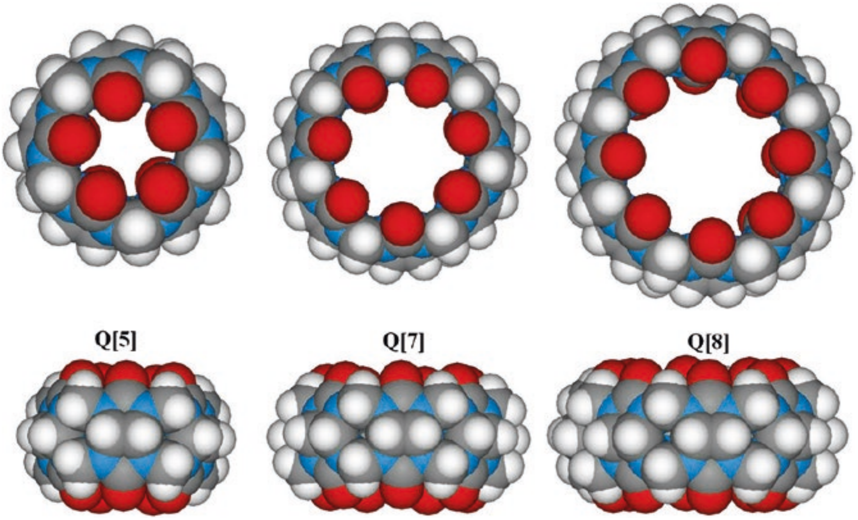

Fig. 1.2 X-ray crystal structure of Q[5], Q[7], and Q[8]

Less than two years later, Day and coworkers crystallized and identified the structure of Q[10], which always includes a Q[5] molecule in synthetic processes (Fig. 1.3 left) [10]. Most interesting is our recent discovery of cucurbit[14]uril, the largest Q[*n*], which has 14 normal glycoluril units linked with 28 methylene bridges. However, it seems to be formed from 14 units of the glycoluril–$(CH_2)_2$– moiety with a 180° twist. As a consequence, it does not have a normal cavity like most cucurbit[*n*]urils, but instead has a folded, figure-of-eight conformation. We have therefore named it twisted cucurbit[14]uril (tQ[14]) (Fig. 1.3 right) [11]. Furthermore, tQ[14] has good solubility in both water (41.0 mmol/L) and organic solvents such as dimethylsulfoxide (18.0 mmol/L). Overall, these results strongly deliver some important conclusions: larger homologs of Q[*n*]s ($n > 10$) could be obtained by the traditional synthetic route.

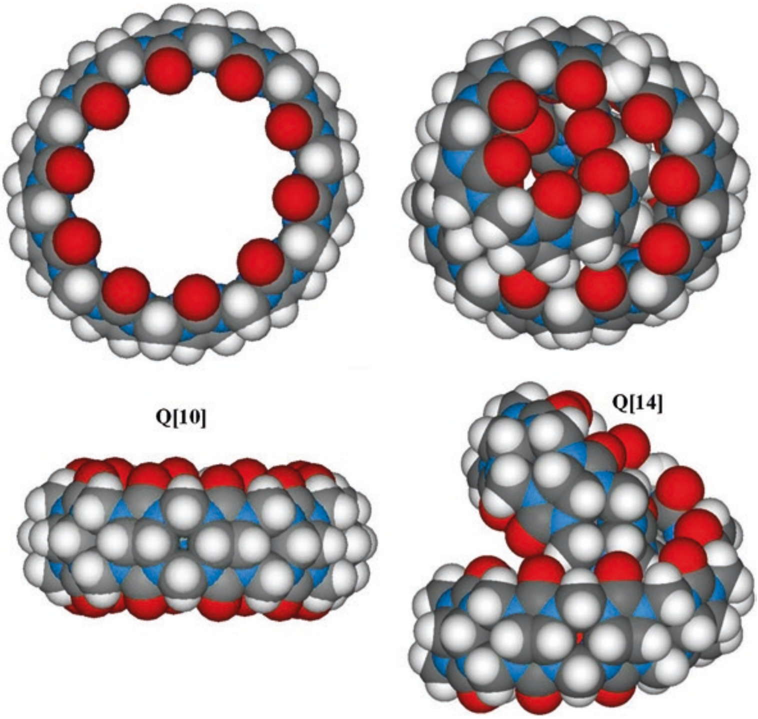

Fig. 1.3 X-ray crystal structure of Q[10] and twisted tQ[14]

Moreover, a number of substituted cucurbit[n]urils (SQ[n]s) and their derivates were reported during the last decade. Stoddart and coworkers first reported an alkyl-substituted cucurbit[5]uril, decamethylcucurbit[5]uril ($Me_{10}Q[5]$) by self-assembly of dimethylglycouril; unexpectedly, none of its homologs were found in 1992 [12]. Following this discovery, a number of fully and partially substituted Q[n] derivatives have been reported since 2001. These include the fully or partially substituted $(CyH)_nQ[n]$s (cyclohexano = CyH; $n = 5$–8) [13], $Me_{12}Q[6]$ [14, 15], and $(CyP)_nQ[n]$ [16], the partially substituted $Ph_2Q[6]$ [17], HMeQ[6] [18], TMeQ[6] [19], $(CyH)_2Q[6]$ [20], and $(Me_2CyP)_nQ[6]$ [14]. Issacs and coworkers reported some water soluble, fluorescence-sensitive cucurbit[n]uril analogues, which were obtained starting with S- and C-shaped diastereomeric methylene-bridged glycoluril dimers [21–23]. Moreover, they found a series of glycouril oligomers [24] and used these oligomers to synthesize a number of novel cucurbit[n]uril derivates [24–27]. Kim, Isaacs, and other groups synthesized and exploited various functionalized Q[n]s. For example, in 2003, Kim and coworkers demonstrated the first reactive cucurbit[n]urils, perhydroxycucurbit[n]urils [$(HO)_{2n}Q[n]$ ($n = 5$–8)], by direct oxidation of Q[n]s with $K_2S_2O_8$ in water [28]. In particular, Scherman recently reported a monohydroxylated cucurbit[6]uril in 2012 [29]. Recently, Isaacs and coworkers also reported a series of functionalized

Q[*n*]s [30–33]. Very recently, Sindelar and coworker first introduced a substituted group onto the bridged methylene moiety and obtained a bridged methylene functionalized Q[6] [34]. All these developments of cucurbit[*n*]urils and their derivates try to overcome the low solubility of the normal Q[*n*]s in water [35, 36], and the difficulty in introducing functional groups on their surfaces. Moreover, such discoveries have led to tremendous growth in the field of Q[*n*] chemistry. Areas of developments include host–guest interactions, supramolecular assemblies, coordination as well as materials science, and relevant applications in sensing, catalysis, drug delivery, biomolecular recognition, polymer chemistry, electrochemistry, photochemistry, and molecular machines [36–61]. Generally speaking, the interaction of Q[*n*]s with various guest molecules has led to the development of Q[*n*]-based host–guest chemistry, which has become mainstream in the Q[*n*] chemistry [36–54]. On the other hand, the interaction of Q[*n*] with various metal ions establishes the Q[*n*]-based coordination chemistry, an increasingly important area in Q[*n*] chemistry [55–61]. A combination of Q[*n*]-based host–guest chemistry and coordination chemistry could create a different branch in the Q[*n*] chemistry: Q[*n*]-based host–guest/coordination chemistry [62] (Scheme 1.1). For example, based on the interaction of Q[6] with long chain guests that end with active moieties and thread through Q[6] to form pseudorotaxanes, Kim and coworkers proposed a type of novel architectures by joining these pseudorotaxanes with metal ions as "linkers" that give rise to one-, two-, or three-dimensional (1D, 2D, or 3D, respectively) polyrotaxane structures [36, 37]. Another typical instance is the summaries on the Q[8]-stabilized charge-transfer (CT) interactions and supramolecular assemblies that result in a series of remarkable achievements in establishing

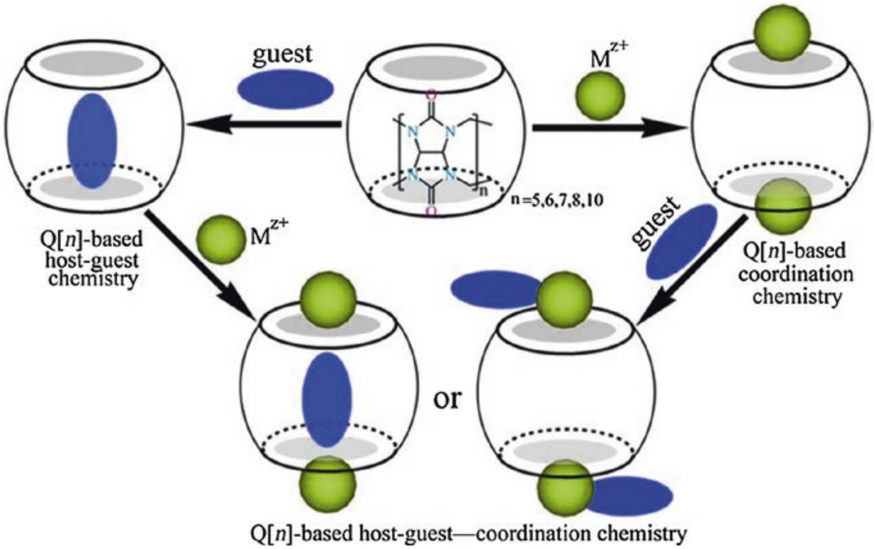

Scheme 1.1 Gross branches in the cucurbit[*n*]uril chemistry

a strategy for synthesizing new types of polymers, nanoscience, surface immobilization, and so on [45, 63]. In particular, they have led Scherman and coworkers to publish their first paper on Q[*n*] chemistry in *Science* in 2012 [64].

Compared to the significant achievements in Q[*n*]-based host–guest chemistry, Q[*n*]-based coordination chemistry or Q[*n*]-based host–guest/coordination chemistry was gradually developing in the last several years [60]. In fact, the establishment of Q[*n*] chemistry started with Q[*n*]-based coordination chemistry because the structural characteristics of the first-characterized member of the Q[*n*] family, Q[6], was based on the determination of the linear coordination polymer of Q[6] molecules with Ca^{2+} cations [2]. ~15 % of studies (among ~1800 papers and patents before the beginning of October 2014, according to a survey by SciFinder), are directly related to coordination of Q[*n*]s with metal ions. Moreover, recent works have revealed that Q[*n*]-based coordination chemistry is gradually changing from simple coordination to novel Q[*n*]/metal ions complex-based polydimensional coordination polymers or supramolecular assemblies. Such structures could be useful in applications in the areas of nanotechnology, molecular sieves, sensors, gas absorption and separation, ionic or molecular transport, and heterogeneous catalysis [62, 65–72]. This book mainly highlights achievements based on the direct coordination of Q[*n*]s with metal ions, their complexes, and corresponding coordination supramolecular assemblies in the areas of Q[*n*]-based coordination chemistry and Q[*n*]-based host–guest/coordination chemistry.

1.2 General Properties of Outer-Surface Interactions of Q[*n*]s

Electrostatic potential surface calculations on Q[*n*]s (Fig. 1.4) indicated that the regions around the portal carbonyl groups on Q[*n*]s are significantly negatively charged, the inner surface of the cavities is close to electrostatically neutral, whereas the outer surface of Q[*n*]s is electrostatically positive. It is not surprising that almost all research in Q[*n*] chemistry has been focused on utilizing the portals and cavities to construct supramolecular assemblies through the strong charge–dipole and hydrogen bonding interactions, as well as hydrophobic and hydrophilic effect derived from the negative portals and rigid cavities of Q[*n*]s. However, few of them focus on the interaction of outer surface of Q[*n*]s on the Q[*n*]-based coordination polymer and supramolecular assemblies [61].

In fact, Chen and coworkers first proposed that the chemical behavior of the convex outer walls of Q[*n*]s could be explored to develop novel structures and functional materials when they investigated iodine-assisted supramolecular assemblies of helical coordination polymers of Q[*n*] and asymmetric copper(II) complexes [73]. Further investigation reveals that the outer surface of Q[*n*] exhibits much higher affinity to the aromatic moieties of an aromatic organic molecule or ligand in a complex anion than to the other Q[*n*] units; we call the resulting interactions as outer-surface interaction of Q[*n*]s, such as those involved in C–H···π,

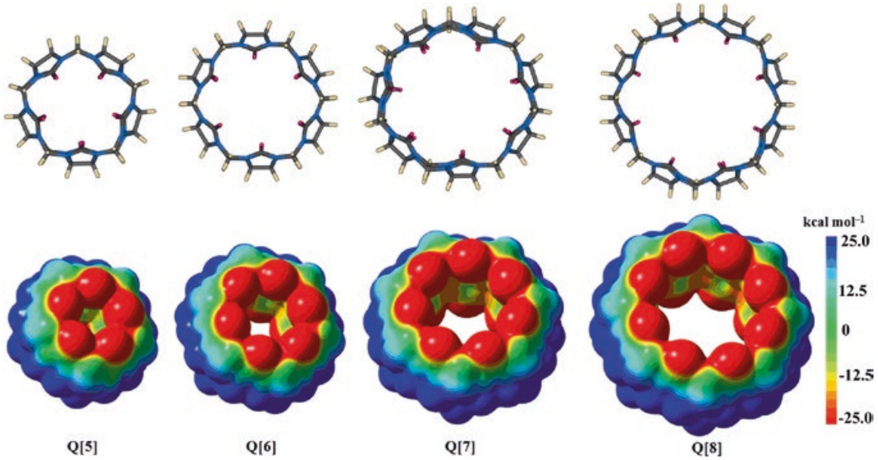

Fig. 1.4 Electrostatic potential maps (ESPs) for Q[5], Q[6], Q[7], and Q[8], respectively. ESPs are mapped on electron density isosurfaces (0.001 e/au^3) for cucurbit[*n*]urils at the B3LYP/6-311G (d, p) level of theory with Gaussian09

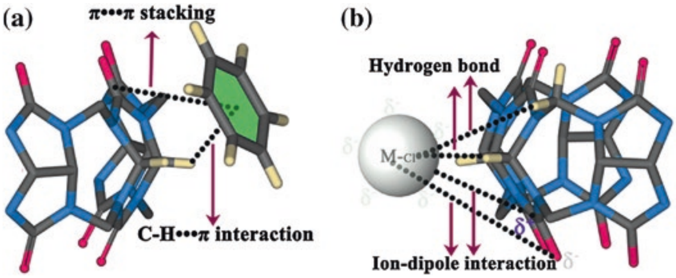

Scheme 1.2 **a** The outer-surface interactions between Q[*n*]s and aromatic molecules; **b** The outer-surface interactions between Q[*n*]s and inorganic complex anion

π interaction, hydrogen bonding, and ion–dipole interactions, which could generate numerous novel Q[*n*]-based supramolecular assemblies and result in a new branch of Q[*n*] chemistry based on the outer-surface interactions (Scheme 1.2).

References

1. R. Behrend, E. Meyer, F. Rusche, Justus Liebigs Ann. Chem. **339**, 1 (1905)
2. W.A. Freeman, W.L. Mock, N.-Y. Shih, J. Am. Chem. Soc. **103**, 7367 (1981)
3. W.L. Mock, Top. Curr. Chem. **175**, 1 (1995)
4. R. Hoffmann, W. Knoche, C. Fenn, H.-J. Buschmann, J. Chem. Soc. Faraday Trans. **90**, 1507 (1994)
5. K.-M. Park, J. Heo, S.-G. Roh, Y.-M. Jeon, D. Whang, K. Kim, Mol. Cryst. Liq. Cryst. Sci. Technol. Sect. A **327**, 65 (1999)
6. K. Kim, Supramol. Chem. **5**, 371 (1999)

7. J. Kim, I.S. Jung, S.Y. Kim, E. Lee, J.K. Kang, S. Sakamoto, K. Yamaguchi, K. Kim, J. Am. Chem. Soc. **122**, 540 (2000)
8. A.I. Day, A.P. Arnold, Method for synthesis cucurbiturils. WO 0068232, **8** (2000)
9. A.I. Day, A.P. Arnold, R.J. Blanch, B. Snushall, J. Org. Chem. **66**, 8094 (2001)
10. A.I. Day, R.J. Blanch, A.P. Arnold, S. Lorenzo, G.R. Lewis, I. Dance, Angew. Chem. Int. Ed. **41**, 275 (2002)
11. X.J. Cheng, L.L. Liang, K. Chen, N.N. Ji, X. Xiao, J.X. Zhang, Y.Q. Zhang, S.F. Xue, Q.J. Zhu, X.L. Ni, Z. Tao, Angew. Chem. Int. Ed. **52**, 7252 (2013)
12. A. Flinn, G.C. Hough, J.F. Stoddart, D.J. Williams, Angew. Chem. Int. Ed. **31**, 1475 (1992)
13. J.Z. Zhao, H.J. Kim, J. Oh, S.Y. Kim, J.W. Lee, S. Sakamoto, K. Yamaguchi, K. Kim, Angew. Chem. Int. Ed. **40**, 4233 (2001)
14. S. Sasmal, M.K. Sinha, E. Keinan, Org. Lett. **6**, 1225 (2004)
15. L.B. Lu, Y.Q. Zhang, Q.J. Zhu, S.F. Xue, Z. Tao, Molecules **12**, 716 (2007)
16. F. Wu, L.H. Wu, X. Xiao, Y.Q. Zhang, S.F. Xue, Z. Tao, A.I. Day, J. Org. Chem. **77**, 606 (2012)
17. H. Isobe, S. Sato, E. Nakamura, Org. Lett. **4**, 1287 (2002)
18. A.I. Day, A.P. Arnold, R.J. Blanch, Molecules **8**, 74 (2003)
19. Y.J. Zhao, S.F. Xue, Q.J. Zhu, Z. Tao, J.X. Zhang, Z.B. Wei, L.S. Long, M.L. Hu, H.P. Xiao, A.I. Day, Chin. Sci. Bull. **49**, 1111 (2004)
20. L. Zheng, J. Zhu, Y. Zhang, Z. Tao, S. Xue, Q. Zhu, Z. Wei, L. Long, Chin. J. Inorg. Chem. **21**, 1583 (2005)
21. B.D. Wagner, P.G. Boland, J. Lagona, L. Isaacs, J. Phys. Chem. B. **109**, 7686 (2005)
22. J. Lagona, J.C. Fettinger, L. Isaacs, J. Org. Chem. **70**, 10381 (2005)
23. J. Lagona, B.D. Wagner, L. Isaacs, J. Org. Chem. **71**, 1181 (2006)
24. W.H. Huang, P.Y. Zavalij, L. Isaacs, J. Am. Chem. Soc. **130**, 8446 (2008)
25. W.H. Huang, P.Y. Zavalij, L. Isaacs, J. Am. Chem. Soc. **127**, 18000 (2005)
26. W.H. Huang, S.M. Liu, P.Y. Zavalij, L. Isaacs, J. Am. Chem. Soc. **128**, 14744 (2006)
27. W.-H. Huang, P.Y. Zavalij, L. Isaacs, Angew. Chem. Int. Ed. **46**, 7425 (2007)
28. S.Y. Jon, N. Selvapalam, D.H. Oh, J.-K. Kang, S.-Y. Kim, Y.J. Jeon, J.W. Lee, K. Kim, J. Am. Chem. Soc. **125**, 10186 (2003)
29. N. Zhao, G.O. Lloyd, O.A. Scherman, Chem. Comm. **48**, 3070 (2012)
30. W.-H. Huang, P.Y. Zavalij, L. Isaacs, Org. Lett. **10**, 2577 (2008)
31. D. Lucas, T. Minami, G. Iannuzzi, L. Cao, J.B. Wittenberg, P. Anzenbacher Jr, L. Isaacs, J. Am. Chem. Soc. **133**, 17966 (2011)
32. L. Cao, L. Isaacs, Org. Lett. **14**, 3072 (2012)
33. B. Vinciguerra, L. Cao, J.R. Cannon, P.Y. Zavalij, C. Fenselau, L. Isaacs, J. Am. Chem. Soc. **134**, 13133 (2012)
34. L. Gilberg, M.S.A. Khan, M. Enderesova, V. Sindelar, Org. Lett. **16**, 2446 (2014)
35. M.E. Bush, N.D. Bouley, A.R. Urbach, J. Am. Chem. Soc. **127**, 14511 (2005)
36. J.W. Lee, S. Samal, N. Selvapalam, H.-J. Kim, K. Kim, Acc. Chem. Res. **36**, 621 (2003)
37. K. Kim, Chem. Soc. Rev. **31**, 96 (2002)
38. O.A. Gerasko, D.G. Samsonenko, V.P. Fedin, Russ. Chem. Rev. **71**, 741 (2002)
39. J. Lagona, P. Mukhopadhyay, S. Chakrabarti, L. Isaacs, Angew. Chem. Int. Ed. **44**, 4844 (2005)
40. K. Kim, N. Selvapalam, Y.H. Ko, K.M. Park, D. Kim, J. Kim, Chem. Soc. Rev. **36**, 267 (2007)
41. L. Isaacs, Chem. Commun. **619** (2009)
42. R.N. Dsouza, U. Pischel, W.M. Nau, Chem. Rev. **111**, 7941 (2011)
43. B.C. Pemberton, R. Raghunathan, S. Volla, J. Sivaguru, Chem. Eur. J. **18**, 12178 (2012)
44. E. Masson, X.X. Ling, R. Joseph, L. Kyeremeh-Mensah, X.Y. Lu, RSC Adv. **2**, 1213 (2012)
45. Y.L. Liu, H. Yang, Z.Q. Wang, X. Zhang, Chem. Asian J. **2013**(8), 1626 (2013)
46. V. Sindelar, S. Silvi, S.E. Parker, D. Sobransingh, A.E. Kaifer, Adv. Funct. Mater. **17**, 694 (2007)
47. W. Wang, A.E. Kaifer, Adv. Polym. Sci. **222**, 205 (2009)

48. S. Gadde, E.K. Batchelor, A.E. Kaifer, Aust. J. Chem. **63**, 184 (2010)
49. S. Gadde, A.E. Kaifer, Cur. Org. Chem. **15**, 27 (2011)
50. V. Mandadapu, A.I. Day, A. Ghanem, Chirality **26**, 712 (2014)
51. M.-G. Veronica, P.-J. Jorge, P.-S. Isabel, M.L.-M. Luis, Chem. Eur. J. **20**, 10874 (2014)
52. L. Isaacs, Acc. Chem. Res. **47**, 2052 (2014)
53. B. Cornelia, Chem. Soc. Rev. **43**, 4037 (2014)
54. J. Vazquez, P. Remon, R.N. Dsouza, A.I. Lazar, J.F. Arteaga, W.M. Nau, U. Pischel, Chem. Eur. J. **20**, 9897 (2014)
55. M.N. Sokolov, D.N. Dybtsev, V.P. Fedin, Russ. Chem. Bull. Int. Ed. **52**, 1041 (2003)
56. O.A. Gerasko, M.N. Sokolov, V.P. Fedin, Pure Appl. Chem. **76**, 1633 (2004)
57. V.P. Fedin, Russ. J. Coordin. Chem. **30**, 151 (2004)
58. H. Cong, Q.J. Zhu, S.F. Xue, Z. Tao, G. Wei, Chin. Sci. Bull. **55**, 3633 (2010)
59. J. Lü, J.X. Lin, M.N. Cao, R. Cao, Coord. Chem. Rev. **257**, 1334 (2013)
60. X.L. Ni, X. Xiao, H. Cong, L.L. Liang, K. Chen, X.J. Cheng, N.N. Ji, Q.J. Zhu, S.F. Xue, Z. Tao, Chem. Soc. Rev. **42**, 9480 (2013)
61. X.L. Ni, X. Xiao, H. Cong, Q.J. Zhu, S.F. Xue, Z. Tao, Acc. Chem. Res. **47**, 1386 (2014)
62. S.D. Choudhury, J. Mohanty, H. Pal, A.C. Bhasikuttan, J. Am. Chem. Soc. **132**, 1395 (2010)
63. Y.H. Ko, E. Kim, I. Hwang, K. Kim, Chem. Commun. **1305** (2007)
64. J. Zhang, R.J. Coulston, S.T. Jones, J. Geng, O.A. Scherman, C. Abell, Science **335**, 690 (2012)
65. M. Cao, J. Lin, H. Yang, R. Cao, Chem. Commun. **46**, 5088 (2010)
66. X. Feng, K. Chen, Y.-Q. Zhang, S.-F. Xue, Q.-J. Zhu, Z. Tao, A.I. Day, CrystEngComm **13**, 5049 (2011)
67. N.-N. Ji, X.-J. Cheng, Y. Zhao, L.-L. Liang, K. Chen, X. Xiao, Y.-Q. Zhang, Q.-J. Zhu, S.-F. Xue, Z. Tao, Eur. J. Inorg. Chem. **1435** (2014)
68. B.-X. Han, C.-Z. Wang, K. Chen, X. Xiao, Z. Tao, S.-F. Xue, Y.-Q. Zhang, Q.-J. Zhu, CrystEngComm **16**, 1615 (2014)
69. N.-N. Ji, X.-J. Cheng, Y. Zhao, L.-L. Liang, X.-L. Ni, X. Xiao, Q.-J. Zhu, S.-F. Xue, N. Dong, Z. Tao, Inorg. Chem. **53**, 21 (2014)
70. X.-J. Cheng, N.-N. Ji, Y. Zhao, L.-L. Liang, X. Xiao, Y.-Q. Zhang, S.-F. Xue, Q.-J. Zhu, Z. Tao, CrystEngComm **16**, 144 (2014)
71. Y. Zhao, L.-L. Liang, K. Chen, T. Zhang, X. Xiao, Y.-Q. Zhang, Z. Tao, S.-F. Xue, Q.-J. Zhu, CrystEngComm **15**, 7987 (2013)
72. T. Sun, N. Ji, M. Qi, Z. Tao, R. Fu, J. Chromatogr. A **1343**, 167 (2014)
73. F. Zhang, T. Yajima, Y.Z. Li, G.Z. Xu, H.L. Chen, Q.T. Liu, O. Yamauchi, Angew. Chem. Int. Ed. **44**, 3402 (2005)

Chapter 2
Simple Coordination Complexes of Cucurbit[*n*]urils with Metal Ions

Abstract Generally, the noncovalent interaction of Q[*n*]s with various guest molecules has led to the development of Q[*n*]-based host–guest chemistry, which has become the mainstream in Q[*n*] chemistry. In fact, the establishment of Q[*n*] chemistry started with Q[*n*]-based coordination chemistry because the structural characteristics of the first characterized member of the Q[*n*] family, Q[6], was based on the determination of the complex of Q[6] molecules with Ca^{2+} cations. From a structural viewpoint, the two preorganized (identical) carbonyl fringed portals in Q[*n*]s are ideal for acting as a rigid platform for developing a variety of Q[*n*]-metal derived coordination structures. In this chapter, a number of Q[*n*]-based metallo-supramolecular coordination fashions and examples are reviewed in detail. Overall, molecular bowls, molecular capsules, sandwich pairs, and heterometallic complexes are the general structures in the solid state. We therefore describe them in this chapter as simple coordination complexes of Q[*n*]s with metal ions.

Keywords Cucurbit[*n*]urils · Coordination complexes · Metal ions, molecular bowls · Molecular capsules · Sandwich pairs · Heterometallic complexes

It is well known that Q[*n*]s [1–5] readily coordinate with metal ions because of their two open polar portals rimmed with carbonyl groups (referring to Scheme 1.2). However, Q[*n*]s of various portal sizes appear to have different coordination abilities with metal ions, and various metal ions seem to show different affinities for a specific Q[*n*]. Moreover, environmental factors, such as coordination geometry or radius of metal ions, temperature, counter-anions, steric bulk, solvent, metal-to-ligand ratio, and pH of the system, influence the coordination and supramolecular assemblies of a Q[*n*] with a certain metal ion.

X.-L. Ni et al., *Supramolecular Assemblies of Cucurbit[*n*]urils with Metal Ions*,
SpringerBriefs in Molecular Science, DOI 10.1007/978-3-662-46629-2_2

2.1 Simple Coordination of Cucurbit[5]urils with Metal Ions

The unsubstituted or substituted cucurbit[5]urils (Q[5] and SQ[5]s, respectively) are the smallest members or homologs in the Q[*n*] family. The first known Q[5] is decamethylcucurbit[5]uril (Me_{10}Q[5]), which was reported in 1992 [6]. The host–guest chemistry of the Q[5]s has received less attention than their larger homologs because of the limited size of the portals and the capacity of their cavities [7–10]. To the best of our knowledge, the first reported crystal structure is a Q[5]-based coordination complex with a molecular bowl confirmation by covering a barium ion on one portal of a decamethylcucurbit[5]uril molecule, and the "bowls" further construct a honeycomb-like supramolecular assembly through hydrogen bonding and ion-dipole interactions (Fig. 2.1) [11].

Unsubstituted Q[5] and its substituted derivatives SQ[5]s are the smallest members of their respective homologous families. Although the smaller portal size of Q[5]s inhibits the entry of most organic molecules into the central cavity, and hence reduces the possible range of Q[5]-based host–guest inclusion complexes, it offers a "concentrated" set of five portal carbonyl oxygens so that larger metal ions are able to fully cover the portal and bind to all five oxygens to yield a stable metal-Q[5] complex. Recent studies reveal that Q[5]s have a strong tendency to coordinate with metal ions and form metal-ion-lidded molecular capsules or molecular bowls because Q[5]s have the smaller portal size and more concentrated portal carbony oxygens at portals, which could directly coordinate with metal ions, including alkali, alkaline earth, transition, and lanthanide or uranium [12–16]. Moreover, different Q[5]s, such as the unsubstituted Q[5], and some representative alkyl-substituted Q[5]s, like Me_{10}Q[5], dimethylcucurbit[5]uril (DMeQ[5]), 1,2,4-hexamethylcucurbit[5]uril

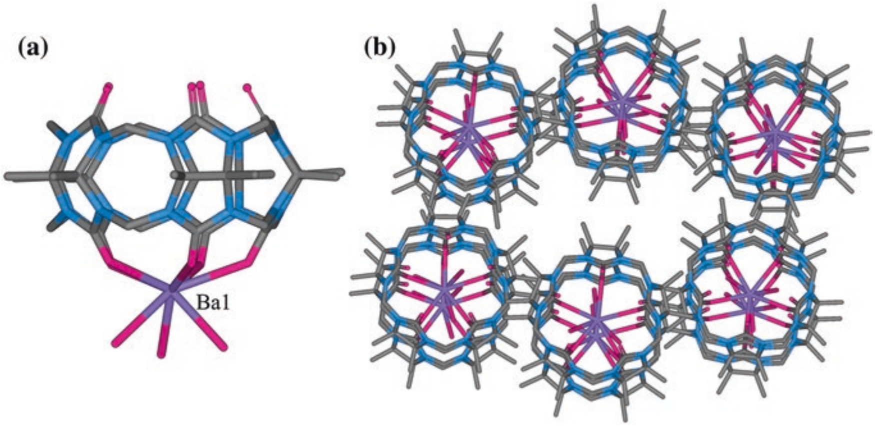

Fig. 2.1 **a** Complex cation of $[Me_{10}Q[5](H_2O)_3Ba]^{2+}$. **b** Stacking of the complexes in the crystals

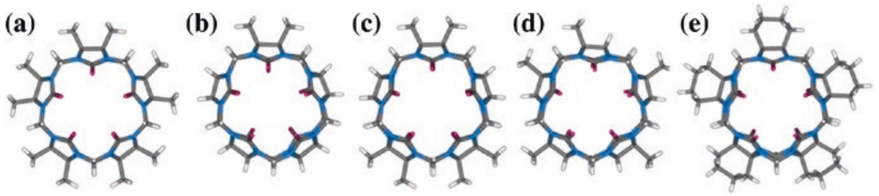

Fig. 2.2 Structures of five representative alkyl-substituted Q[5]s: **a** $Me_{10}Q[5]$; **b** DMeQ[5]; **c** 1,2,4-HMeQ[5]; **d** PMeQ[5] and **e** $CyH_5Q[5]$

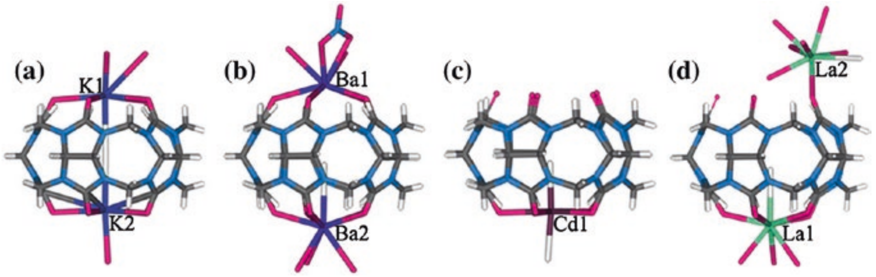

Fig. 2.3 X-ray crystal structures of molecular capsules and molecular bowls of Q[5] with various metal ions: **a** alkali (K^+); **b** alkaline earth (Ba^{2+}); **c** transition (Cd^{2+}); and **d** lanthanide (La^{3+}) metal ions

(1,2,4-HMeQ[5]), pentamethylcucurbit[5]uril (PMeQ[5]), pentacyclopentanocucurbit[5]uril ($CyH_5Q[5]$), and so on show no obvious difference in affinity to the metal ions (Fig. 2.2).

For example, a series of molecular capsules or molecular bowls of Q[5] with various metal ions, including alkali (K^+), alkaline earth (Ba^{2+}), transition (Cd^{2+}), and lanthanide (La^{3+}) metal ions (Fig. 2.3) [17, 18]. Moreover, these Q[5]-based complexes exhibited the remarkable property of encapsulating a negatively charged ion. Its easy synthesis, rigid structure, and chemical and thermal stability could make Q[5] very attractive for complexation of anions in aqueous solution [18]. Further experiments reveal that Q[5] shows special selectivity for including "naked" chloride anion or nitrate anion under certain conditions. The metal-free host has been demonstrated to selectively include nitrate ion, whereas the lanthanide-capped molecular capsule showed preference toward the inclusion of chloride ion (Fig. 2.4) [19].

Our group synthesized complexes of alkyl-substituted Q[5]s (referring to Fig. 2.2) with various metal ions. Most of them were molecular bowls or molecular capsules. The metal ions included alkali [12, 13], alkaline earth [14], transition [15], and lanthanide [16] metal ions. For example, we evaluated the effect of a series of alkaline earth metal ions (Ca^{2+}, Sr^{2+}, and Ba^{2+}) on their complexes with $CyH_5Q[5]$ by mixing their chloride salts with $CyH_5Q[5]$ [20]. The experimental results revealed that coordination of $CyH_5Q[5]$-based molecular capsules

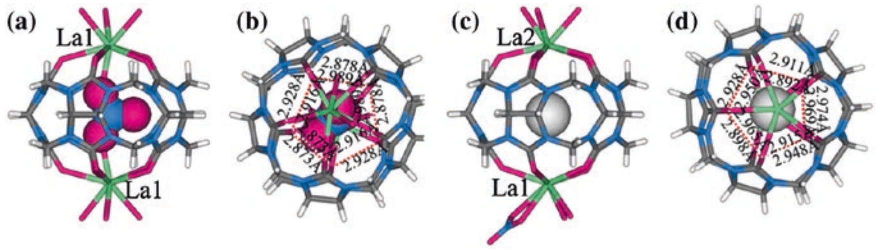

Fig. 2.4 X-ray structures of dinuclear capsule-like complexes of La^{3+}-Q[5]: **a** complex with an included nitrate anion; **b** the corresponding portal sizes; **c** complex with an included chloride ion; **d** the corresponding portal sizes

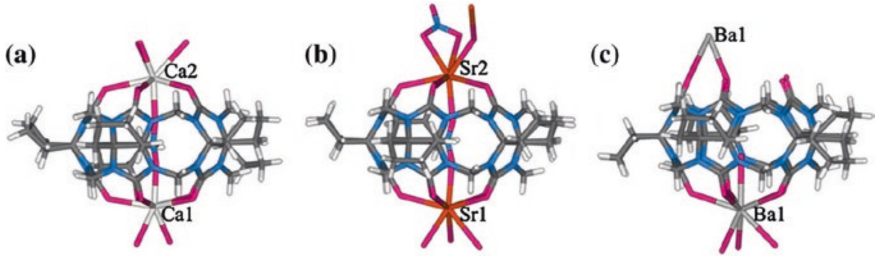

Fig. 2.5 X-ray crystal structures of molecular capsules and molecular bowls of $CyH_5Q[5]$ with alkaline earth metal ions: **a** Ca^{2+}; **b** Sr^{2+}; and **c** Ba^{2+}

and molecular bowls depended on the ionic radius of the metal cation (Fig. 2.5). In the $CyH_5Q[5]/Ca^{2+}$ complex, the $CyH_5Q[5]$ portal is larger than the calcium cation. Thus, the $CyH_5Q[5]$-based molecular capsule is not completely closed, and the $CyH_5Q[5]$ molecule even experiences some deformation. In the $CyH_5Q[5]/Sr^{2+}$ complex, the radius of the strontium cation is slightly larger than the $CyH_5Q[5]$ portal, and thus they form a completely closed molecular capsule. In the $CyH_5Q[5]/Ba^{2+}$ complex, the barium ion can only cover one portal of the $CyH_5Q[5]$ molecule and juxtaposes itself near the portal of other $CyH_5Q[5]$ molecule, generating an opened molecular capsule. Based on the radii of these three metal ions, which are 0.99, 1.12, and 1.34 Å, the radius of the metal ion is the underlying reason behind these differences.

Generally, metal ions that can cover the portals of a Q[5] molecule have a radius larger than 0.84 Å, which is the radius of the Cd^{2+} cation. Nevertheless, there are other factors that could lead to the formation of Q[5]s with metal ions with a smaller radius, such as Hg^{2+} (0.69 Å) [21]. In recent years, there has been a trend toward the use of third species as structure directing agents in Q[*n*]–metal systems, and the driving forces could be the so-called outer surface interactions of Q[*n*]s [22]. These species produce Q[*n*]-based supramolecular assemblies whose properties, structural novelties, and functionalities exceed those

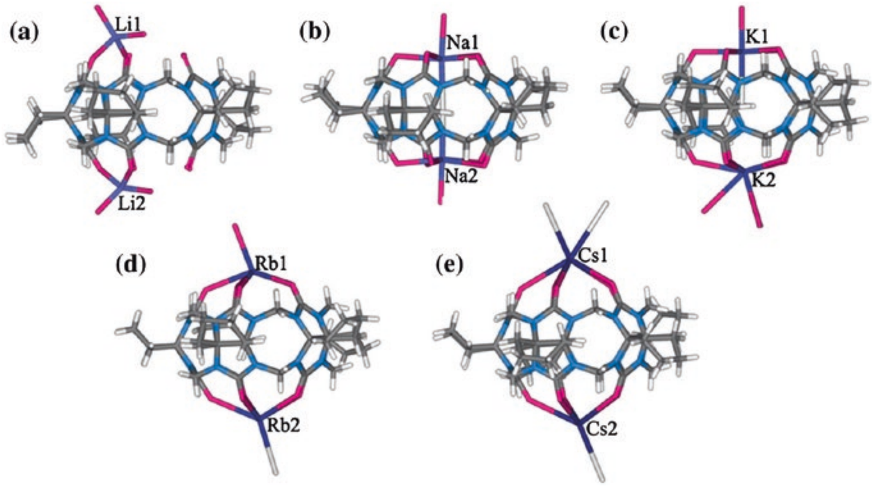

Fig. 2.6 X-ray crystal structures of molecular capsules of $CyH_5Q[5]$ with alkali metal ions: **a** Li^+; **b** Na^+; **c** K^+; **d** Rb^+; and **e** Cs^+

of assemblies obtained in the absence of such agents. For example, we cannot obtain all complexes of $CyH_5Q[5]$ with all alkali metal ions by simple combination of $CyH_5Q[5]$ with alkali metal salts. However, in the presence of $ZnCl_2$ in an acidic medium (HCl), the formed $[ZnCl_4]^{2-}$ anions behave as "structure directing agent", and facilitate the formation of all five $CyH_5Q[5]/M_{alkali}$ complexes (Fig. 2.6a–e). Among these complexes are those with the smallest (Li^+, 0.59 Å) and largest (Cs^+, 1.67 Å) metal radii (except Fr^+, 1.80 Å) [23]. All four alkali metal ions, Na^+ (0.97 Å), K^+ (1.33 Å), Rb^+ (1.43 Å), and Cs^+ (1.67 Å) which have larger metal radii, coordinate to the five carbonyl oxygen atoms and fully cover the portals of the $CyH_5Q[5]$ molecules. An exception to this trend is the Li^+ cation, which has the smallest metal radius and can only coordinate to two portal carbonyl oxygen atoms. The $CyH_5Q[5]$-based complexes with the fully capped portals initially appear to crystallize with similar molecular structures, such as opened molecular capsules or molecular capsules. The distances of the capped metal ions to the mean planes of the five portal carbonyl oxygens appear to increase with increasing atomic numbers of the alkali metals. But a close inspection shows that the capsules contain different core molecules: a chloride anion for the $CyH_5Q[5]/Na^+$ and $CyH_5Q[5]/K^+$ complexes, a water molecule for the $CyH_5Q[5]/Rb^+$ complex, and none for the $CyH_5Q[5]/Cs^+$ complex. Additionally, the interaction between the capped alkali metal ions and the included ion or molecule could affect the distances of the capped metal ions from the portal plane.

An example of the $Me_{10}Q[5]–M_{alkali}$ system can show this trend better [24]. Figure 2.7 shows four $Me_{10}Q[5]/M_{alkali}$ molecular bowls or capsules obtained by reactions of $Me_{10}Q[5]$ with the corresponding alkali metal salts (NaCl, KCl, RbCl, and CsCl) in the presence of hydroquinone (Hyq) as a structure directing agent.

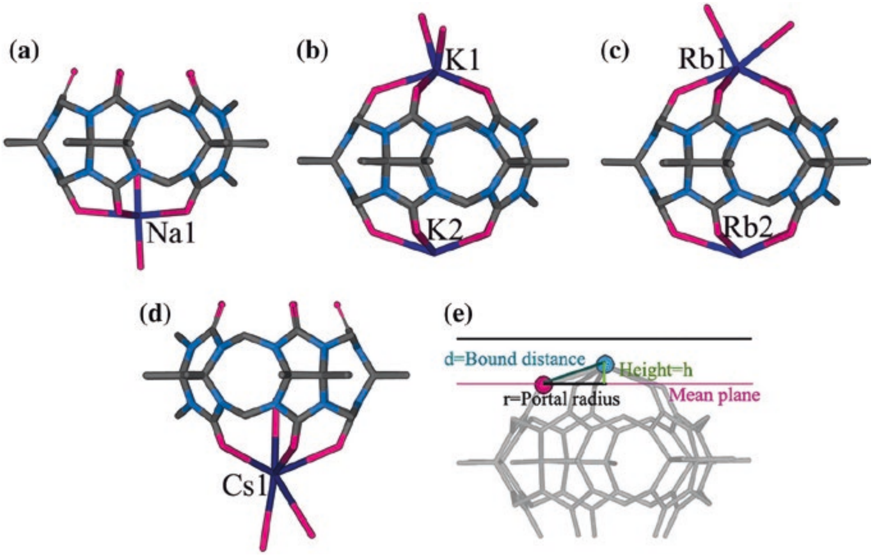

Fig. 2.7 X-ray crystal structures of molecular capsules and molecular bowls of $Me_{10}Q[5]$ with alkali metal ions **a** Na^+; **b** K^+; **c** Rb^+; and **d** Cs^+; **e** representation of bonding distance of $Me_{10}Q[5]$ with metal ions

Table 2.1 Comparison of the structural parameters of four $(Me_{10}Q[5])/M_{alkali}$ complexes

Parameters	$Me_{10}Q[5]/Na^+$	$Me_{10}Q[5]/K^+$	$Me_{10}Q[5]/Rb^+$	$Me_{10}Q[5]/Cs^+$
d (Å)	2.627	2.775	2.870	3.009
h (Å)	~0	0.832	1.028	1.175
r (Å)	2.627	2.647	2.680	2.770

A careful comparison reveals that a structural trend holds for the four $Me_{10}Q[5]$ complexes. These four complexes were all isolated as the sole products of seemingly straightforward reactions of the relevant alkali metal salt with the $Me_{10}Q[5]$ ligand. It should be interesting and essential to compare the related structural data of the four complexes. As shown in Fig. 2.7e and Table 2.1, the average metal–carbonyl oxygen bond lengths (*d*; $O_{Me10Q[5]}$–M_{alkali}) vary from complex to complex. It is well known that the radius of alkali metal ions increases with increasing atomic number. As a result, the metal–carbonyl oxygen bond lengths in the four complexes follow the order $Me_{10}Q[5]/Na^+ < Me_{10}Q[5]/K^+ < Me_{10}Q[5]/Rb^+ < Me_{10}Q[5]/Cs^+$ (Table 2.1). Their crystal data suggest that the height of the alkali cation out-of-portal plane (*h*) of the four complexes follows the same order (Table 2.1). According to the Pythagorean theorem, the portal radius of the $Me_{10}Q[5]$ ligand (*r*) for the four compounds has the same order. Obviously, all these structural trends can be attributed to the fact that the radii of alkali cations are of the order $Na^+ < K^+ < Rb^+ < Cs^+$, and this suggests that the portal size of a Q[*n*] could be transformed in a certain range. Unexpectedly, all four complexes include a water molecule instead of an anion in the cavity of the $Me_{10}Q[5]$ molecule. In other words, the opened or closed molecular capsules in the four compounds could not recognize or encapsulate the chloride anion. A similar structural feature can be observed in the complexes of SQ[5]s with alkaline earth metal ions [25].

Although the first reported Ln^{3+}-Q[5] complex of this type was $\{(LaCl@Q[5])LaCl(H_2O)_9\}Cl_4 \cdot HCl \cdot 7H_2O$, obtained from an HCl solution (~3 M) containing $La(NO_3)_2$ and Q[5], La^{3+} cation has 14 lanthanide group members, which could show similar interaction properties with Q[5]s due to the so-called lanthanide contraction. The La^{3+} cation fully caps one portal of the Q[5] molecule, while a second La^{3+} partially caps the second portal via coordination to two carbonyl oxygens and a chloride ion is included in the Q[5] cavity (Fig. 2.3d) [18]. A similar arrangement occurs in the product obtained from the coordination of Pr^{3+} to Q[5] [26]. The coordination of Gd^{3+} to the dimethyl-substituted derivative ($Me_2Q[5]$), or Nd^{3+} to the decamethyl $Me_{10}Q[5]$ derivative, once again results in products exhibiting similar structural arrangements (Fig. 2.8b and c respectively) [16].

In recent years, Thuéry focused on the coordination of Q[*n*]s with lanthanide and actinide cations and synthesized two Q[5]/UO_2 complexes. One of these complexes, which has a stoichiometry of $\{UO_2Q[5]\}(ReO_4)_2 \cdot 2H_2O$, was prepared

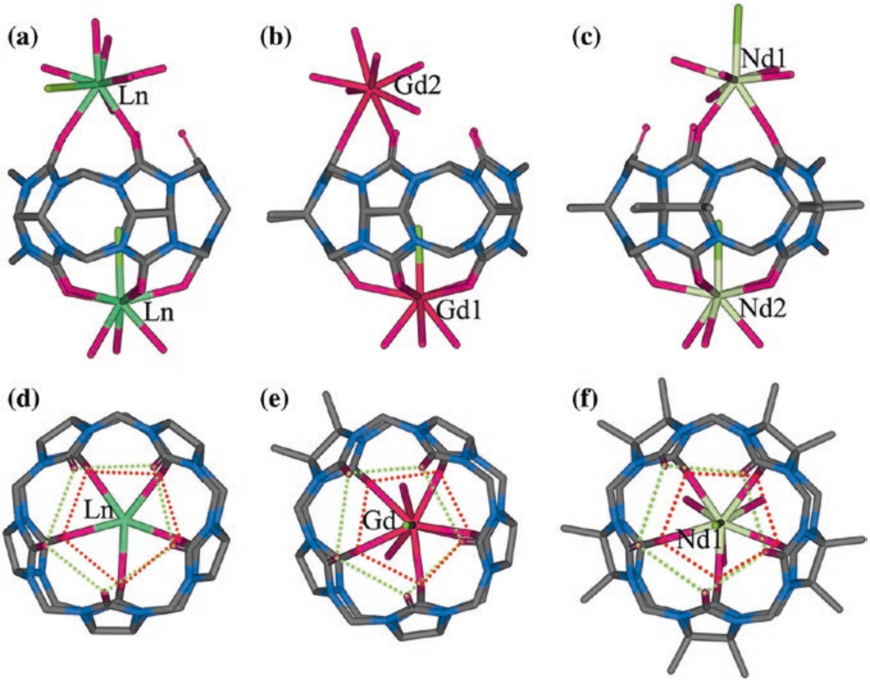

Fig. 2.8 X-ray crystal structures of the complexes of selected Ln^{3+} cations with Q[5] and its $Me_2Q[5]$ and $Me_{10}Q[5]$ substituted derivatives: **a** Ln^{3+}-Q[5] (Ln = La, Pr); **b** Gd^{3+}-$Me_2Q[5]$; **c** Nd^{3+}-$Me_{10}Q[5]$; **d–f** the portal sizes of the corresponding complexes

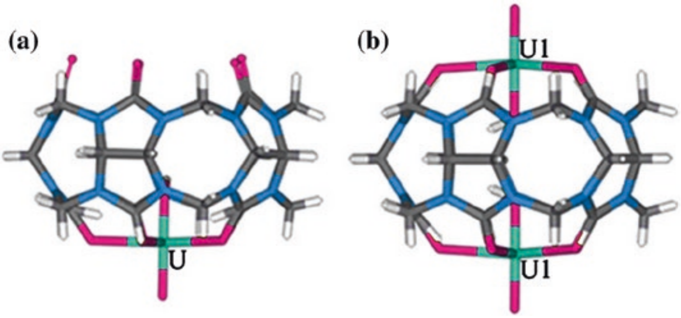

Fig. 2.9 X-ray crystal structures of Q[5] with uranyl ions: **a** molecular bowl; **b** molecular capsule

by mixing Q[5] with excess UO_3 in an aqueous $HReO_4$ solution. The other, with a stoichiometry of $\{(UO_2)_2Q[5]\}(NO_3)_4 \cdot 4HNO_3 \cdot 3H_2O$, was prepared by mixing Q[5] with excess of $(UO_2)_2NO_3$ in an aqueous HNO_3 solution. The Q[5]/UO_2 complexes had characteristic features of the molecular bowl [27] and molecular capsule [28] respectively (Fig. 2.9).

On the other hand, addition of the second metal ion as a structure directing agent could also result in the formation of unusual complexes or novel Q[*n*]-based supramolecular assemblies. For example, when Thuéry investigated the inclusion properties of Q[*n*]/Ln^{3+} complexes for the perrhenate anion, he introduced potassium cation (KNO_3) into the Q[*n*]–Ln^{3+}–ReO_4^- system. A series of Ln^{3+}/K^+ heterometallic capped Q[5]-based capsules were formed (Ln = Ce, Sm, Gd), but no suitable crystal could be obtained in the absence of the KNO_3 reactant in this series (Fig. 2.10a) [27]. In his previous work, U^{6+}/K^+ or Cs^+ heterometallic capped Q[5]-based capsules were obtained by introducing alkali metal ions in the form of their salts, such as KNO_3 or $CsNO_3$, into a Q[5]–$UO_2(NO_3)_2 \cdot 6H_2O$ system (Fig. 2.10b) [28]. Our group also discovered some heterometallic capped Q[5]-based capsules, for example, a Zn^{2+}/K^+ Q[5]-based capsule that could be

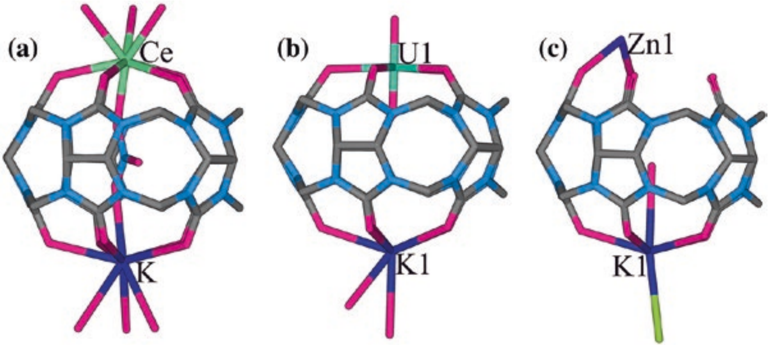

Fig. 2.10 X-ray crystal structures of heterometallic capped molecular capsules: **a** K^+/Ce^{3+} complex and **b** K^+/U^{6+} complex; and molecular bowl **c** K^+/Zn^{2+} complex

obtained by introducing KCl into a Q[5]–$ZnCl_2$ system (Fig. 2.10c) [14]. The Zn^{2+} cation coordinates to the two carbonyl oxygens of a Q[5] portal because of its shorter ionic radius.

When a second larger metal ion is introduced to the singularly capped mononuclear Ln^{3+}-Q[5] system, such as K^+, then in particular cases fully doubly capped heterometallic molecular capsules form. Thuéry [27] first reported a series of heterometallic K^+/Ce^{3+}, K^+/Sm^{3+} (2 complexes) and K^+/Gd^{3+} Q[5] capsules of this type which were obtained under hydrothermal conditions in the presence of perrhenic acid. Five complexes were isolated with all but the fifth, a Yb^{3+} complex (see below), containing K^+. Each capsule included a bound nitrate ion in its cavity (the cavity of Q[5] is too small to include an $[ReO_4]^-$ anion, contrasting with Q[6] which is able to include this anion—see discussion in Sect. 2.2). In the first four complexes the lanthanide ion is nine-coordinate with a capped square antiprismatic geometry. The $[ReO_4]^-$ anions are present as hydrogen bonded counter ions, although in the case of the Sm^{3+} complex this anion is also present as a monodentate ligand. The Ce^{3+}/K^+ complex forms linear columns along the *c*-crystallographic axis in which the cerium and potassium metal centers from adjacent capsules are bridged by two water molecules and a nitrate ion. The Sm^{3+}/K^+ and Gd^{3+}/K^+ complexes are effectively isomorphous and differ from the Ce^{3+}/K^+ complex in that zigzag columns are present (involving one carbonyl and one water bridge between hetero-metal centers), with the K^+ and Ln^{3+} ions also bound to one and two terminal water ligands, respectively. A corresponding K^+/Nd^{3+} capsule was subsequently reported by our group [29] and this product was also found to include a nitrate ion.

The general arrangement of the metal centers in the heterometallic Ln^{3+}-K^+-Q[5] (Ln = Ce, Nd, Sm, Gd) capsule motifs just discussed is represented schematically in Fig. 2.11a [27, 29], with, for comparison, that for a related Gd^{3+}/K^+ complex of dimethyl-substituted Q[5}, $Me_2Q[5]$, given in Fig. 2.11b [30]. Comparison of the two portals in each of these doubly capped species reveals that the portals capped by a K^+ ion are larger than those capped by an Ln^{3+} ion. Reflecting this, there is a difference of ~0.3 Å in the average separation between adjacent carbonyl oxygens rimming the pair of portals in the respective capsules (Fig. 2.11d, e). Our group has demonstrated that reaction of $PrCl_3$ with Q[5] in the presence of $CaCl_2$ (Ca^{2+} has a comparable ionic radius to the lanthanides) leads to a heterometallic (Ca^{2+}/Pr^{3+}) *dinuclear* Ca^{2+}-bridged complex with the structure shown in Fig. 2.11c [29]. In this complex two Pr^{3+} ions fully cap the respective outer portals of the dimer while two Ca^{2+} ions link and partially cap each of the "inner" portals. As might be anticipated, in this arrangement the difference in the respective ("outer" vs. "inner") portal sizes (as expressed by the adjacent carbonyl oxygen internuclear distances—see Fig. 2.11f) show a similar trend to that for the homo-dinuclear Ln^{3+}-Q[5] complexes (see Fig. 2.8a) containing both a fully capped and a partially capped portal [18, 26].

In summary, the smaller portal size of Q[5]s offers related concentrated bonding sites so that a metal ion can coordinate with more portal carbonyl oxygens and form a stable Q[5]/metal complex. Therefore, metal ions suitable for coordination to Q[5] molecules have a wider distribution.

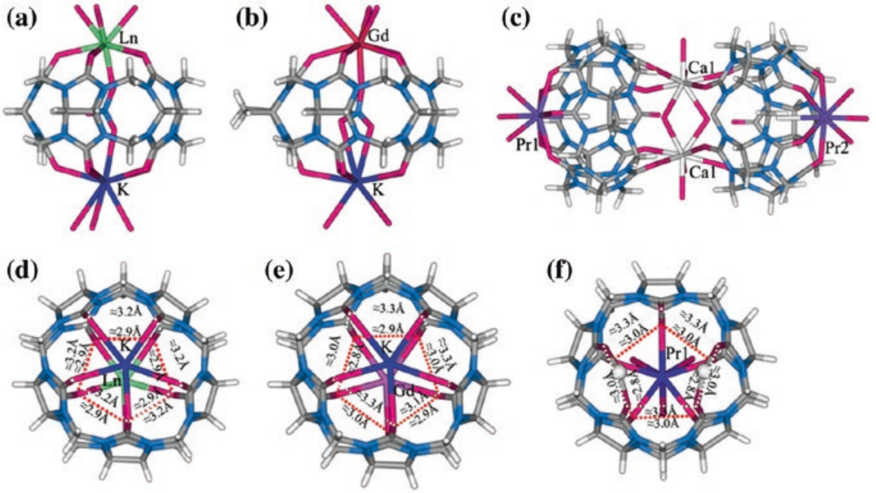

Fig. 2.11 X-ray crystal structures of heterometallic Ln^{3+} and K^+ Q[5] complexes: **a** Ln^{3+}/K^+-Q[5] (Ln = Ce, Nd, Sm, Gd); **b** Gd^{3+}/K^+-DMeQ[5]; **c** $(Pr^{2+})_2/(Ca^{2+})_2$-2Q[5]; **d**–**f** comparison of the portal sizes in the complexes **a**–**c**, respectively

2.2 Simple Coordination Complexes of Cucurbit[6]urils with Metal Ions

Compared with Q[5]s, Q[6]s have a larger portal size. The portal (*r*) radius of Q[6] molecules is within 3.3–3.4 Å, similar to the longest M_{Cs}–$O_{carbonyl}$ bond lengths (3.0–3.3 Å) observed in $CyH_5Q[5]/Cs^+$ or $Me_{10}Q[5]/Cs^+$ complexes. Thus, it is believed that no other single metal ion can fully cover the portal of the Q[6] molecule except the Cs^+ cation, which has the second longest ionic radius. For example, we reported a simple complex of methyl-substituted Q[6], namely symmetrical α,α′,δ,δ′-tetramethylcucurbit[6]uril (TMeQ[6]) with a Cs^+ cation (Fig. 2.12) [31]. The Cs1 atom seems to cover a portal of the TMeQ[6] molecule, and coordinates to five portal carbonyl oxygens. The length of the bond between

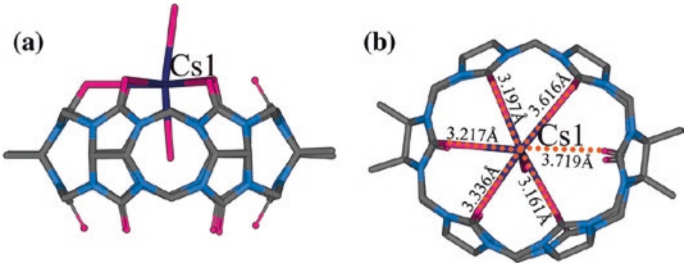

Fig. 2.12 X-ray crystal structures of the $TMeQ[6]/Cs^+$ complex: **a** side view; **b** top view

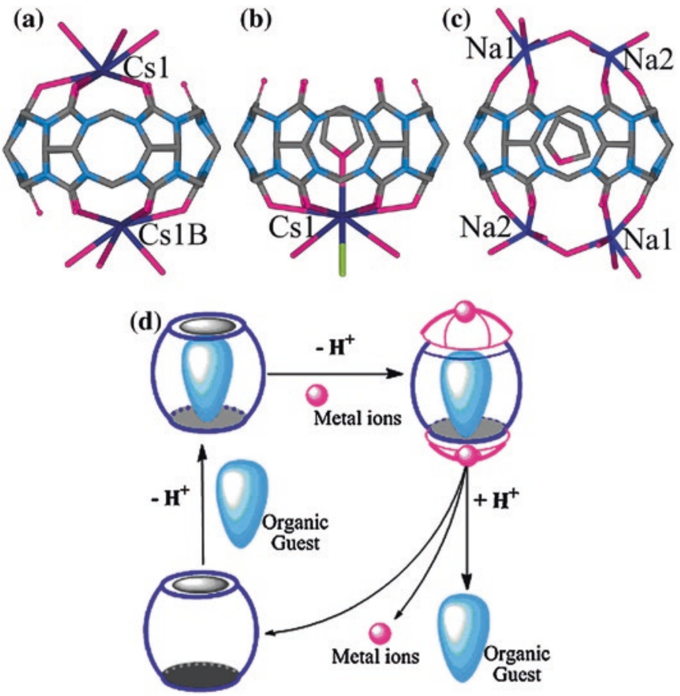

Fig. 2.13 X-ray crystal structures of Q[6] with the alkali metal ion: **a** molecular capsule with Cs^+; **b** molecular bowl with Cs^+; **c** molecular capsule with Na^+; and **d** the representation of molecular capsule and molecular bowl built by Q[*n*]s

Cs1 and the portal carbonyl oxygens is 3.305 Å on average, and can reach a maximum of 3.616 Å.

Kim and coworkers first reported a simple Q[6]/Cs^+ complex in 1998 [32], in which the Cs^+ cation can effectively coordinate only four of six carbonyl oxygens of a portal of a Q[6] molecule. The lengths of the Cs–$O_{carbonyl}$ bonds are in the range 3.100–3.378 Å (Fig. 2.13a). However, with the aid of an organic guest (tetrahydrofuran, THF), the Cs^+ cation fully covers the portal of the Q[6] molecule, and forms a typical molecular bowl. The resulting Cs–$O_{carbonyl}$ bond lengths are in the range 3.144–3.584 Å. In particular, the bond length of Cs–O_{THF} is only 2.934 Å, suggesting that the strong bonding between the Cs^+ cation and the included THF further draws the Cs^+ cation toward the portal of the Q[6] molecule, resulting in the formation of the fully covered Q[6]/THF/Cs^+ molecular bowl (Fig. 2.13b). Such phenomenon exemplifies a typical instance involving Q[*n*]-based host–guest/coordination chemistry. An earlier case involving Q[*n*]-based host–guest/coordination chemistry is the Q[6]/THF/Na^+ molecular capsule also reported by Kim and coworkers in 1996 [33]. In this complex, two Na^+ cations are capped at each of the two portals of the Q[6] molecule, and a THF molecule is included in the cavity of the Q[6] molecule; thus, a sealed molecular capsule is formed (Fig. 2.13c). The bonding and release of the included THF can be controlled by pH-dependent complexation and decomplexation of metal ions at the portals of the Q[6] molecule (Fig. 2.13d). Their observations suggest that the sodium ion “lids” are removed in strongly acidic solution because of the protonation of the carbonyl groups at the cucurbituril portals; consequently, the encapsulated THF molecule can readily escape from the cavity (Fig. 2.13). Raising the pH of the solution restores the sodium ion “lids” of cucurbituril and, therefore, the capability for encapsulating THF. Interestingly, similar supramolecular interaction behaviors may be observed with other guest molecules such as benzene, cyclopentanone, and furan, as well as with other metal ions such as cesium. Knoche and Buschmann first introduced metal ions into a Q[6]–$G_{\text{organic molecule}}$ system to determine the stability constants and the mechanism of formation of association and inclusion complexes of cucurbituril with the 4-methylbenzylammonium ion [34]. Although they only focused on the solution structure of the Q[6]–$G_{\text{organic molecule}}$–$M_{\text{alkali}}$ systems, their seminal work on Q[*n*]-based host–guest/coordination chemistry is a significant contribution. We will further demonstrate more cases in the succeeding parts of this chapter.

Returning to the coordination features of Q[6]/metal complexes, we note that they are clearly different from those of Q[5] complexes because of their larger portal size. In typical Q[6]-based complexes, a metal ion with a smaller ionic radius can only coordinate to a limited number of portal carbonyl oxygens (one to three). This restriction results in the formation of Q[6]-based capsules or bowls in which a portal of the Q[6] molecule could be coordinated with multiple metal ions. The aforementioned Q[6]/THF/Na^+ molecular capsule is a typical instance, in which two coordinated Na^+ cations at each of the two portals of Q[6] coordinates to two portal carbonyl oxygens. Fedin and coworkers made the greatest contribution to Q[6]-based coordination chemistry; they studied almost all alkaline earth, transition, lanthanide, actinide metal ions, as well as their aqueous complexes, clusters, and so on. For example, they demonstrated that Q[6]/Sr^{2+} capsules may be obtained by slow concentration of an aqueous solution of $Sr(NO_3)_2$ and Q[6] (Fig. 2.14a) [35]. Each Q[6] molecule is bound to four strontium cations (two cations per portal), forming a molecular capsule that includes a nitrate anion. The coordination of the four Sr^{2+} ions in the Q[6] molecular capsule is different, in that they coordinate two or three portal carbonyl oxygens by sharing a nitrate anion (N31). This sharing results in the formation of infinite 1D supramolecular chains through electrostatic interaction. Furthermore, Fedin and coworkers recently discovered a Q[6]/Mg^{2+} complex that involves the interaction between Q[6] with the amino acid tryptophan and its decarboxylation product tryptamine in the solid state [36]. This complex is the first known supramolecular assembly of cucurbituril with magnesium ion, which has the smallest ionic radius (0.49 and 0.72 Å for hexacoordinated Mg^{2+}) among metals studied for their coordination to unsubstituted cucurbituril ligands (Fig. 2.14b). Generally, Q[6] molecules show affinity to alkali and alkaline earth metal ions, and form molecular bowls or capsules [37–39]. However, their interaction with metal ions in the presence of a third species could result in the formation of novel coordination polymers and supramolecular assemblies, which will be described in detail later.

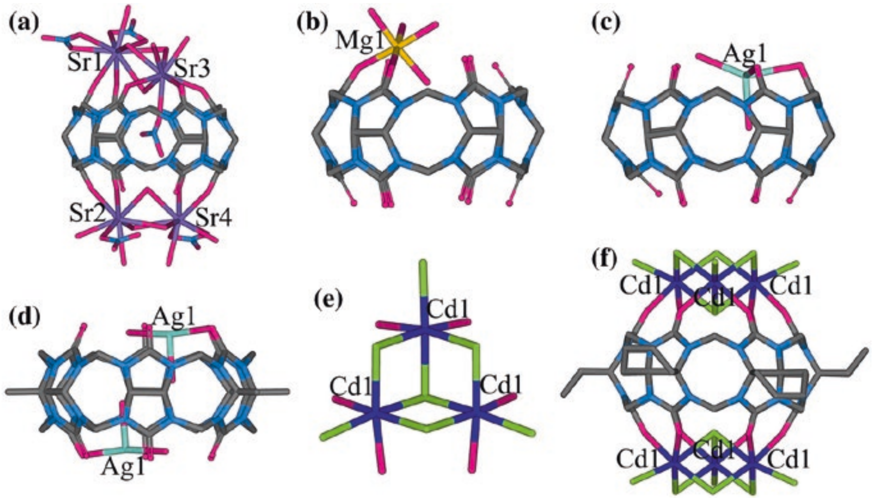

Fig. 2.14 X-ray crystal structures of **a** a Q[6]/Sr^{2+} complex; **b** a Q[6]/Mg^{2+} complex; **c** a Q[6]/Ag^{+} complex; **d** a TMeQ[6]/Ag^{+} complex; **e** a $[\text{Cd}_3\text{Cl}_3(\mu_2\text{-Cl})_3(\mu_3\text{-Cl})]^{-}$ cluster; and **f** a CyH_6Q[6]/Cd^{2+} complex

In aqueous solution, the interaction of Q[6] with transition metal salts prefer to form adducts of Q[6] with metal aqua complexes through hydrogen bonding. There are a few exceptions to the usual products, such as Q[6]/Ag^{+} complexes from a solution containing a Q[6]/isonicotinic acid/La^{3+} host–guest complex in the presence of AgNO_3, as shown in Fig. 2.14c [39]. Another is the complex formed by tetramethyl-substituted Q[6] (TMeQ[6]) and AgNO_3 [40, 41]. In the resulting Q[6]/Ag^{+} complex, only one Ag^{+} cation coordinates to two carbonyl oxygens of a Q[6] portal, whereas in the TMeQ[6]/Ag^{+} complex, both portals of TMeQ[6] are coordinated to an Ag^{+} cation and form a molecular capsule feature (Fig. 2.14d). Another example is the complex of cyclohexanocucurbit[6]uril (CyH_6Q[6]) with Cd^{2+} cations [42]. Interestingly, two $[\text{Cd}_3\text{Cl}_3(\mu_2\text{-Cl})_3(\mu_3\text{-Cl})]^{-}$ cluster anions effectively cover each portal of CyH_6Q[6], forming one sealed molecular capsule (Fig. 2.14e, f).

Professor Zhang in our laboratory investigated coordination assemblies by reactions between alkali metal salts and a *meta*-hexanomethyl-substituted cucurbit[6]uril (*m*-HMeQ[6]) in aqueous solutions. X-ray diffraction analysis revealed that each *m*-HMeQ[6] coordinates with three alkali metal ions, K^{+}, Rb^{+}, or Cs^{+} and forms a 1:2, *m*-HMeQ[6]:$\text{M}^{+}_{\text{alkali}}$ complex (Fig. 2.15) [43].

In 2002 Fedin and coworkers reported the first lanthanide complex of Q[6] (a Sm^{3+} species) [44]. The product formed on slow evaporation of an aqueous solution of SmBr_3 and Q[6] and had an Sm^{3+}:Q[6] stoichiometry of 2:3. The X-ray structure shows a triple-decker sandwich arrangement (height: ~33 Å) of type $\{(\text{Q[6]})[\text{Sm}(\text{H}_2\text{O})_4](\text{Q[6]})[\text{Sm}(\text{H}_2\text{O})_4](\text{Q[6]})\}^{6+}$ (Fig. 2.16). Each Sm^{3+} is coordinated by four waters and two Q[6] units. Relative to Q[5], Q[6] has a larger

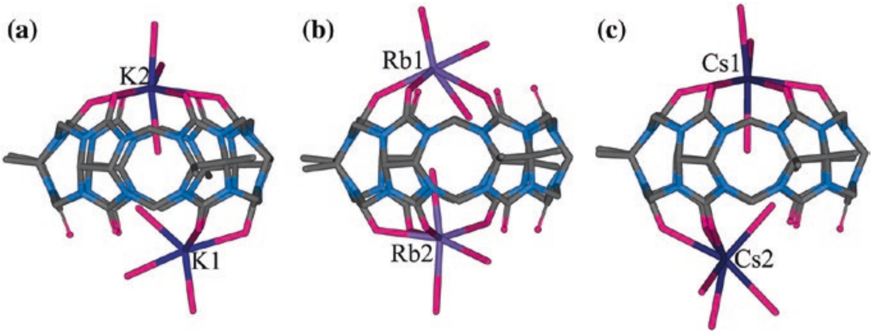

Fig. 2.15 X-ray crystal structures of molecular capsules of *m*-HMeQ[6] with metal ions: **a** K^+; **b** Rb^+; **c** Cs^+

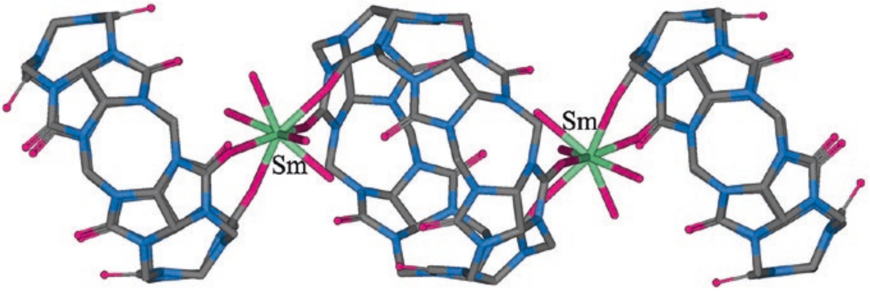

Fig. 2.16 X-ray crystal structure of the Sm^{3+}-Q[6] triple-decker sandwich

portal size with a portal radius of 3.3–3.4 Å. This radius is substantially longer than the bond length range observed for Ln^{3+}-$O_{carbonyl}$ bonds: 2.223–2.478 Å. As a consequence a single lanthanide cation is unable to coordinate simultaneously to all six carbonyl oxygens lining a Q[6] portal; generally only one to three portal carbonyl oxygens have been found to bind. In the above complex, each Sm^{3+} cation ion coordinates to two portal carbonyl oxygens from each of two Q[6]s, with the average bond length being 2.401 Å; each metal center achieves 8-coordination.

In a further paper Fedin reported a systematic study of Q[6] coordination with La^{3+}, Ce^{3+}, Gd^{3+}, Ho^{3+}, and Yb^{3+} nitrates or bromides in aqueous solution [45]. While Q[6] is not soluble in water, it readily dissolves on heating with a saturated solution of the above Ln^{3+} salts. Seven complexes were isolated—the first five were obtained from the corresponding Ln^{3+} nitrate salt while the remaining two were from the corresponding bromide salt: (i) $[Gd(NO_3)(H_2O)_4(Q[6])](NO_3)_2 \cdot 7H_2O$, (ii) $[Ho(NO_3)(H_2O)_4(Q[6])](NO_3)_2 \cdot 7H_2O$, (iii) $[Yb(NO_3)(H_2O)_4](Q[6])](NO_3)_2 \cdot 6H_2O$, (iv) $[La(H_2O)_6(SO_4)(Q[6])](NO_3) \cdot 12H_2O$, (v) $[Gd(NO_3)(C_2H_5OH)(H_2O)_2(H_2O@Q[6])](NO_3)_2 \cdot 5.5H_2O$. Two additional complexes $\{[Gd(H_2O)_4]_2(Q[6])_3\}Br_6 \cdot 45H_2O$ and $\{[Ce(H_2O)_5]_2(Q[6])_2\}Br_6 \cdot 26H_2O$, obtained employing the corresponding La^{3+} bromide salts, were also isolated (see later). With the exception of $[La(H_2O)_6(SO_4)(Q[6])](NO_3) \cdot 12H_2O$ (iv), all of these products were isolated either directly from water or following diffusion of ethanol into their aqueous solution. While the X-ray structure of (i) was not determined, the 1:1 (Ln^{3+}:Q[6]) complexes (ii) and (iii) were shown to be isostructural (Fig. 2.17a). In the case of (iv), the reaction solution contained lanthanum nitrate, Q[6], and copper sulfate. The X-ray structure of the latter product showed that the complex consists of an La^{3+} bound to a portal of Q[6] via two oxygens, with the nine-coordinate coordination sphere of the metal center being completed by six water molecules and a monodentate sulfate ligand (Fig. 2.17b). The X-ray structure of $[Gd(NO_3)(C_2H_5OH)(H_2O)_2(H_2O@(Q[6])](NO_3)_2 \cdot 5.5H_2O$ (v), which crystallized from the reaction solution following the slow diffusion of alcohol, showed that the Gd^{3+} is eight-coordinate with the coordination sphere consisting of a bidentate Q[6] unit, an ethanol molecule, a bidentate nitrate, and three aqua ligands (Fig. 2.17c) [45]. This product incorporates one water molecule in the Q[6] cavity (not shown in Fig. 2.17c). In a related study, it was shown that Gd^{3+} chloride reacts with Q[6] to yield $\{[Gd(H_2O)_6]_2[(H_2O@Q[6])\}Cl_6 \cdot 4H_2O$ in which Q[6] acts as a bis-bidentate ligand such that a pair of carbonyl oxygens

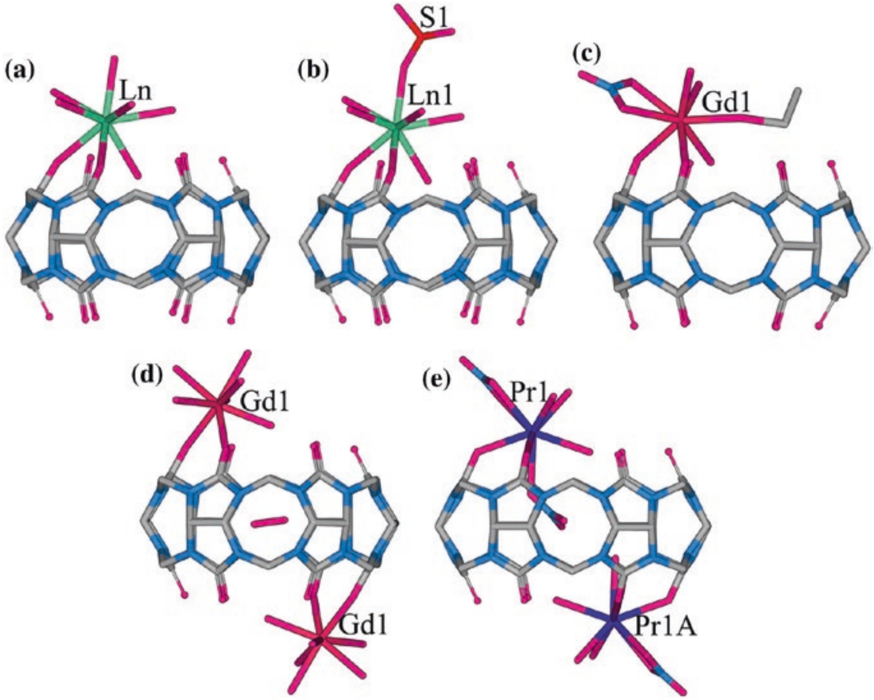

Fig. 2.17 X-ray crystal structures of selected Ln^{3+}-Q[6] complexes prepared from La^{3+} nitrate salts: **a** the isostructural complexes $[Ho(NO_3)(H_2O)_4(Q[6])]^{2+}$ and $[Yb(NO_3)(H_2O)_4](Q[6])]^{2+}$; **b** $[La(H_2O)_6(SO_4)(Q[6])]^{+}$ with bound sulfate group; **c** $[Gd(NO_3)(C_2H_5OH)(H_2O)_2(H_2O@Q[6])]^{2+}$ with coordinated ethanol molecule, the included water molecule is not shown; **d** $\{[Gd(H_2O)_6]_2[(H_2O@Q[6])\}^{6+}$, included water molecule not shown; **e** $[\{Pr(NO_3)_2(H_2O)_3\}\{Pr(NO_3)(H_2O)_3(H_2O@Q[6])\}]^{3+}$, the included (bound) nitrate ion and water molecule not shown

at each portal coordinate to a Gd^{3+} cation along with six water molecules [46]. A guest water molecule resides in the cavity of the Q6 and is disordered between two positions (Fig. 2.17d). Under hydrothermal conditions (at 120 °C) $Pr(NO_3)_3$ reacts with Q[6] in water to yield $[\{Pr(NO_3)_2(H_2O)_3\}\{Pr(NO_3)(H_2O)_3(H_2O@Q[6])\}](NO_3)_3 \cdot 4H_2O$ [47]. An X-ray diffraction study (Fig. 2.17e) demonstrated that the two metal centers in this complex are each linked to the Q[6] through tridentate coordination of three portal oxygens from the respective portals. Each metal center is also bound to a bidentate nitrato ligand and three water molecules located exo to the central cavity. The cavity encapsulates both a nitrate ion and a water ligand (both disordered over two positions) which are each bound in a monodentate fashion to the respective metal centers, each of which achieves a coordination number of nine.

Use of a lanthanide bromide salt rather than a nitrate salt has been shown to result in changes in both the composition and the structure of the corresponding Ln^{3+}-Q[6] complexes—once again emphasizing the difficulties in predicting the nature of the product from a given synthetic procedure [45]. Thus, complex crystallization from an aqueous solution containing cerium bromide and Q[6] results in a 2:2 Ce^{3+}-Q[6] sandwich complex incorporating two cucurbituril ligands linked by two bound $[Ce(H_2O)_5]^{3+}$ units (Fig. 2.18a). Each nine-coordinated Ce^{3+} has four carbonyl oxygens and five aqua ligands in its coordination sphere. The 2:2 structure contrasts with the 1:1 arrangements found in the (Ln^{3+}:Q[6]) complexes (a)–(e) discussed above (see Fig. 2.17)—all of which employed the corresponding lanthanide nitrate salt as a precursor [45]. The trigonal crystal packing of the above sandwich complex is shown in Fig. 2.18b. Triangular channels with a van der Waals diameter of ~4.3 Å are filled with disordered water molecules and bromide anions (omitted in Fig. 2.18b for clarity). In contrast, the corresponding $GdBr_3$-Q[6] system results in a triple-decker sandwich (Fig. 2.18c). The latter is related to that described above for the Sm^{3+}-Q[6] triple-decker sandwich [44] shown in Fig. 2.16.

As discussed already for Q[5]-based complex systems [24], there are also examples of Q[6] systems prepared in the presence of added small organic molecules that appear to play a structure directing role. Thus, Fedin and coworkers showed that the interaction of aqueous Gd^{3+} nitrate with Q[6] in the presence of pyridine yielded a hydrogen-bonded (supramolecular) adduct between the aqua nitrate complex $[Gd(NO_3)(H_2O)_7]^{2+}$ and Q[6] (Fig. 2.19a) [48]. In the above assembly the water molecules coordinated to the Gd^{3+} center are hydrogen bonded to carbonyl groups of Q[6], with the cavity of the Q[6] molecule encapsulating a pyridine molecule. These workers also reported a further La^{3+}-Q[6] capsule-like complex of type $[La(H_2O)_6(X@Q[6])(NO_3)]^{2+}$ ($X = 0.5\ C_5H_5N + 0.5\ H_2O$) [49] in which a pyridine molecule occupies the internal cavity of one half of the Q[6] molecules (Fig. 2.19b), while a water molecule occupies the other half. The La^{3+} center is bound to two adjacent carbonyl oxygens, a bidentate nitrato ligand and six aqua ligands to yield a coordination number of ten. The metal center is disordered between the two portal faces (with both occupancy positions shown in Fig. 2.19b). In a related study Liu and coworkers [50] crystallized a 1:1

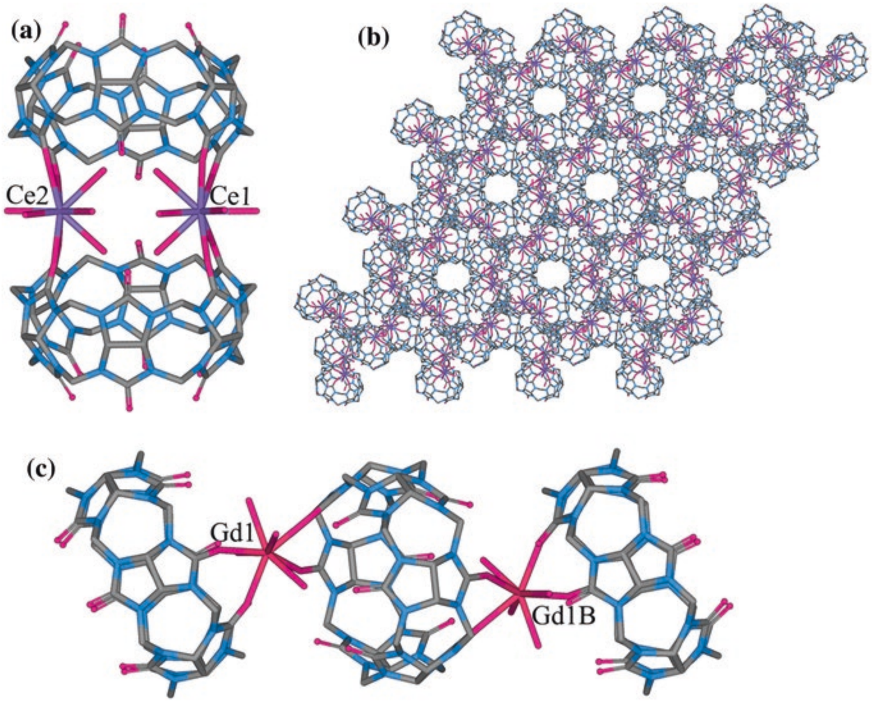

Fig. 2.18 X-ray crystal structures of **a** the Ce^{3+}-Q[6] sandwich complex; **b** the 3D Ce^{3+}-Q[6] packing in **a** showing the presence of nanochannels; **c** the Gd^{3+}-Q[6] triple-decker sandwich complex

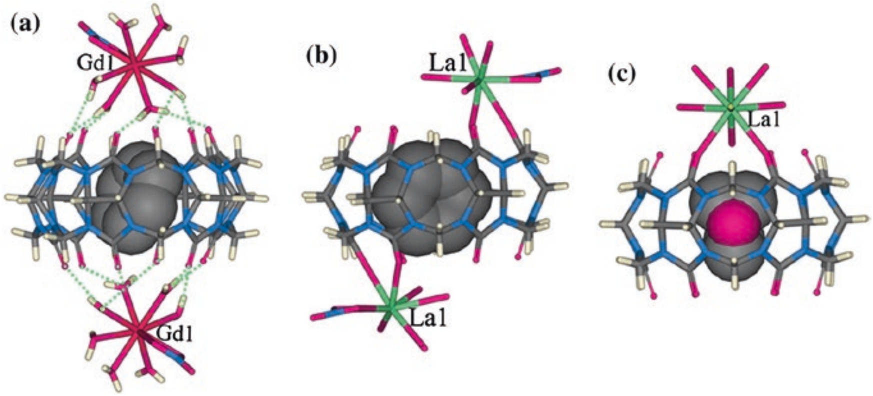

Fig. 2.19 X-ray crystal structures of Ln^{3+}-Q[6] assemblies: **a** hydrogen-bonded host–guest assembly of two $[Gd(H_2O)_7NO_3]^{2+}$ cations with Q[6] which encapsulates a pyridine molecule in its cavity; **b** a La^{3+}-Q[6] complex incorporating an encapsulated pyridine molecule (pyridine encapsulation occurs for half the complexes while the other half encapsulate a water molecule); the La^{3+} site is disordered between each portal (both positions shown); **c** La^{3+}-Q[6] complex incorporating an encapsulated tetrahydrofuran molecule

(La^{3+}:Q[6]) cationic inclusion complex of type $\{[La(H_2O)_6Cl](THF@Q[6])\}^{2+}$ (THF = tetrahydrofuran) through slow diffusion of THF vapor into a solution containing Q[6] and lanthanum nitrate in 3 M HCl (Fig. 2.19c). The La^{3+} coordination sphere in this case consists of two carbonyl oxygens, six water molecules and a chloride ion.

Fedin and coworkers have synthesized a series of polynuclear lanthanide complexes by reacting Q[6] with aqueous solutions of lanthanide(III) nitrates [51], chlorides [52] or bromides [39], Q[6], and 4-cyanopyridine under hydrothermal conditions (130 °C). These μ-hydroxo polynuclear lanthanide complexes are formed in aqueous solution and their formation involves hydrolysis of the corresponding Ln^{3+} salts with, under the conditions employed, the 4-cyanopyridine also being hydrolyzed to isonicotinic acid. Thus, for example, using lanthanide nitrates, a series of tetranuclear aqua-hydroxo-carboxylate complexes of type $\{[Ln_4(\mu_3\text{-}OH)_4(\mu_2\text{-}OH)_2(C_5NH_4COO)_2(H_2O)_4(Q[6])_2][Ln(H_2O)_8]_{1.5}[Ln(H_2O)_6(NO_3)_2]_{0.5}\}(NO_3)_9 \cdot nH_2O$ (Ln = Ho, Gd, or Er) was obtained and characterized by X-ray diffraction analysis, elemental analysis, infrared spectrophotometry, and electrospray ionization (ESI) mass spectrometry [51]. The sandwich structure involves coordination of a central tetrahedral lanthanum cluster to two Q[6] via four oxygens (two per Ln^{3+} cent) at each portal (Fig. 2.20a). The presence of bridging bidentate carboxylate groups in the tetranuclear cluster was postulated to stabilize the observed structure by inhibiting formation of infinite polymeric species.

The above products are generally similar to a range of complexes formed from chloride [52] and bromide [39] lanthanide salts (Fig. 2.20b) in that sandwich complexes are generated; although, in particular complexes, some structural differences do occur—reflecting variation in the synthetic conditions and/or due to the intrinsic differences in the properties of the lanthanide cations themselves. Some variations on the basic structure are illustrated in Fig. 2.20c–f. All these complexes incorporate a tetranuclear lanthanide cluster (Ln1-Ln4) core positioned between two neighboring Q[6] molecules. Ln1 and Ln2 each coordinate to two portal carbonyl oxygens of a Q[6] molecule while Ln3 and Ln4 coordinate to two portal carbonyl oxygens of the second Q[6] molecule in the sandwich complex, with the carboxylate groups (O1, O2 and O3, O4) from two isonicotinates coordinating to Ln1, Ln2 and Ln3, Ln4, respectively. The aromatic ring of each bridging bidentate isonicotinate is included in a Q[6] cavity. The four Ln^{3+} cations are linked by four μ_3-OH groups and from one to four μ_2-OH groups (depending on the particular lanthanide involved). Thus, for example, there are four μ_3-OH groups and one μ_2-OH group in the structure shown in Fig. 2.20c. In particular complexes, one or two additional isonicotinate ligands also bind to particular Ln^{3+} sites (Fig. 2.20c–f) while in other cases the carbonyls from the second ("outside") portal of each Q[6] also bind to further Ln^{3+} cations (Fig. 2.20d, e). Selected compounds from the above series have been employed as precursors for the synthesis of lanthanide-silver heterometallic coordination polymers [39]. In these heteronuclear compounds the affinity of the isonicotinate pyridyl nitrogen for Ag^+ has been exploited to produce chain polymers in which La^{3+}, Pr^{3+} and Dy^{3+} sandwich complexes are

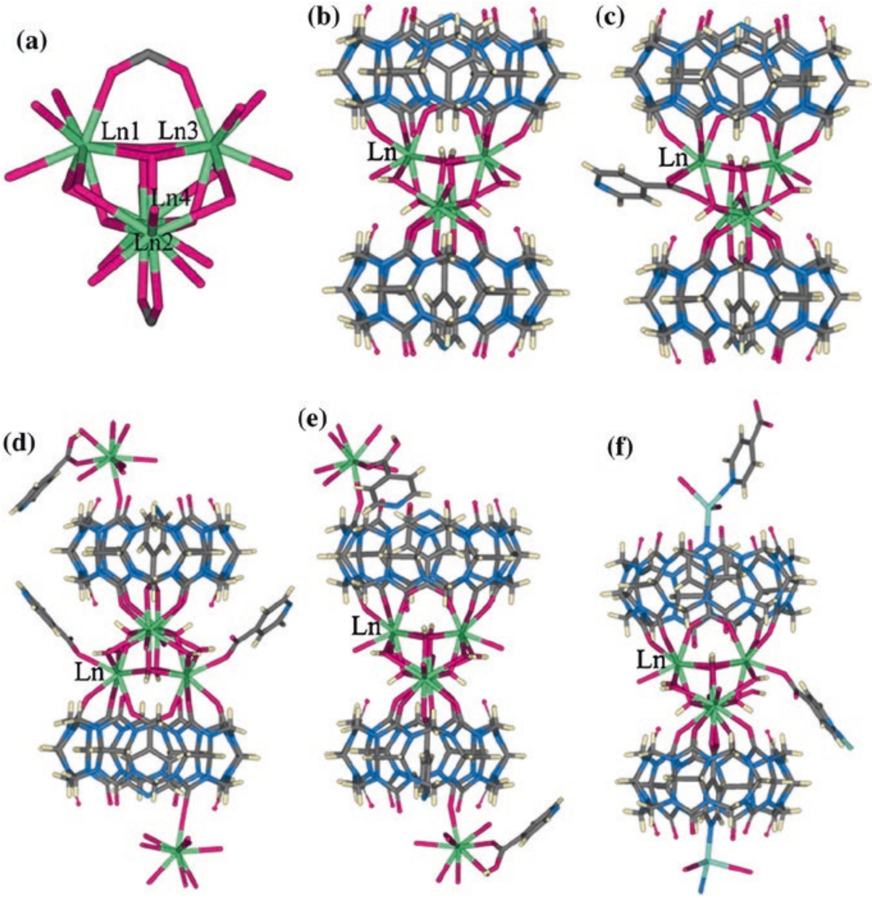

Fig. 2.20 X-ray crystal structures of tetranuclear lanthanide aqua hydroxo-Q[6] sandwich complexes: **a** representative tetranuclear lanthanide aqua hydroxo core; typical sandwich complexes in which **b** Ln = Gd [55], Ho [55], Er [55, 56], Yb [56]; **c** Ln = Dy [57], Ho [57], Er [57]; **d** Ln = La [57]; **e** Ln = Pr [56, 57], Nd [56]; and **f** Ln = La [57], Pr [57], Dy [57]; the tetrahedral Ag^+ centers are shown above and below the *top* and *bottom* portals of the Q[6] sandwich structure

linked via coordination of their nitrogen atoms to Ag^+ ions to yield repeating units of the type shown in Fig. 2.20f.

Although Fedin et al. originally focused on the preparation of polynuclear lanthanide complexes, the approaches that they adopted greatly aided the developments in Q[*n*]-based host–guest coordination chemistry.

Since 2008, Thuéry have synthesized numerous Q[6]-based complexes with lanthanides and actinides in various media, such as neutral aqueous solution, nitric acid, sulfuric acid, formic acid, and perrhenic acid. These reactions have been carried out in the presence of various species, which could behave as structural inducers: examples include sebacic acid, L-(+)-tartaric acid, citric acid, and second metal salts. For example, Thuéry characterized a series of Q[6]/Ln^{3+}-based molecular capsules (Ln = Ce^{3+}, Pr^{3+}) and molecular bowls (Ln = Yb^{3+}, Lu^{3+}) including a perrhenate anion in perrhenic acid (Fig. 2.21a, b). Only the coordination of Sm^{3+} cations with Q[6] form a molecular pair in which two Sm^{3+} cations link two neighboring Q[6] molecules (Fig. 2.21c) [53]. In the presence of the α-amino acid L-cysteine (L-cys), the reaction of $Nd(NO_3)_3$, $Eu(NO_3)_3$, or $Tb(NO_3)_3$ salts with Q[6] gives simple complexes that belong to Q[*n*]-based host–guest/coordination chemistry, as shown in Scheme 1.1. In all three cases, each metal cation is bound to the bidentate Q[6] and the monodentate L-cys molecules, with the latter in the zwitterionic form, and the ammonium group of L-cys is directed away from Q[6] (Fig. 2.21d) [27]. In the presence of *p*-sulfobenzoic acid (4-SB), combination of Q[6] with $Nd(NO_3)_3$ seems to give a molecular pair in which two Q[6]-based capsules are close to each other (the two Nd^{3+} cations between the two capsules have 50 % occupancy). However, the Nd^{3+} cation at the other portal of Q[6] coordinates to both the Q[6] molecule and 4-SB (Fig. 2.21e) [53]. It is interesting to compare the former two Q[6]/Ln^{3+}/guest complexes

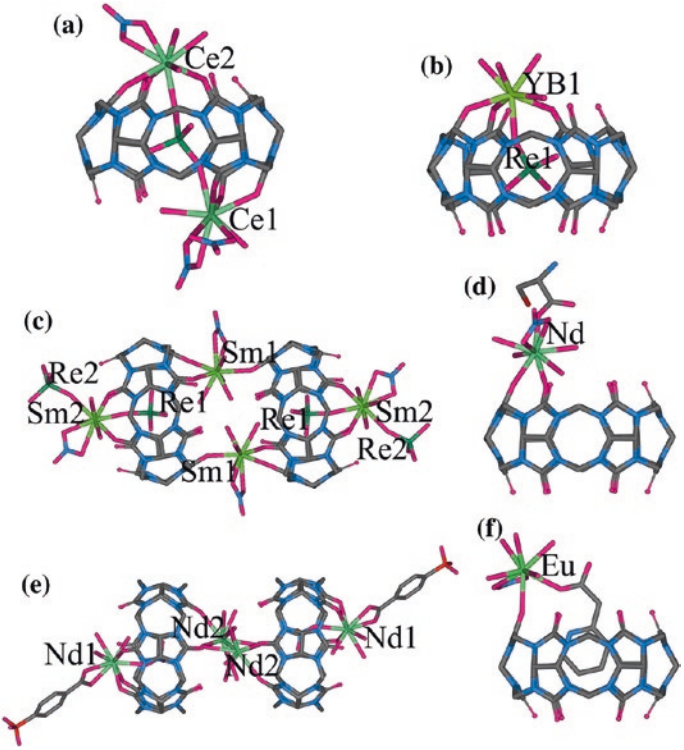

Fig. 2.21 X-ray crystal structures of simple complexes of Q[6]/Ln^{3+} cations and the corresponding supramolecular assemblies: **a** a molecular capsule of Q[6]/Ln^{3+} (Ln = Ce, Pr); **b** a molecular bowl of Q[6]/Ln^{3+} (Ln = Yb, Lu), **c** a molecular pair of Q[6]/Sm^{3+}; **d** a Q[6]/Ln^{3+}/L-cys complex (Ln = Nd, Eu, Tb); **e** a Q[6]/Nd^{3+}4-SB complex pair; and **f** a Q[6]/Eu^{3+}/HPA complex

with that obtained from the anion derived from 2-pyridylacetic acid (HPA). The crystal structure of the Q[6]/Eu^{3+}/AP^- complex shows that the Q[6] molecule coordinates with a Eu^{3+} cation, and includes the aromatic moiety of the organic guest. Moreover, the anion moiety (COO^-) of the guest further coordinates to the capped Eu^{3+} cation, resulting in the formation of the typical organic-guest-induced Q[6]/metal complex (Fig. 2.21f) [54].

Using a hydrothermal method, Thuéry obtained some simple Q[6]/UO_2^{2+} complexes by combination of Q[6] and UO_3 or $UO(NO_3)_2 \cdot 6H_2O$ in the presence of perrhenic acid and formic acid, respectively [55]. The crystal structure of the complex with perrhenic acid shows a dinuclear species in which one uranyl ion is bound to each Q[6] portal through bidentate coordination, to one perrhenate ion located *trans* with respect to the macrocycle, and to half a perrhenate ion, which occupies the same coordination site as an aqua ligand. Both are given occupancy parameters of 0.5 (Fig. 2.22a) [55]. The crystal structure of the complex with sebacic acid shows uranyl coordination by Q[6]. Each U1 atom is bound to two carbonyl atoms from two Q[6] molecules, which are adjacent in its equatorial plane. The average length of such bond is 2.38(4) Å, in agreement with the average value of 2.36(4) Å for urea derivatives reported in the Cambridge Structural Database (CSD) (Fig. 2.22b) [56]. Heterometallic Q[*n*]-based complexes commonly feature coordination of two different metal ions at both portals of the Q[*n*] molecule. Thuéry demonstrated an unusual case in which a series of novel heterometallic uranyl–lanthanide molecular complexes (Q[6]/UO_2^{2+}/Ln^{3+}, Ln = Sm, Eu, Gd, Lu) are obtained from the reaction of uranyl and lanthanide nitrates with Q[6] in the presence of perrhenic acid under hydrothermal conditions. Both metal cations of UO_2^{2+} and Ln^{3+} are bound to carbonyl groups of the same Q[6] portal (Fig. 2.22c) [57].

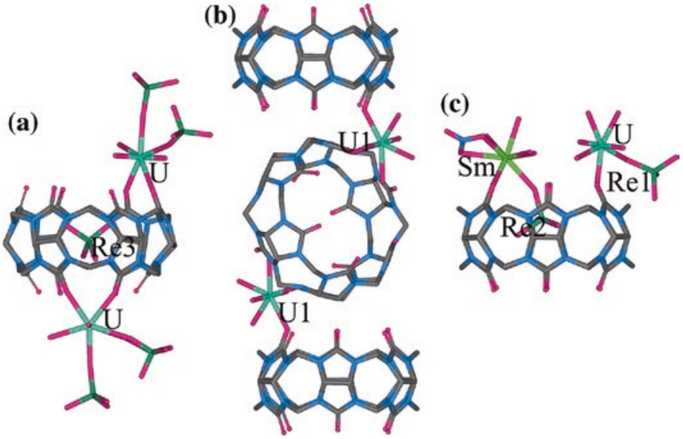

Fig. 2.22 X-ray crystal structures of two Q[6]/UO_2^{2+} complexes formed in the presence of **a** perrhenic acid; **b** formic acid; and **c** the heterometallic Q[6]/UO_2^{2+}/Ln^{3+} complexes (Ln = Sm, Eu, Gd, Lu)

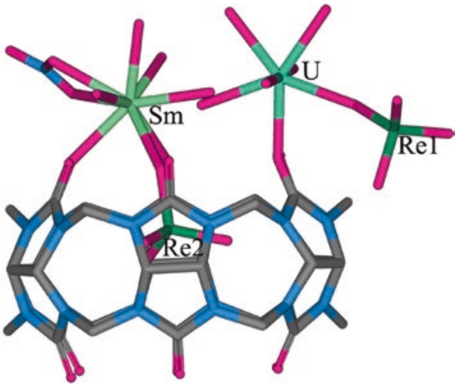

Fig. 2.23 X-ray structure of the isomorphous heterometallic complexes of type $[UO_2Ln(Q[6])(ReO_4)_2(NO_3)(H_2O)_7]$ (Ln = Sm, Eu, Gd, Lu), shown for Ln = Sm

Initial attempts by Thuéry to prepare heteronuclear uranyl-lanthanide Q[6] complexes were unsuccessful [27]. However, four such species of type $[UO_2Ln(Q[6])(ReO_4)_2(NO_3)(H_2O)_7](ReO_4)_2$ (Ln = Sm, Eu, Gd, Lu) were subsequently isolated following reaction of a mixture of uranyl nitrate and lanthanide nitrate with Q[6] in the presence of $[ReO_4]^-$ under hydrothermal conditions [57]. In an unusual arrangement both the UO_2^{2+} and Ln^{3+} cations bind to carbonyl groups on the *same* Q[6] portal (Fig. 2.23). The UO_2^{2+} also binds to a monodentate $[ReO_4]^-$ group as well as to three waters while the Ln^{3+} binds to a monodentate $[ReO_4]^-$ and a nitrato ligand together with four waters, with the latter $[ReO_4]^-$ included in the Q[6] cavity. This was the first reported example of the inclusion of a tetrahedral oxoanion in Q[6].

In a subsequent study it was shown that UO_2^{2+} combined with Nd^{3+}, Dy^{3+}, Er^{3+}, or Yb^{3+} nitrate in each case reacts with Q[6] and 1,2-ethanedisulfonate (EDS^{2-}) under hydrothermal conditions to yield heterometallic complexes of type $[(UO_2)_4Nd_2(EDS)_4(OH)_4(Q[6])(H_2O)_{16}](NO_3)_2 \cdot 8H_2O$, and $[(UO_2)_2Ln_{1.5}(EDS)_2(OH)_2(NO_3)_{1.5}(Q[6])(H_2O)_{7.5}][(UO_2)_2(EDS)\text{-}(OH)_2(H_2O)_4]NO_3 \cdot 5.5H_2O$ (where Ln = Dy, Er and Yb) [58]. In each complex the Ln^{3+} ion is bound to a Q[6] and partially caps a portal. Each EDS^{2-} co-ligand binds to a UO_2^{2+} and an Ln^{3+} ion via its two sulfonate groups in a bis-monodentate manner, with the UO_2^{2+} ion also being part of a bis(hydroxide)-bridged dinuclear unit that forms part of a link between adjacent Q[6] units such that each complex adopts a ribbon-like 1D assembly.

In summary, unlike in the coordination of Q[5] with the metal ions, a wider bonding site distribution is available because of the larger portal size of Q[6]s. With such distribution, the metal ion can generally coordinate to one to three portal carbonyl oxygens, and more than one metal ion may be located at the same portal of a Q[6] molecule.

2.3 Simple Coordination Complexes of Cucurbit[n, $n \geq 7$]urils with Metal Ions

A comparison of complexes of Q[n, $n \geq 7$]s and Q[5 or 6]s shows that the coordination of Q[n, $n \geq 7$]s with metal ions is more difficult than that of Q[5 or 6] with metal ions. Few of the simple complexes involving with Q[n, $n \geq 7$]s have been reported in Q[n]-based coordination chemistry. The larger portal size of Q[n, $n \geq 7$]s result in an even wider distribution of the carbonyl oxygens, which may be a reason for the difficulty in the coordination of Q[n, $n \geq 7$] with metal ions. The first crystal structures of Q[7]/metal-based coordination complexes were obtained by Thuéry. He investigated the influence of perrhenate ions on the structure of lanthanide complexes with Q[n]s to further probe the properties of Q[n]s in perrhenate encapsulation [27]. The compound has a very large assembly uniting two different Q[7]/Yb^{3+} complexes: The first comprises two Q[7] molecules bridged by one Yb^{3+} cation, with two partially included (but not coordinated) $[Yb(ReO_4)(NO_3)(H_2O)_5]^+$ cations (Fig. 2.24a). The second is built from one bidentate Q[7], one coordinated cation that is disordered over two positions related by a mirror plane, and one coordinated and included ReO_4^- anion (Fig. 2.24b). However, in the presence of $CsNO_3$ or aqueous formic acid, combination of Q[7] with $UO_2(NO_3)_2$ or UO_3 can yield simple Q[7]/UO_2^{2+} complexes, as shown in Fig. 2.24c, d, respectively [59]. In both Q[7]/UO_2^{2+} complexes, the UO_2^{2+} cation coordinates one portal carbonyl oxygen, and a pair of OH^- anions link two UO_2^{2+} cations.

Even though more Q[8]/metal-based simple complexes have been reported, only two typical Q[8]/metal-based coordination complexes have been synthesized

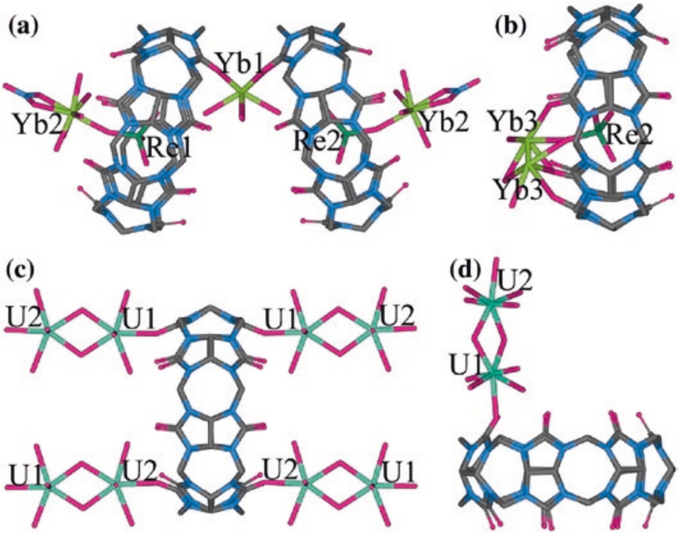

Fig. 2.24 X-ray crystal structures of **a** and **b** two different Q[7]/Yb^{3+} complexes and two different Q[7]/UO_2^{2+} complexes in the presence of **c** $CsNO_3$ and **d** formic acid

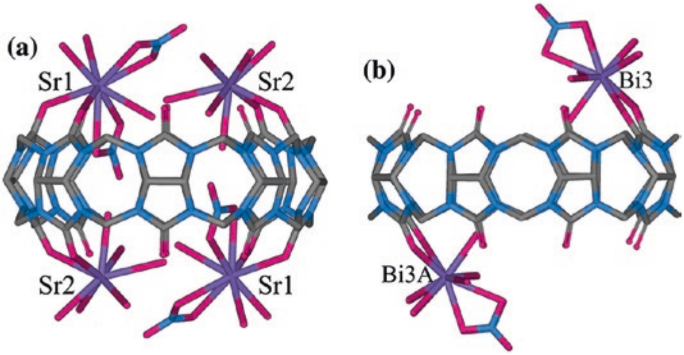

Fig. 2.25 X-ray crystal structures of two different Q[8]/Metal complexes **a** Q[8]/Sr^{2+} complex and **b** Q[8]/Bi^{3+} complex

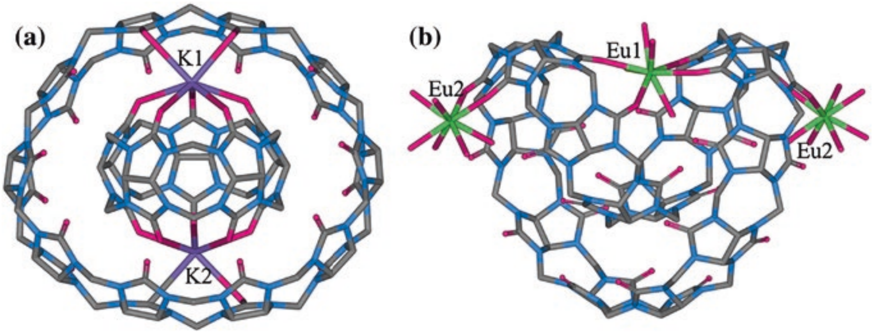

Fig. 2.26 X-ray crystal structures of **a** the Q[5]@Q[10]/K^+ complex and **b** tQ[14]/Eu^{3+}

and characterized by X-ray diffraction in the early development of cucurbituril chemistry. One was obtained by slow concentration of aqueous solutions containing strontium nitrate and Q[8]. The crystal structure of this Q[8]/Sr^{2+} complex shows that each Q[8] molecule is bound to four strontium cations (two cations per each portal), and the strontium atoms linked to the portal of the larger macrocycle are remote from each other and are not linked to each other through the bridging ligands (Fig. 2.25a) [60]. The other Q[8]/metal-based coordination complex was obtained by reacting $Bi(NO_3)_3$ with Q[8] in 3M HNO_3. This complex has a Q[8] molecule coordinated by two $[Bi(NO_3)(H_2O)_5]^{2+}$ fragments (Fig. 2.25b) [61].

Cucurbit[10]uril (Q[10]), which was discovered by Day in 2002, used to be the largest member in the Q[*n*] family. However, it is rare to see a simple complex of Q[10] or its derivatives [4, 62, 63] with metal ions not only because Q[10] itself is rare, but also because of the wider carbonyl oxygen distribution. A host–guest/M^{n+} complex, Q[5]@Q[10]/K^+ was synthesized by Liu and coworkers (Fig. 2.26a) [64]. A Q[5] molecule is included in the cavity of Q[10], and two K^+ cations, each of which does not fully cover portal of Q[5] molecule, coordinates two portal carbonyl oxygens of the Q[10] molecule. As mentioned previously, we recently reported the new largest member of the Q[*n*] family, namely tQ[14]. In fact, determination of the structural characteristics of tQ[14] was also first based on the determination of the complex of tQ[14] molecules with the aid of Eu^{3+} cations (Fig. 2.26b) [5]. This was accomplished because the tQ[14]/Eu^{3+} structures belong to coordination polymers, which will be presented in detail later.

Based on the above results, we summarized the main simple Q[*n*]-based complexes, in which Q[*n*]s play the role of poly-dentate ligands and interact with metals through direct coordination to the portal carbonyl oxygens. These simple complexes could be applied to selective inclusion of anions, absorption of molecules, drug delivery, and so forth.

References

1. W.A. Freeman, W.L. Mock, N.-Y. Shih, J. Am. Chem. Soc. **103**, 7367 (1981)
2. J. Kim, I.S. Jung, S.Y. Kim, E. Lee, J.K. Kang, S. Sakamoto, K. Yamaguchi, K. Kim, J. Am. Chem. Soc. **122**, 540 (2000)
3. A.I. Day, A.P. Arnold, Method for synthesis cucurbiturils. WO **0068232**, 8 (2000)
4. A.I. Day, R.J. Blanch, A.P. Arnold, S. Lorenzo, G.R. Lewis, I. Dance, Angew. Chem. Int. Ed. **41**, 275 (2002)
5. X.J. Cheng, L.L. Liang, K. Chen, N.N. Ji, X. Xiao, J.X. Zhang, Y.Q. Zhang, S.F. Xue, Q.J. Zhu, X.L. Ni, Z. Tao, Angew. Chem. Int. Ed. **52**, 7252 (2013)
6. A. Flinn, G.C. Hough, J.F. Stoddart, D.J. Williams, Angew. Chem. Int. Ed. **31**, 1475 (1992)
7. D.M. Rudkevich, Angew. Chem. Int. Ed. **43**, 558 (2004)
8. H. Zhang, E.S. Paulsen, K.A. Walker, K.E. Krakowiak, D.V. Dearden, J. Am. Chem. Soc. **125**, 9284 (2003)
9. K.A. Kellersberger, J.D. Anderson, S.M. Ward, K.E. Krakowiak, D.V. Dearden, J. Am. Chem. Soc. **123**, 11316 (2001)
10. Y. Miyahara, K. Abe, T. Inazu, Angew. Chem. Int. Ed. **41**, 3020 (2002)
11. Y.-J. Zhao, S.-F. Xue, Q.-J. Zhu, Y.-Q. Zhang, Z. Tao, Z.-B. Wei, L.-S. Long, Chin. J. Inorg. Chem. **22**, 129 (2006)
12. X.L. Ni, X. Xiao, H. Cong, L.L. Liang, K. Chen, X.J. Cheng, N.N. Ji, Q.J. Zhu, S.F. Xue, Z. Tao, Chem. Soc. Rev. **42**, 9480 (2013)
13. W.J. Chen, J.P. Zeng, J.M. Yi, Y.Q. Zhang, Q.J. Zhu, S.F. Xue, Z. Tao, G. Wei, Chin. J. Inorg. Chem. **26**, 2018 (2010)
14. F.G. Zhou, L.H. Wu, X.J. Lu, Y.Q. Zhang, Q.J. Zhu, S.F. Xue, Z. Tao, J. Mol. Struct. **927**, 14 (2009)
15. X. Xiao, Y.Q. Zhang, Q.J. Zhu, S.F. Xue, Z. Tao, G. Wei, J. Mol. Struct. **969**, 216 (2010)
16. Y.Q. Zhang, J.P. Zeng, Q.J. Zhu, S.F. Xue, Z. Tao, J. Mol. Struct. **929**, 167 (2009)
17. H. Cong, C.-Z. Wang, W.X. Zhao, L.-L. Liang, X. Xiao, Y.-Q. Zhang, Z. Tao, S.-F. Xue, Q.-J. Zhu, Chin. J. Inorg. Chem. **2014** (In press)
18. J.X. Liu, L.S. Long, R.B. Huang, L.S. Zheng, Cryst. Growth Des. **6**, 2611 (2006)
19. J.X. Liu, L.S. Long, R.B. Huang, L.S. Zheng, Inorg. Chem. **46**, 10168 (2007)
20. Y.F. Hu, K. Chen, R.L. Lin, W.Q. Sun, J. Zhu, J.X. Liu, S.F. Xue, Q.J. Zhu, Z. Tao, RSC Adv. **2**, 5663 (2012)
21. J.X. Liu, Y.F. Hu, R.L. Lin, W.Q. Sun, X.H. Liu, W.R. Yao, J. Coord. Chem. **63**, 1369 (2010)
22. X.L. Ni, X. Xiao, H. Cong, Q.J. Zhu, S.F. Xue, Z. Tao, Acc. Chem. Res. **47**, 1386 (2014)
23. J.X. Hu, Y.F. Hu, X. Xiao, Y.Q. Zhang, Z. Tao, S. F. Xue, J.X. Liu, Q.J. Zhu, Eur. J. Inorg. Chem. **3632** (2013)

24. Y.F. Hu, K. Chen, J.X. Liu, R.L. Lin, W.Q. Sun, S.F. Xue, Q.J. Zhu, Z. Tao, Polyhedron **31**, 632 (2012)
25. X. Feng, H. Du, K. Chen, X. Xiao, S.X. Luo, S.F. Xue, Y.Q. Zhang, Q.J. Zhu, Z. Tao, X.Y. Zhang, W. Gang, Cryst. Growth Des. **10**, 2901 (2010)
26. Y.Q. Zhang, Q.J. Zhu, S.F. Xue, Z. Tao, Molecules **12**, 1325 (2007)
27. P. Thuéry, Inorg. Chem. **48**, 4497 (2009)
28. P. Thuéry, Cryst. Growth Des. **9**, 1208 (2009)
29. L.L. Liang, K. Chen, X. Feng, Y.Q. Zhang, Q.J. Zhu, S.F. Xue, Z. Tao, J. Mol. Struct. **1006**, 87 (2011)
30. Y.J. Ma, W.J. Chen, D.H. Yu, Y.Q. Zhang, Z. Tao, S.F. Xue, Q.J. Zhu, Chin. J. Inorg. Chem. **3**, 626 (2012)
31. W.J. Chen, D.H. Yu, Y.Q. Zhang, Q.J. Zhu, S.F. Xue, Z. Tao, G. Wei, Inorg. Chem. **50**, 6956 (2011)
32. D. Whang, J. Heo, J.H. Park, K. Kim, Angew. Chem. Int. Ed. **37**, 78 (1998)
33. Y.M. Jeon, J. Kim, D. Whang, K. Kim, J. Am. Chem. Soc. **118**, 9790 (1996)
34. R. Hoffmann, W. Knoche, C. Fenn, H.J. Buschmann, J. Chem. Soc., Faraday Trans. **90**, 1507 (1994)
35. O.A. Gerasko, J. Lipkowski, A.V. Virovets, V.P. Fedin, Russ. Chem. Bull. **52**, 585 (2003)
36. O. Danylyuk, V.P. Fedin, Cryst. Growth Des. **12**, 550 (2012)
37. D.H. Yu, X.L. Ni, Y.Q. Zhang, S.F. Xue, Q.J. Zhu, Z. Tao, J. Mol. Struct. **882**, 128 (2008)
38. Y.Q. Zhang, L.M. Zhen, D.H. Yu, Y.J. Zhao, S.F. Xue, Q.J. Zhu, Z. Tao, J. Mol. Struct. **875**, 435 (2008)
39. O.A. Gerasko, E.A. Mainicheva, M.I. Naumova, M. Neumaier, M.M. Kappes, S. Lebedkin, D. Fenske, V.P. Fedin, Inorg. Chem. **47**, 8869 (2008)
40. J.P. Zeng, S.M. Zhang, Y.Q. Zhang, Z. Tao, Q.J. Zhu, S.F. Xue, G. Wei, Crystal. Growth Des. **10**, 4509 (2010)
42. J.P. Zeng, H. Cong, K. Chen, S.F. Xue, Y.Q. Zhang, Q.J. Zhu, J.X. Liu, Z. Tao, Inorg. Chem. **50**, 6521 (2011)
42. X. Feng, Z.-F. Li, S.-F. Xue, Z. Tao, Q.-J. Zhu, Y.-Q. Zhang, J.-X. Liu, Inorg. Chem. **49**, 7638 (2010)
43. H.T. Hou, W.J. Chen, Y.Q. Zhang, Q.J. Zhu, S.F. Xue, Z. Tao, Polyhedron (In press)
44. G. Samsonenko, O.A. Gerasko, J. Lipkowski, A.V. Virovets, V.P. Fedin, Russ. Chem. Bull. **2002**, 51 (1915)
45. D.G. Samsonenko, J. Lipkowski, O.A. Gerasko, A.V. Virovets, M.N. Sokolov, V.P. Fedin, J.G. Platas, R. Hernandez-Molina, A. Mederos, Eur. J. Inorg. Chem. **2380** (2002)
46. G.L. Zhang, Z.Y. Wu, Y.T. Li, D.Q. Wang, J.M. Dou, Chin. Chem. Lett. **17**, 93 (2006)
47. E.A. Mainicheva, A.A. Tripolskaya, O.A. Gerasko, D.Y. Naumov, V.P. Fedin, Russ. Chem. Bull. **55**, 1566 (2006)
48. A.A. Tripolskaya, E.A. Mainicheva, O.A. Gerasko, D.Y. Naumov, V.P. Fedin, J. Struct. Chem. **48**, 547 (2007)
49. A.A. Tripolskaya, O.A. Gerasko, D.Y. Naumov, V.P. Fedin, J. Struct. Chem. **48**, 949 (2007)
50. R.-L. Lin, J.-X. Liu, L.-S. Long, R.-B. Huang, L.-S. Zheng, J. Incl. Phenom. Macrocycl. Chem. **62**, 263 (2008)
51. E.A. Mainicheva, O.A. Gerasko, J. Lipkowski, A.V. Virovets, V.P. Fedin, Russ. Chem. Bull. **2006**, 55 (1956)
52. O.A. Gerasko, E.A. Mainicheva, M.I. Naumova, O.P. Yurjeva, A. Antonio, C. Vicent, R. Llusar, V.P. Fedin. Eur. J. Inorg. Chem. **416**, (2008)
53. P. Thuéry, Inorg. Chem. **50**, 10558 (2011)
54. P. Thuéry, Cryst. Growth Des. **12**, 1632 (2012)
55. P. Thuéry, Cryst. Growth Des. **10**, 716 (2010)
56. P. Thuéry, Cryst. Growth Des. **8**, 4132 (2008)
57. P. Thuéry, Inorg. Chem. **48**, 825 (2009)
58. P. Thuéry, Cryst. Eng. Comm. **14**, 3363 (2012)

59. P. Thuéry, Cryst. Eng. Comm. **11**, 1150 (2009)
60. O.A. Gerasko, V. Aian. Virovets, D.G. Samsonenko, A.A. Tripolskaya, V.P. Fedin, D. Fenske, Russ. Chem. Bull. **52**, 585 (2003)
61. M.N. Sokolova, T.V. Mitkinaa, O.A. Geraskoa, V.P. Fedina, A.V. Virovetsa, R. Llusar, Z. Anorg. Allg. Chem. **629**, 2440 (2003)
62. S. Liu, A.D. Shukl, S. Gadde, B.D. Wagner, A.E. Kaifer, L. Isaacs, Angew. Chem. Int. Ed. **47**, 2657 (2008)
63. S. Liu, P.Y. Zavalij, L. Isaacs, J. Am. Chem. Soc. **127**, 16798 (2005)
64. J.X. Liu, R.L. Lin, L.S. Long, R.B. Huang, L.S. Zheng, Inorg. Chem. Comm. **1085**, 11 (2008)

Chapter 3
Coordination Polymers of Cucurbit[*n*]urils with Metal Ions

Abstract The recent work has revealed that Q[*n*]-based coordination chemistry is gradually changing from simple coordination to novel polydimensional coordination polymers of metal ions to Q[*n*]s. In particular, our recent study revealed that the coordination of Q[*n*]s with metal ions in the presence of a third species (often an anionic species or an organic molecule), that is, a structure inducer, can result in the formation of various cucurbit[*n*]uril-based polydimensional supramolecular coordination architectures and polymers. Weak noncovalent interactions derived from the "outer-surface interactions" of Q[*n*]s, such as hydrogen bonding, $\pi\cdots\pi$ stacking, and C–H$\cdots\pi$ and ion–dipole interactions, have important roles in those systems. Detailed investigations have indicated that such noncovalent interactions can be the main driving forces in the formation of Q[*n*]-based supramolecular assemblies and functional materials. For example, the pore sizes and hydrophobic cavities of these compounds that lead to unprecedented properties, and potential applications in gas absorption, polycyclic aromatic hydrocarbons (PAHs) separation, and so on.

Keywords Coordination polymers · Metal ions · Structure inducer · Hydrophobic cavities · Gas absorption · PAHs separation · Polydimensional supramolecular coordination · Supramolecular assemblies

3.1 Coordination Polymers Prepared by Simple Reaction of Cucurbit[*n*]urils with Metal Ions

Generally, interaction of Q[*n*]s with metal ions give rise to simple complexes, such as molecular bowl conformation, or molecular capsule conformation, and so on, occasionally, give rise to some coordination polymers and supramolecular assemblies. To the best of our knowledge, the only Q[5]-based linear coordination polymer was first reported by Liu and coworkers in 2006 by simply mixing

X.-L. Ni et al., *Supramolecular Assemblies of Cucurbit[*n*]urils with Metal Ions*,
SpringerBriefs in Molecular Science, DOI 10.1007/978-3-662-46629-2_3

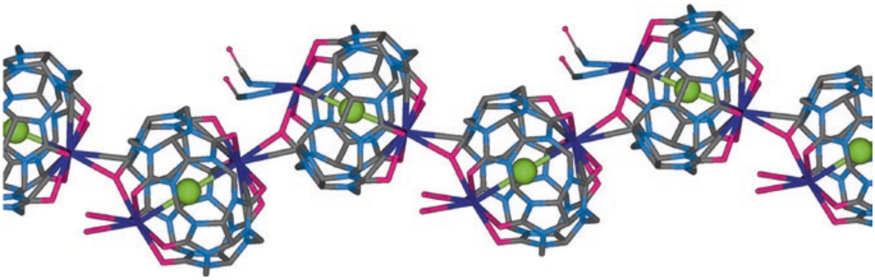

Fig. 3.1 Linear coordination polymer of Q[5]s and K^+ cations

up Q[5] and potassium chloride in 1.5 M hydrochloric acid, in which lidded Q[5] molecules link to one another through coordination of their carbonyl groups to the potassium cations in between (Fig. 3.1) [1].

Compared to Q[5]-based coordination polymer, Q[6] offered more chances to form linear coordination polymers due to the larger portals, which can attract more than one metal ion at one portal. Mock and Freeman first characterized it in 1981, although they did not give the structural details of the Q[6]/Ca^{2+} complex, and instead focused on the remarkable structure of Q[6] itself [2]. Freeman described this complex in his succeeding paper in 1984 [3]. In the Q[6]/Ca^{2+} complex, each Ca^{2+} ion is coordinated to three carbonyl O atoms; two at a portal of one cage and the third at a portal of an immediate neighboring Q[6] (Fig. 3.2a). Thus, a 1D polymer is formed through direct coordination of Q[6] molecules and Ca^{2+} cations. Materials with tubular architectures have attracted considerable interest in the areas of nanotechnology, molecular sieves, ion sensors, and fluidic transport systems [4–6]. Q[*n*]s readily coordinate with various metal ions to form 1D tubular polymers through direct coordination. The coordination of Q[6] with alkali metal ions could result in common 1D coordination polymers in which every two Q[6] molecules are linked by two alkali metal ions, and the two metal ions may be bridged by sharing water molecules or not bridged (Fig. 3.2b–d) [7–9]. In particular, the Q[6]/Rb^+ coordination polymer chains are arranged to form a honeycomb structure with large linear hexagonal channels running parallel to the polymer chains (Fig. 3.2e, f).

When we summarized the simple coordination complexes of Q[6]s with metal ions, we mentioned that the interaction of Q[6]s with transition metal salts formed mainly adducts of Q[6] with metal aqua complexes [10]. It is even more rare to observe the coordination polymers based on Q[6]s with transition metal ions. An interesting exception was demonstrated by Liu and coworkers in 2009. They chose the copper(II) ion, nitrate, and the weak-field ligand, chloride, to construct transition metal cucurbituril-based coordination tubes. They obtained a 1D zigzag coordination polymer $\{[Cu(H_2O)_4Q[6]] \cdot (NO_3)_2 \cdot 8H_2O\}_n$, and the tubular coordination polymer $\{[Cu(H_2O)_2Cl_2Q[6]]\ 1/3 \cdot (H_2O)_3\}_n$, and demonstrated a means of enhancing the coordination ability of the terminal carbonyl group of cucurbituril under the direction of coordination chemistry [11]. The zigzag 1D

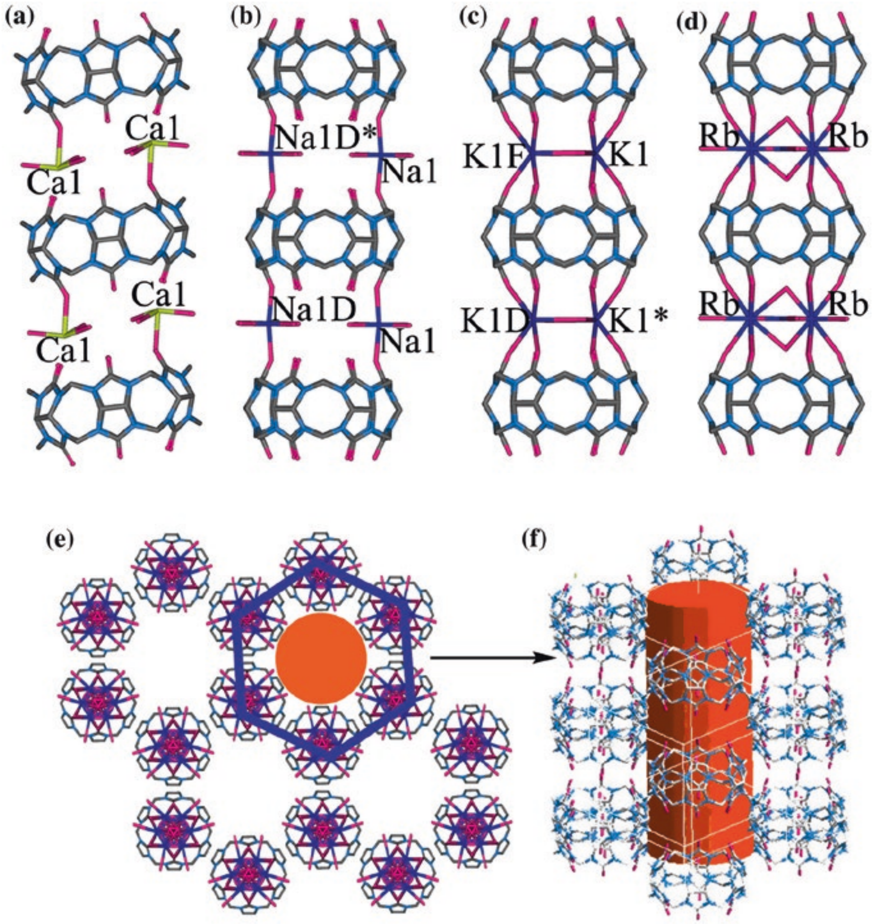

Fig. 3.2 X-ray crystal structures of a 1D polymer formed through direct coordination of Q[6] molecules. **a** Ca^{2+} cations; **b** Na^{+} cations; **c** K^{+} cations; **d** Rb^{+} cations; **e** honeycomb-like arrangement of the Q[6]/Rb^{+} coordination polymers and **f** a large hexagonal channel with a mean diameter of about 10 Å constructed from the Q[6]/Rb^{+} coordination polymers. Rb^{+} cations are omitted for clarity in Fig. 3.2e, f

coordination polymer was formed through coordination of each copper(II) ion with two terminal carbonyl groups from two adjacent cucurbiturils (Fig. 3.3a, b). The assembly of a cucurbituril-based coordination polymer occurs through interactions with the weak-field ligand, Cl^{-}. The tubular structure is formed from three copper(II) ions linked to six carbonyl groups from two adjacent cucurbiturils, three of which derive from one cucurbituril unit and the remaining alternating groups from the adjacent one (Fig. 3.3c, d).

Under hydrothermal conditions (at 120 °C) $Nd(NO_3)_3$ reacts with Q[6] in water to yield Polymeric $[\{Nd(NO_3)(H_2O)_4\}_2(NO_3@Q[6])][Nd(NO_3)_6]_n$. Its structure

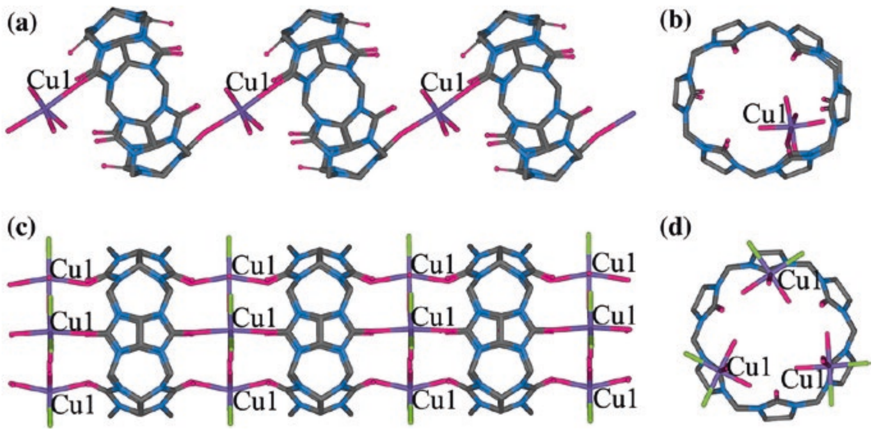

Fig. 3.3 X-ray crystal structures of a 1D polymer through direct coordination of [6] molecules and Cu^{2+} cations in the presence of NO_3^- anions **a** side view and **b** top view; Cu^{2+} cations in the presence of Cl^- anions **c** side view, and **d** top view

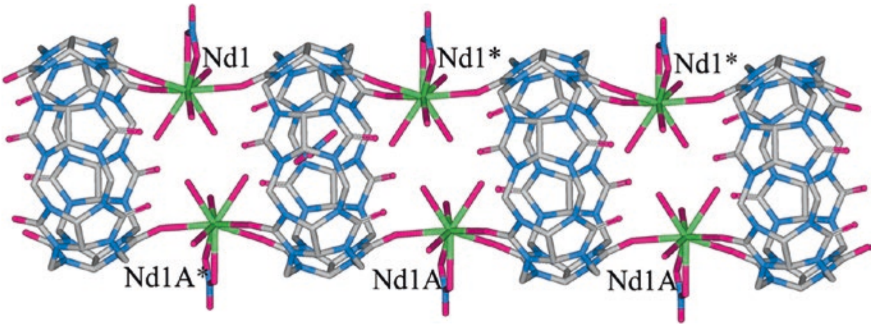

Fig. 3.4 X-ray crystal structures of the $[\{Nd(NO_3)(H_2O)_4\}_2(NO_3@Q[6])][Nd(NO_3)_6]_n$ coordination polymer

shows pseudohexagonal packing of polymeric chains that consist of Q[6] molecules linked via pairs of neodymium cations bound to portal carbonyl groups (see Fig. 3.4) [12]. In this arrangement, each Q[6] molecule is thus coordinated to four Nd^{3+} ions, with each Nd^{3+} bound to two Q[6] molecules (by one carbonyl group from one Q[6] molecule and two carbonyl groups from the adjacent Q[6] molecule). Each Nd^{3+} site also binds to four water molecules and a bidentate nitrate anion so that each metal center is again nine-coordinate. $[Nd(NO_3)^6]^{3-}$ counter ions are located between the polymeric $[\{Nd(NO_3)(H_2O)_4\}_2(NO_3@Q[6])]^{3+}$ chains.

3.2 Induced Coordination Polymers of Cucurbit[5]urils with Metal Ions

As mentioned already, there has been a trend toward the use of third species as structure directing agents in Q[*n*]–metal systems, and the driving forces could be the so-called outer surface interactions of Q[*n*]s [13]. These species produce Q[*n*]-based supramolecular assemblies whose properties, structural novelties, and functionalities exceed those of assemblies obtained in the absence of such agents. For example, the coordination behavior of the light lanthanides can sometimes show a marked difference to that of the heavier lanthanides. This was clearly demonstrated in a study by Thuéry [14] who attempted to prepare a similar K^+/Ln^{3+} complex of the “heavy” lanthanide ion, Yb^{3+}, by employing a corresponding Yb^{3+}/K^+-Q[5] perrhenic acid reaction mixture that is used to prepare the heterometallic Ln^{3+}/K^+-Q[5] complexes of Ce^{3+}, Sm^{3+}, Gd^{3+} (represented schematically by Fig. 2.11). Instead, in this case the procedure resulted in the formation of a colorless crystalline product whose X-ray structure showed it to be a 1D coordination polymer of type $\{[Yb(Q[5])(H_2O)_4](ReO_4)_3 \cdot H_2O\}_n$. Unexpectedly, K^+ does not coordinate, while Yb^{3+} ions bind simultaneously to adjacent Q[5] portals so that $\cdots Yb^{3+}$-Q[5]-Yb^{3+}-Q[5]-Yb^{3+}-$\cdots$ metallo-supramolecular chains are generated (Fig. 3.5); once again the $[ReO_4]^-$ counter ions occupy positions between the chains. In discussing his results, Thuéry pointed out that both the presence of K^+ and perrhenic acid in the reaction medium are important for the successful isolation of both the heteronuclear Ln^{3+}/K^+-Q[5] complexes and the homonuclear polymeric Yb^{3+}-Q[5] complex [14].

Although we have not observed linear coordination polymers by simply mixing the unsubstituted Q[5] with alkali or alkaline earth metal salts other than potassium salts, we obtained such supramolecular polymers constructed from SQ[5]s with other metal ions by simply mixing the two species. For example, the reaction of $CyH_5Q[5]$ with NaCl can give a 1D coordination polymer (Fig. 3.6a) [15]. Close inspection reveals that Na1 and Na2 also fully cover the two portals of a $CyH_5Q[5]$ molecule, resulting in the formation of typical molecular capsules. These capsules are linked by the third sodium cations (Na3) through direct coordination with two neighboring $CyH_5Q[5]$ molecules, and form the 1D

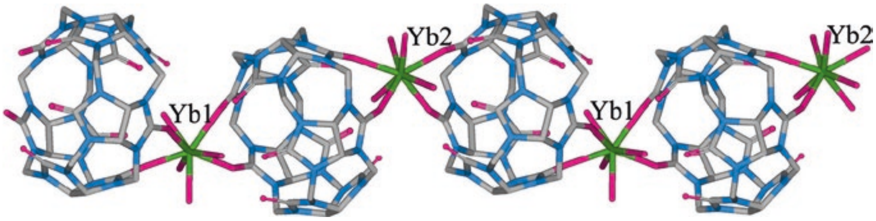

Fig. 3.5 X-ray crystal structure of the Yb^{3+}-Q[5] 1D coordination chain polymer present in $\{[Yb(Q[5])(H_2O)_4](ReO_4)_3 \cdot H_2O\}_n$

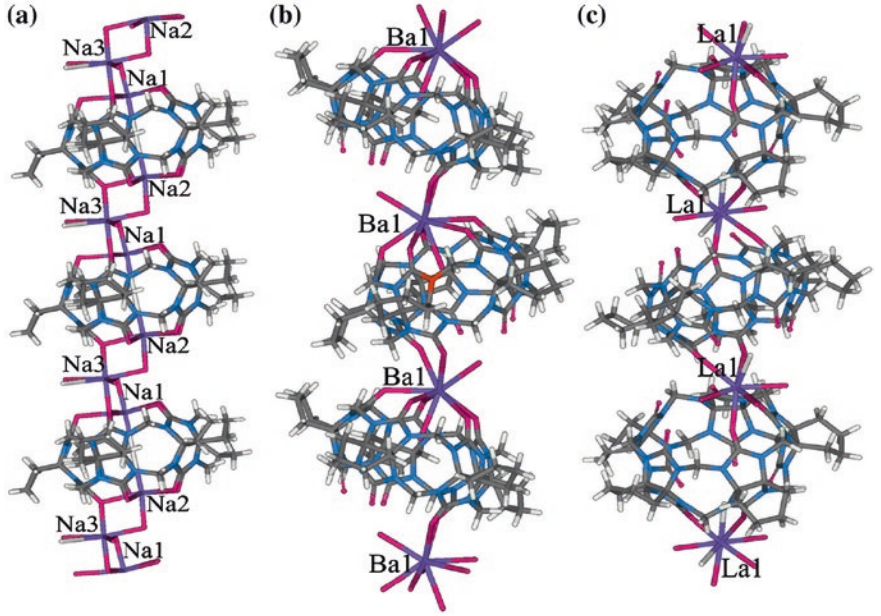

Fig. 3.6 X-ray crystal structures of 1D coordination polymers consisting of **a** $CyH_5Q[5]/Na^+$; **b** $CyH_5Q[5]/Ba^{2+}$; and **c** $CyH_5Q[5]/La^{3+}$

coordination polymer [15]. In contrast, Ba^{2+} fully covers a portal of $CyH_5Q[5]$ in the $CyH_5Q[5]/Ba^{2+}$-based 1D coordination polymer, and coordinates to two portal carbonyl oxygens of the neighboring $CyH_5Q[5]$ molecule. This coordination results in the formation of an 1D polymer constructed from alternating $CyH_5Q[5]$ molecules and Ba^{2+} cations (Fig. 3.6b) [16]. Although the atomic radii of lanthanides are generally shorter than those of the alkali or alkaline earth cations, 1D coordination polymers from alternating $CyH_5Q[5]$ molecules, and La^{3+} cations (Fig. 3.6c) may be observed. No portal of the $CyH_5Q[5]$ molecule is fully covered with La^{3+}, but it offers two portal carbonyl oxygens to coordinate with La^{3+} [17].

Why do the alkyl-substituted SQ[5]s show such different coordination and supramolecular assemblies from the unsubstituted Q[5]? A comparison of electrostatic potential surface calculations based on density functional theory (B3LYP/3-21G* basis set) for three typical Q[5]s—Q[5], $Me_{10}Q[5]$, and $CyP_5Q[5]$ (Fig. 3.7) shows that the mapped on electron density isosurfaces (0.001 e/au^3) for the portal carbonyl oxygens on the three Q[5]s are different, the alkyl-substituted SQ[5]s are generally more negatively charged as a consequence of the electron donating effect of the alkyl substituents, we call them as self-structure directing agents, resulting in more affinity for metal ions, and form novel coordination polymers and supramolecular assemblies [18–20]. The alkyl-substituted SQ[5]s can not only form 1D coordination polymers and supramolecular assemblies as shown in Fig. 3.6, but can also be linked directly by metal ions to create supramolecular

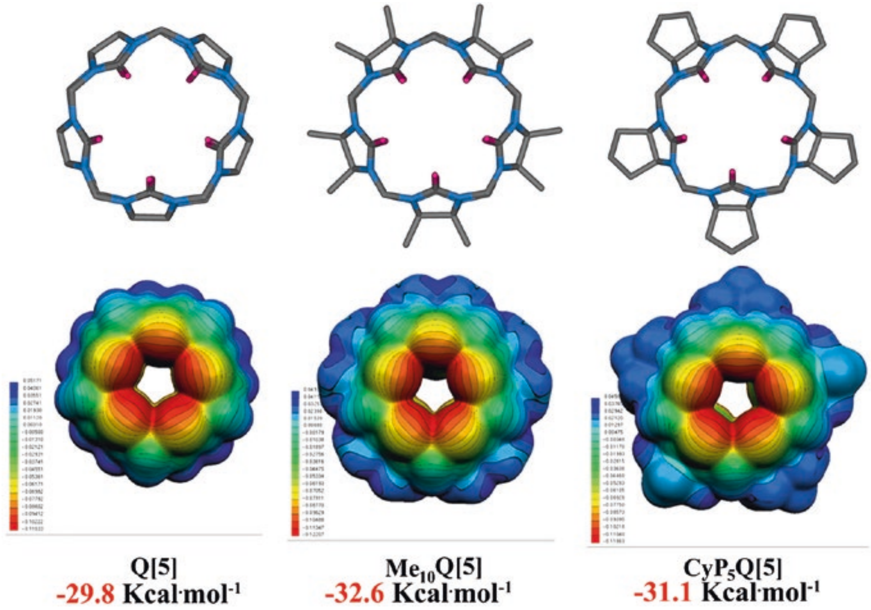

Fig. 3.7 Electrostatic potential maps (ESPs) for Q[5], $Me_{10}Q[5]$, and $CyP_5Q[5]$, respectively. ESPs are mapped on electron density isosurfaces (0.001 e/au^3) for cucurbit[*n*]urils at the B3LYP/6-311G (d, p) level of theory with Gaussian09

rings (Scheme 3.1a), which may further fuse into 2D networks (Scheme 3.1b). The first SQ[5]-based supramolecular ring was constructed from α,α′-dimethylcucurbit[5]uril (DMeQ[5] though direct coordination of metal ions to the carbonyl oxygen of the substituted glycoluril moieties of DMeQ[5] [18]. Further studies have revealed that it is a common feature of the alkyl-substituted SQ[5]s to coordinate directly with metal ions and to form a SQ[5]-based supramolecular ring which can fuse into various SQ[5]-based metal-organic networks (Fig. 3.8) [18]. In all of these cases, a common structural motif, i.e., a trigonal-planar branch, can be observed. Each branch contains 12 metal ions (the metal ion is K^+) coordinated in a similar way and three SQ[5] moieties; each K^+ ion not only coordinates to the portal carbonyl oxygens of an SQ[5], but also directly coordinates to one of the carbonyl oxygens of the neighboring SQ[5]. The branches can fuse into six-membered "bracelets," and these can further fuse into 2D networks (Scheme 3.1b and Fig. 3.8).

X-ray crystal structures show that these SQ[5]/K^+-based networks are assembled from trigonal-planar branches in which each of three SQ[5] "beads" is linked by K^+ ions, as shown in Fig. 3.8. Six-membered rings with different geometric patterns can be identified in the corresponding 2D SQ[5]/K^+-based networks. These patterns include trigonal (Fig. 3.8d, q), hexagonal (Fig. 3.8c), and quadrilateral patterns (Fig. 3.8h, u). At first glance, all five trigonal-planar branches of the respective compounds are structurally similar. In reality, however, they have many

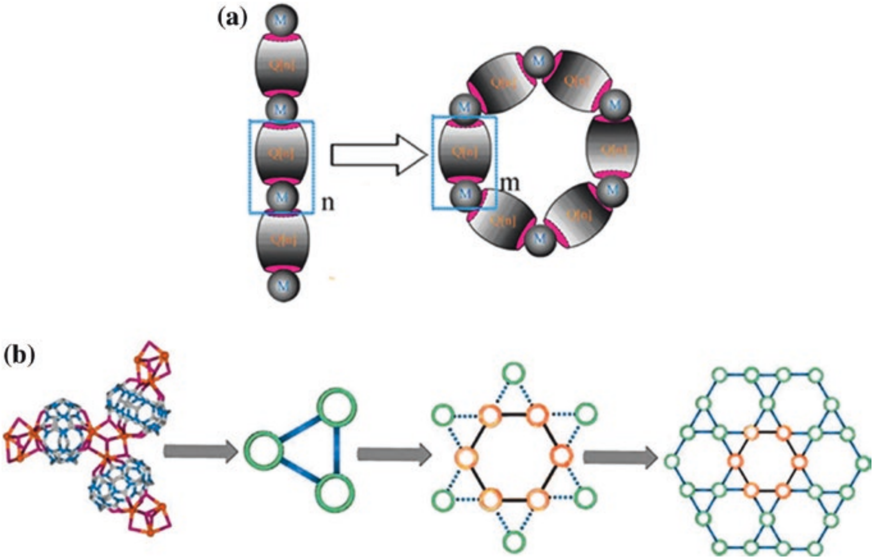

Scheme 3.1 Assembly of 1D (**a**) and 2D (**b**) catenated frameworks based on metal-ion-linked cucurbiturils

differences that lead to the formation of different six-membered rings with different geometric patterns. These differences could in turn affect the structural conformation of the formed 2D networks and the superimposition of the networks in the corresponding compounds. We closely inspect the trigonal-planar branch constructed from three DMeQ[5] moieties (Figs. 3.8b and 3.9). Both portals of each DMeQ[5] molecule in the branch are fully covered by potassium cations through direct coordination. Moreover, each capping K^+ ion is coordinated to a portal carbonyl oxygen of a neighboring DMeQ[5] in the trigonal-planar branch. Thus, three capping potassium cations form a junction link of three DMeQ[5] molecules and lead to the formation of the trigonal-planar branch. At the respective portals of the DMeQ[5] molecule, one can see four junctions of three capping K^+, which reside in the same chemical environment. In other words, the four junctions of three capping K^+ are identical. The two adjacent DMeQ[5] portals are mutually offset in the trigonal-planar branch, at offset angles of 61.79°, 62.13°, and 59.03°, as shown in Fig. 3.9. There are four identical junctions linked by three K^+ ions (K1, K2, and K3) in the trigonal-planar branch. The dihedral angles between the junction plane and the center junction plane are 6.75° for $\angle$S0S1, 32.12° for $\angle$S0S2, and 32.12° for $\angle$S0S3. The two junction planes S2 and S3 are clearly parallel in the trigonal-planar branch, with a gap ($d_{S2\text{–}S3}$) of 5.534 Å. The dihedral angle seems to be an important parameter that could indicate the construction of 2D networks or 3D frameworks through SQ[5]/M^{n+} coordination [19].

Much attention in supramolecular chemistry has been focused on the design and synthesis of interlocked molecules, such as rotaxanes, catenanes, and molecular

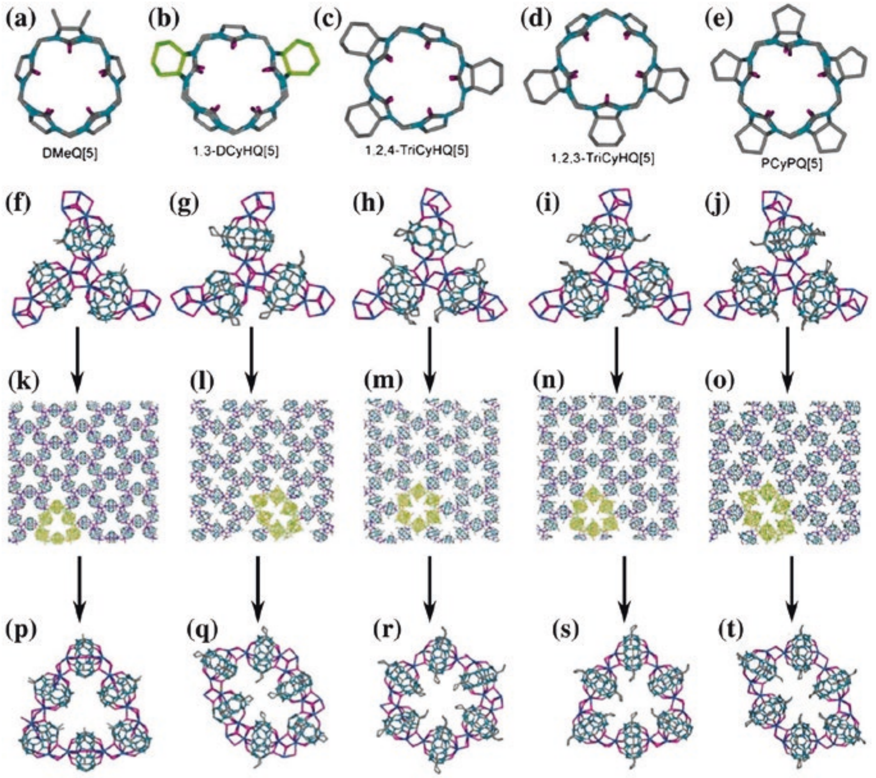

Fig. 3.8 *First row* the structures of the five related SQ[5]s (top view). *Second row* the corresponding trigonal-planar branches constructed from SQ[5]s and K^+ ions. *Third row* 2D networks based on coordination of alkyl-substituted Q[5]s and potassium cations. *Fourth row* the six-membered "bracelets" isolated from the corresponding networks

knots [21–24]. Apart from being esthetically attractive, theses molecules offer the potential for nanoscale applications in molecular devices and new materials [22]. Pioneering work by Kim and coworkers was undertaken utilizing long-chain guests ending with active moieties. They accomplished this by first threading Q[6] to form rotaxanes through the coordination of transition metal ions, and then using catenanes, and molecular necklaces. These achievements have been reviewed by Kim and others [25]. This field has since been extended to include Q[8]. The intrinsic ability of Q[8] to encapsulate two guest molecules, i.e., a pair of electron-rich and electron-deficient guest molecules, has been utilized to form a "molecular necklace" through host-stabilized intermolecular CT complexes (Scheme 3.2) [26]. These novel architectures prompted us to exploit the strategy of changing the Q[n]-based 1D polymer to polydimensional architectures through the direct coordination of Q[n]s with metal ions. The coordination between two adjacent portals and metal ions was anticipated to lead to the formation of a string of Q[5]s. In addition,

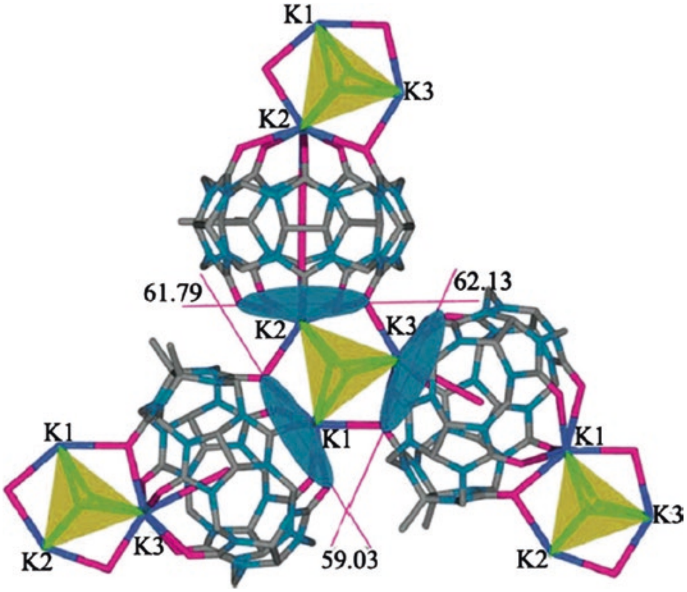

Fig. 3.9 The structural characteristics of the trigonal-planar branch constructed from DMeQ[5] molecules and K^+ ions

the interplay between alkyl substituents of neighboring Q[5]s was expected to lead to novel solid-state structures or metal-organic frameworks (MOFs) with unusual structures, including bracelet motif structures (Scheme 3.3) [20].

Our recent work revealed that SQ[5]s generally coordinate directly with metal ions to form various SQ[5]-based MOFs with unusual structures. In such cases, a common structural motif, the trigonal-planar branching unit, is observed (Fig. 3.9). As mentioned, the dihedral angles between the junction plane and the center junction plane could indicate the construction of 2D networks or 3D frameworks through SQ[5]/M^{n+} direct coordination [18–20]. When the dihedrals between any two K^+-based junction planes have the same angle of 70.53° in the trigonal-planar branch, the trigonal-planar branches fuse into 10-membered SQ[5] bracelets, but the six-membered SQ[5]s can further fuse into 2D network coordination polymers, and which then fuse into 3D frameworks. Remarkably, two identical but independent 3D infinite frameworks are generated, which are mechanically linked through catenation. The resulting 3D frameworks are therefore composed of catenated, multifused 10-membered bracelets incorporating potassium ions that link adjacent SQ[5] units through simultaneous coordination to their portal oxygens. Figure 3.10a–c shows three alkyl-substituted Q[5]s and their supramolecular assemblies through direct coordination with potassium cations.

We closely inspect the trigonal-planar branch constructed from three 1,2,4-HMeQ[5] molecules (Fig. 3.10d). Two different K^+ ions (K1 and K2), located at

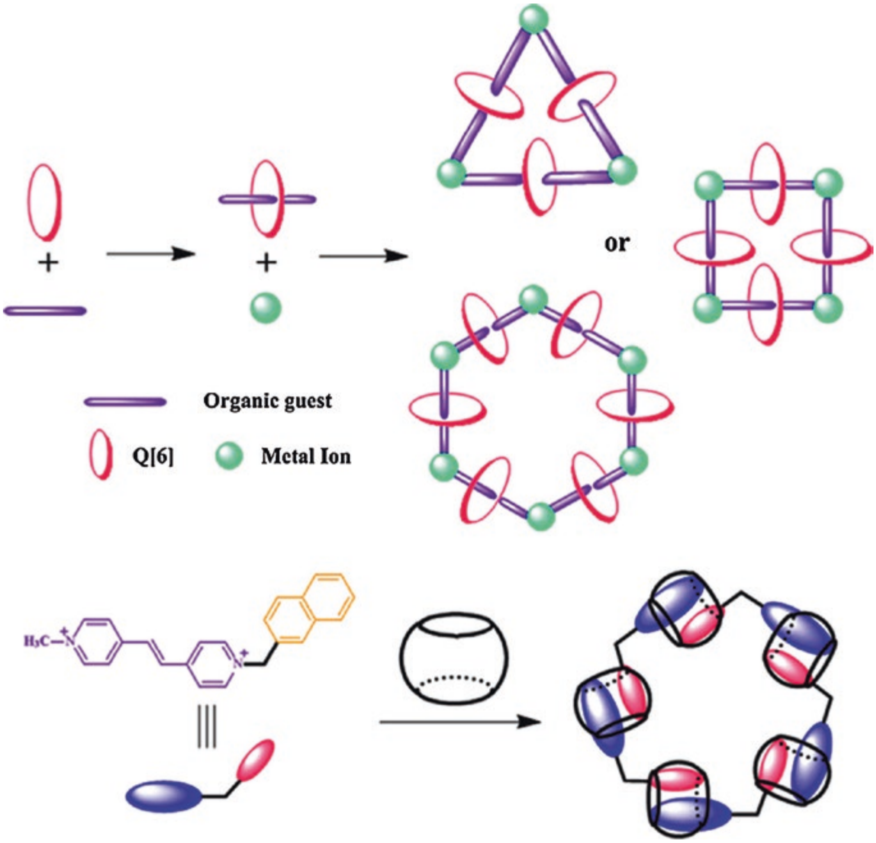

Scheme 3.2 Representation of supramolecular assemblies of Q[6] and Q[8] with metal ions and guests

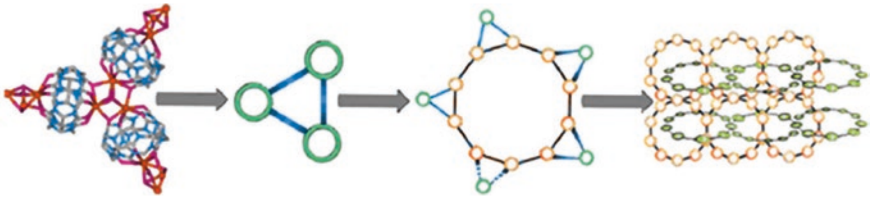

Scheme 3.3 Assembly of 3D catenated frameworks based on trigonal-planar branching units composed of metal-ion-linked SQ[5]s

alternate ends of each 1,2,4-HMeQ[5] molecule, are present in the structure. Each K2 center is directly coordinated to five portal carbonyl oxygens of one 1,2,4-HMeQ[5] molecule, while being bound to one (bridging) portal carbonyl oxygen from an adjacent 1,2,4-HMeQ[5] unit. This coordination pattern is reproduced in a

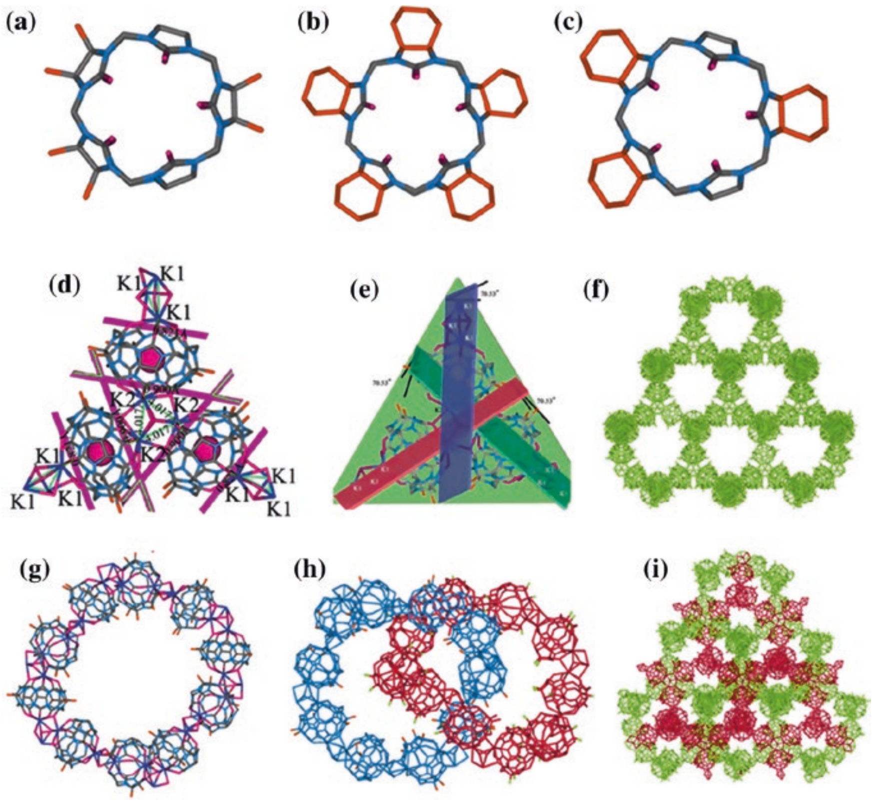

Fig. 3.10 **a–c** The structures of the related three SQ[5]s (top view) used for the preparation of 3D frameworks; **d** the trigonal-planar branches constructed from 1,2,4-HMeQ[5]s and K^+ ions; **e** schematic illustrating the identical dihedrals (70.53°) between any two K1 junction planes in the trigonal-planar branch; **f** part of a single 3D framework incorporating multifused 10-membered 1,2,4-HMeQ[5] bracelets; **g** a single 10-membered 1,2,4-HMeQ[5] "bracelet"; **h** catenation of two 10-membered 1,2,4-HMeQ[5] bracelets; **i** part of the overall structure showing the two multi-catenated 3D frameworks, each composed of multifused 10-membered 1,2,4-HMeQ[5] bracelets

triangular manner such that the edges of three portals are drawn close together to form the trigonal-planar branch, which also incorporates two symmetrically positioned water oxygens. A similar (but not identical) arrangement occurs with the K1 end of each 1,2,4-HMeQ[5] molecule. The offset angles of the adjacent portals in both trigonal-planar branches are all 62.37°, with the distances of K1 and K2 from the corresponding 1,2,4-HMeQ[5] portal coordination planes varying slightly by 0.821 and 0.900 Å, respectively. The two nonequivalent "junctions" are thus constructed around three K1 and three K2 cations in the trigonal-planar branches. The K^+ ions in each K1 junction, as well as in each K2 junction, are positioned at the vertices of an equilateral triangle, as shown in Fig. 3.10d. The separation between K1 cations is 4.135 Å, whereas that between K2 cations is 4.017 Å. The dihedral angles between each K1 junction plane (the plane through the three K1 atoms defining the triangle) and the corresponding adjacent K2 junction plane are identical (70.53°); in addition, the dihedrals between any two K1 junction planes are the same (70.53°) in the trigonal-planar branch (Fig. 3.10e). The constancy of these angles is important for the generation of the observed 3D, 10-membered bracelet frameworks. Figure 3.10f shows part of the 3D framework, illustrating the fused trigonal-planar branches in relation to the unit cell axes. Each of the catenated 3D frameworks is thus constructed from multifused, 10-membered 1,2,4-HMeQ[5] bracelets. Figure 3.10g shows an isolated 10-membered 1,2,4-HMeQ[5] bracelet consisting of a string of 1,2,4-HMeQ[5] "beads" linked by direct coordination to potassium ions. The size of the bracelet is partly dictated by the size of each 1,2,4-HMeQ[5] bead, which has a diameter of ~12 Å (taking into account the presence of the methyl substituents). The 10-membered bracelets have an average diameter of around 19 Å, which is more than enough to fit a 1,2,4-HMeQ[5] unit in the cavity when forming the catenated structure. Figure 3.10h shows two equivalent catenated (noncovalently linked) 10-membered bracelets, while Fig. 3.10i shows part of the two multicatenated 3D frameworks, each composed of multifused 10-membered 1,2,4-HMeQ[5] bracelets (the unit cell axes are also shown).

As mentioned previously, there has been a trend toward the use of a third species as structure inducer in Q[*n*]–metal systems. These species could result novel Q[*n*]-based supramolecular coordination polymers and assemblies with unusual properties, structural features. In that case, the positive outer surface of Q[*n*]s may also play an important role in such supramolecular architectures (Scheme 1.2). For instance, we have not seen polydimensional coordination polymers of Q[5] with metal ions other than potassium cation in the absence of a third species, such as an aromatic organic molecule or polychloridematollate anions as structure directing agents. However, in the presence of *p*-hydroxybenzoic acid (Hyb), Q[5] behaves as a tetradentate ligand and coordinates with two Ca^{2+} cations on both portals, resulting in the formation of a 1D helical coordination polymer. The Hyb molecules surround the helical polymer and form a Hyb-based helix (Fig. 3.11a) [27]. Similar 1D coordination polymers have been assembled from Q[5] and various lanthanide ions (Ln^{3+}) in the presence of Hyq as an organic structure inducer. It should be noted that the coordination of Q[5] with light lanthanide cations leads to the formation of zigzag 1D coordination polymers (Fig. 3.11b) and the coordination of heavy lanthanide cations to Q[5] leads to the formation of homochiral 1D helical coordination polymers (Fig. 3.11c) [28]. Furthermore, the Hyq molecules are distributed around the 1D coordination polymers. In these cases, the radii of the related cations are around 1 Å; generally, such cations cannot fully cover both portals of Q[5]. In order to effectively coordinate to the portals of Q[5] molecules, these metal ions prefer to coordinate to two carbonyl oxygens for each portal of Q[5] molecules, resulting in the formation of the alternating arrangements of metal ions and Q[5] molecules. Figure 3.11d shows a $CyH_5Q[5]/K^+$-based 1D coordination polymer assembled in the presence of an inorganic species, $[ZnCl_3H_2O]^-$. Both portals of each $CyH_5Q[5]$ molecule in the polymer are fully covered by a potassium cation, which further coordinates to a carbonyl oxygen

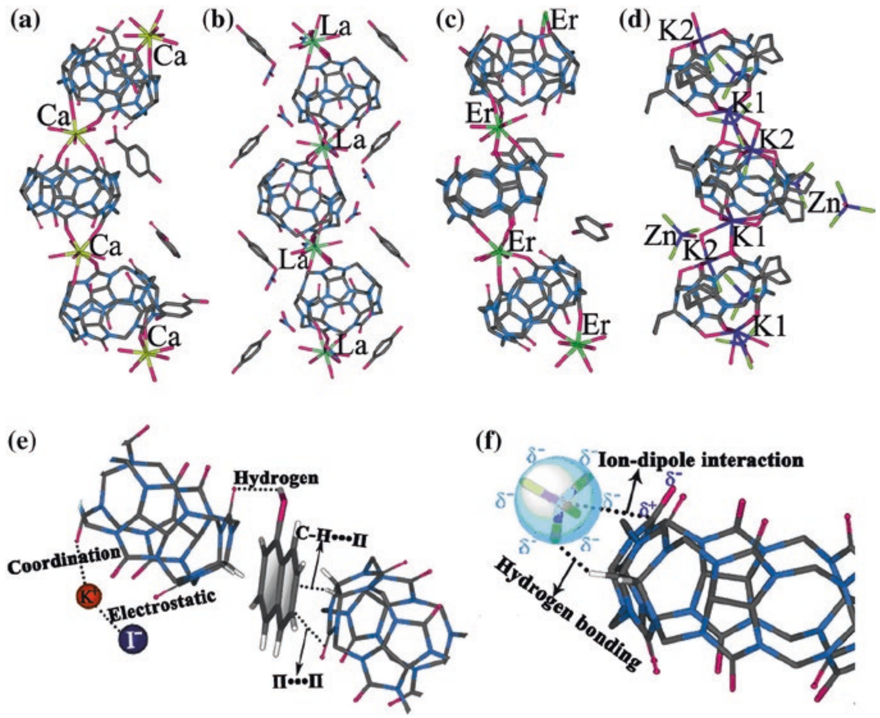

Fig. 3.11 X-ray crystal structure of 1D polymers based on the coordination of **a** unsubstituted Q[5]/Ca^{2+} in the presence of Hyb; **b** $CyH_5Q[5]/Na^+$; **c** $CyH_5Q[5]/Ba^{2+}$ in the presence of Hyq; **d** $CyH_5Q[5]/La^{3+}$ in the presence of $[ZnCl_3H_2O]^-$ anions. The possible interactions between; **e** Q[*n*] molecules and aromatic organic molecules; and **f** Q[*n*] molecules and $[M_{trans}Cl_x]^{n-}$ anions

of the neighboring $CyH_5Q[5]$ molecule. Moreover, the $[ZnCl_3H_2O]^-$ anions are distributed around the $CyH_5Q[5]/K^+$-based 1D coordination polymer [29, 30].

Figure 3.11 shows several typical cases of 1D coordination polymers constructed from Q[5]s and metal ions in the presence of organic molecules or inorganic molecules, which behave as structure inducers. Generally, these molecules closely accompany the polymers. Therefore, interactions between inducers with components in the polymers, such as Q[*n*]s and metal ions, could be important driving forces leading to the formation of Q[*n*]-based supramolecular polymers. Chen and Yamauchi explored the chemical behavior of the convex outer walls of Q[*n*], and found that the convex glycoluril backbones of Q[*n*] displayed a much higher affinity to aromatic rings. Their analysis of the stacking of Q[5] and organic molecules revealed that the aromatic molecules are always arranged between two Q[5] molecules. Moreover, the aromatic plane of the organic molecules is roughly parallel to one of the five-membered rings of glycoluril in the adjacent Q[5]s. This parallel orientation appears to reflect the presence of π–π stacking and C–H$\cdots\pi$ interactions. Therefore, the formation of such coordination polymers could be ascribed to these weak intermolecular interactions (Fig. 3.11e) [31–33]. On the other hand, recent works show that numerous supramolecular polymers are accompanied by polychloride anion complexes ($[MCl_x]^{n-}$) which are formed in HCl solution or in a medium with excess chloride anions. These $[MCl_x]^{n-}$ anions seem to play the role of structure inducers. The driving force behind the formation is the interaction between chloride anions and methenyl or methylene on the back of the Q[*n*] molecules, as well as the ion–dipole interaction between the $[M_{trans}Cl_x]^{n-}$ anion and the carbonyl carbon atom of Q[*n*] molecules (Fig. 3.11f) [34, 35].

The alkyl-substituted Q[5]s present the characteristics of direct coordination with metal ions and spontaneous formation of polydimensional coordination polymers. These characteristics indicate a likely increased electron density as a consequence of the electron donating effect of the alkyl substituents. Many attempts to synthesize similar polydimensional coordination polymers by using Q[5] under the similar synthetic conditions have failed. However, when we introduced Hyb into the Q[5]–KI system, a template or structure inducer, we obtained a stable 2D network-like coordination polymer with accessible channels [36]. The solid-state structure was found to have channels similar to those derived from the aforementioned alkyl-substituted Q[5]s and Sr^{2+}or K^+ [17]. The channels are created by Q[5] “beaded” six-membered rings [36], which are stacked upon one another to form channels (Fig. 3.12b, c). The six-membered rings are joined together to form a netting layer (Fig. 3.12b) through the trigonal-planar branches (Fig. 3.12a). Each of the branches is constructed from three Q[5]molecular “beads” whose portals are bound to three K^+ ions (Fig. 3.12a). The trigonal branches link a layer of molecular netting with hexagonal holes, and each netting layer is stacked upon the next layer below it (Fig. 3.12c, d).

In the above trigonal-planar branch, the radii of the metal ions are generally larger than 1 Å, and the portals of the Q[5]s are generally fully covered by metal ions such as K^+, Sr^{2+}, and so forth. Recent research revealed that in the presence of inorganic structure inducers, such as some transition metal salts, a series of Q[5]–$Ln(NO_3)_3$ systems could yield novel 2D-network coordination polymers. For example, X-ray structural analysis has shown the Q[5]/Sm^{3+} pair (Fig. 3.13a) [30]. The pairs are not discrete, but they are essential building blocks for constructing the Q[5]/Sm^{3+} pair-based 2D-network coordination polymer (Fig. 3.13b). In the Q[5] pair, two Q[5] molecules are linked by a $[Sm_2(H_2O)_4]^{3+}$ cation through direct coordination of the Sm2 cation to two portal carbonyl oxygens of the Q[5]s (O6, O7, and O11, O12). The other portal of the two Q[5] molecules in the pair is fully capped by Sm1 and Sm3 cations. Moreover, Sm1 and Sm3 also coordinate to the neighboring portal oxygens (O14 or O9, respectively). This additional coordination leads to the formation of the novel network constructed from the Q[5] pair (Fig. 3.13b, c). Although the inorganic salt $CuCl_2$ acts as a supramolecular assembly inducer in this case, Cu^{2+} cations do not appear in the crystal structure of the Q[5]/Sm^{3+} complexes. The Sm–Q[5] porous material could have similar or even better absorption properties compared with the KI–Q[5]–Hyb hexagonal netting sheets.

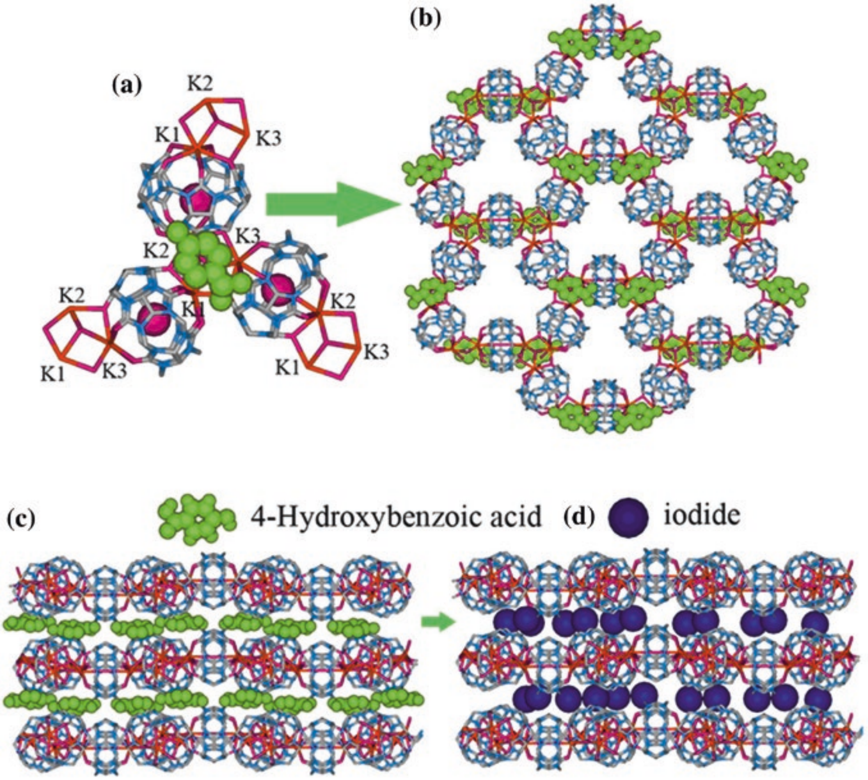

Fig. 3.12 X-ray crystal structures of **a** the trigonal-planar branch of three Q[5] coordinated to potassium ions (*yellow*); **b** the six-membered Q[5] "beaded" rings in a single layer with molecules of Hyb (*green*) centered over each junction. H_2O in the channels is omitted for clarity; **c** a view of the template molecules, Hyb (*green*), between the layers; **d** the location of the I^- ions between the netting layers of Q[5] "beaded" ring. Adapted from Ref. [36] with permission from The Royal Society of Chemistry

More recently, we demonstrated the coordination of neodymium (Nd^{3+}) cations with cucurbit[5]uril (Q[5]) and corresponding supramolecular assemblies in the presence of tetrachlorozincate $[ZnCl_4]^{2-}$ anion [37]. The $[ZnCl_4]^{2-}$ anions gave rise to a "honeycomb effect" that resulted in the formation of Nd^{3+}/Q[5]-based linear coordination polymers and 2D networks. X-ray crystallographic analysis of this compound showed a 2D network (Fig. 3.14a). Close inspection revealed that each Q[5] coordinate with three Nd^{3+} cations (Nd1, Nd3 at one portal, whereas Nd2 at other portal of the Q[5] molecule), each Nd1 or Nd2 coordinates to two neighboring Q[5] molecules with similar manner: fully cover on a portal of Q[5] molecule, and one coordination with one portal carbonyl oxygen of neighboring Q[5] molecules, resulting in the formation of 1D coordination polymers. In addition, the coordinated Nd3 cations coordinate to neighboring Q[5] molecules belonging to adjacent Nd/Q[5]-based linear coordination polymers, thus resulting

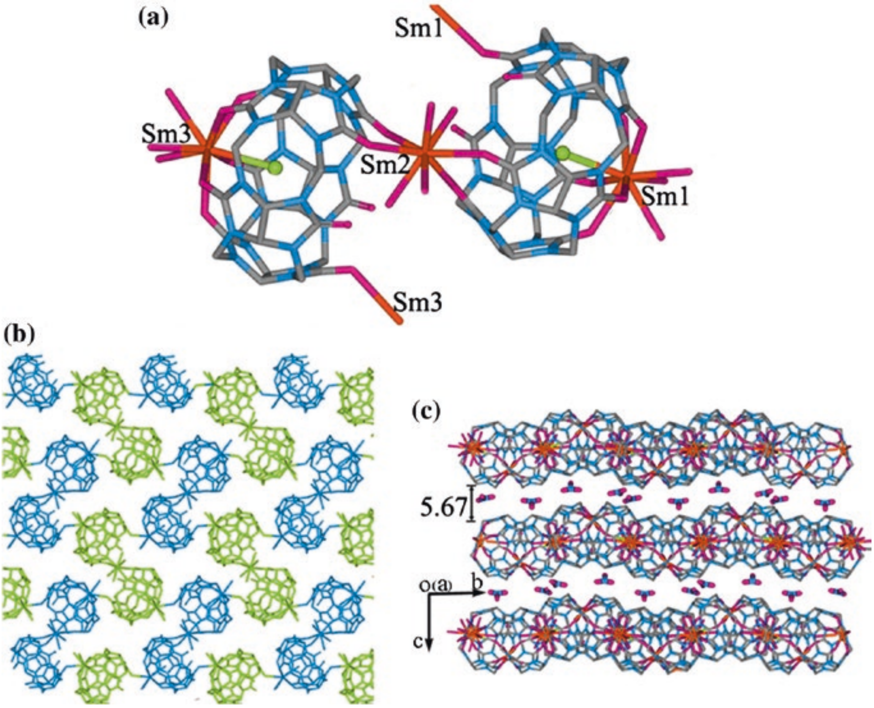

Fig. 3.13 X-ray crystal structure of **a** samarium cation/cucurbit[5]uril pair linked by a $[Sm(H_2O)_4]^{3+}$ cation through direct coordination; **b** the network constructed of the Q[5] pairs; **c** stacking of the networks filled with nitrate anions

in the formation of a 2D network. Figure 3.14b shows the detailed coordination of Q[5] with Nd^{3+} cations. On the other hand, the $[ZnCl_4]^{2-}$ anions, formed from Zn^{2+} cations in HCl solution, are found in association with a distorted honeycomb-like framework (Fig. 3.14c) in which the Nd/Q[5]-based linear coordination polymers are filled in the cells (Fig. 3.14d, e). Electrostatic interactions between the Nd^{3+}/Q[5] complex cations and the surrounded $[ZnCl_4]^{2-}$ anions could be driving forces resulting in the formation of the Nd^{3+}/Q[5]-based supramolecular assembly.

In recent years, our lab investigated the coordination of metal ions to perhyd roxycucurbit[*n*]urils $\{(HO)_{2n}Q[n]s\}$, which can offer not only portal carbonyl oxygens but also the equatorial hydroxyl groups (another kind of self-structure directing agent) as binding sites to metal ions to assemble polydimensional coordination polymers (Fig. 3.15, left). For examples, two novel 2D coordination polymers were obtained by reactions of alkali metal (K^+ and Cs^+) salts with perhydroxycucurbit[5]uril, $\{(HO)_{10}Q[5]\}$, and their structures were determined by single-crystal X-ray diffraction studies [38]. Structure analysis revealed that the $(HO)_{10}Q[5]$ ligands are interlinked into 2D networks through coordination of their carbonyl groups and hydroxyl groups to the alkali metal ions (K^+ and Cs^+)

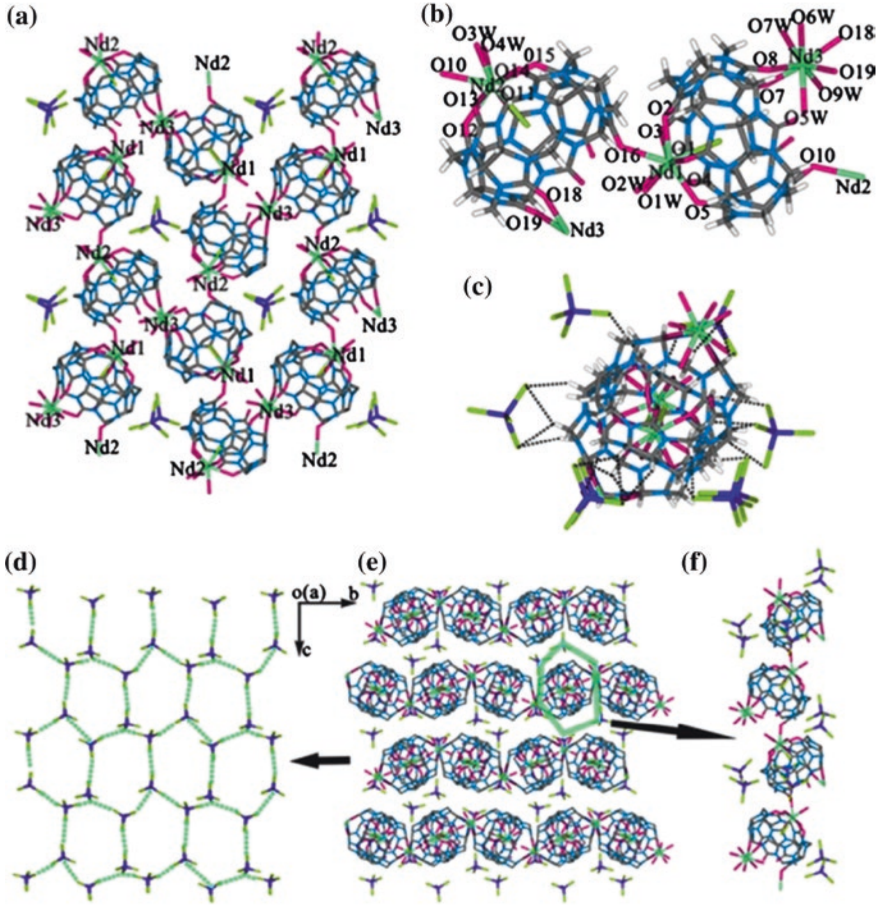

Fig. 3.14 X-ray crystal structure of **a** Nd^{3+}/Q[5]-based 2D coordination polymers; **b** detailed coordination of Q[5] molecules and Nd^{3+} (Nd1, Nd2, and Nd3) cations; **c** overview of the $[ZnCl_4]^{2-}$-based honeycomb framework; **d** overview of the Nd/Q[5]-based supramolecular assembly in the presence of; and **e** a Nd^{3+}/Q[5]-based linear dimensional coordination polymer

in between. The solid-state packing of these complexes shows the formation of open channels occupied by counter ions and noncoordinating water molecules. In the $(HO)_{10}Q[5]/K^+$ 2D network (Fig. 3.15a, b), each $(HO)_{10}Q[5]$ molecule coordinates with four potassium cations, two of which (K1 and K2) fully cover both portals of the $(HO)_{10}Q[5]$ molecule. Meanwhile, K1 and K2 also coordinate two oxygens (O19A and O16A) of the hydroxyl group of neighboring $(HO)_{10}Q[5]$ molecules, respectively. The other two K^+ cations (K1A and K2A) coordinate to two oxygens (O19 and O16, respectively) of the hydroxyl groups on the $(HO)_{10}Q[5]$ molecule, resulting in the formation of the $(HO)_{10}Q[5]/K^+$-based 2D networks. Moreover, the staggered arrangement of these 2D networks along the *c*

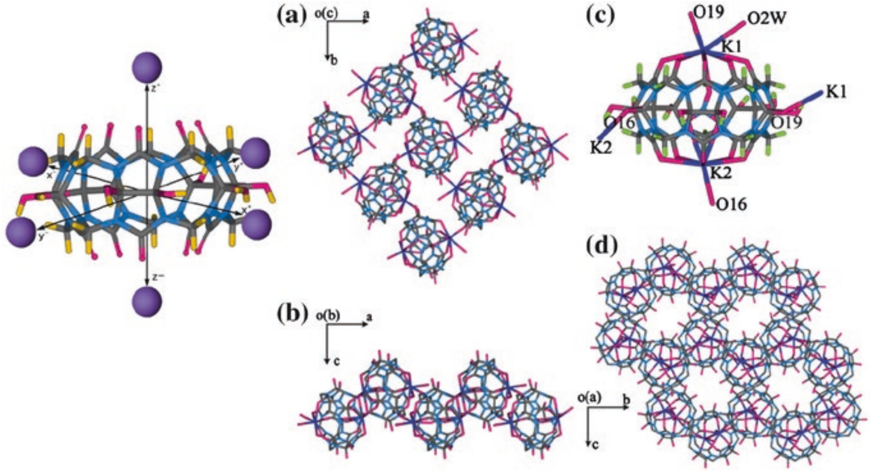

Fig. 3.15 (*Left*) coordination of hydroxyl groups on the outer surface of Q[n]s with metal ions; (*right*) X-ray crystal structure **a** top view; **b** side view of $(HO)_{10}Q[5]/K^{+}$ 2D network; **c** of $(HO)_{10}Q[5]/K^{+}$ complex; **d** stacking of the $(HO)_{10}Q[5]/K^{+}$ 2D networks with honeycomb structure features

axis creates honeycomb-like supramolecular assemblies with infinite 1D channels along the *a* axis, in which the Cl^{-} counter ions and water molecules are entrapped. $(HO)_{10}Q[5]/Cs^{+}$-based 2D networks show similar structure features as those in the $(HO)_{10}Q[5]/K^{+}$-based 2D networks [38].

3.3 Induced Coordination Polymers of Cucurbit[6]urils with Metal Ions

Recently, our lab also prepared a series of 1D polymers constructed from alkyl-substituted Q[6]s with different metal ions. Among them are complexes of TMeQ[6] with alkali and alkaline earth metal ions and their coordination polymers [39]. As ligands, unsubstituted cucurbituril (Q[6]) or partially methyl-substituted cucurbituril, TMeQ[6] can generally coordinate with either alkali or alkaline earth metal ions and with certain complexes. However, the assembly of the complexes of metal ions with Q[*n*]s could depend upon the Q[*n*] ligands. Previous experimental results reveal that the unsubstituted Q[6] ligand can coordinate with alkali metal ions and form a 1D supramolecular assembly of alternating Q[6] molecules and metal ions through direct coordination (referring to Fig. 3.2) [7–9]. The results also reveal that the TMeQ[6] ligand can coordinate with the alkaline earth metal ions and form a 1D supramolecular assembly of alternating TMeQ[6] molecules and metal ions through direct coordination (Fig. 3.16) [39]. The coordination of Q[6] with alkaline earth metal ions also produces common 1D coordination

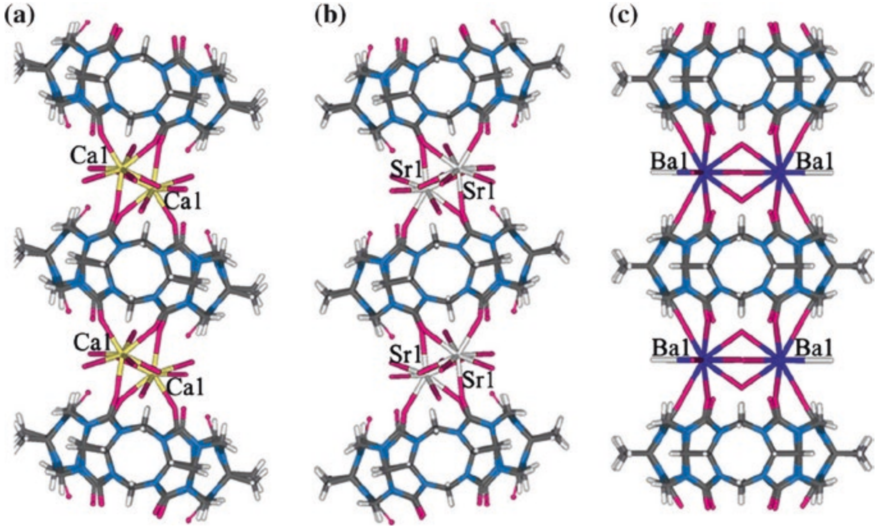

Fig. 3.16 X-ray crystal structures of a 1D polymer formed through direct coordination of TMeQ[6] molecules and **a** Ca^{2+} cations; **b** Rr^{2+} cations; and **c** Ba^{2+} cations

polymers in which every two Q[6] molecules are linked by two alkaline earth metal ions, and the two metal ions are bridged by sharing water molecules or not bridged.

More recently, our group prepared a series of 1D polymers based on direct coordination of lanthanides to alkyl-substituted Q[6] in the absence of structure directing agents or to unsubstituted Q[6] in the presence of structure directing agents [40–42]. As mentioned, alkyl-substituted Q[*n*]s present different characteristics in coordination with metal ions, suggesting a likely increased electron density as a consequence of the electrondonating effect of the alkyl substituents. According to the summary on the coordination of unsubstituted Q[6] with lanthanide metal ions and the formation of Q[6]/Ln^{3+}-based molecular capsules, molecular bowls, or Q[6]/Ln^{3+} pairs are very common, whereas 1D polymers are rare. Under similar synthetic conditions, hexacyclohexanocucurbit[6]uril (HCyHQ[6]) interacts with lanthanide nitrate in water, generating mainly 1D polymers through direct coordination of HCyHQ[6] with lanthanide metal ions (Ln = Y, Sm, Eu, Gd, Tb, Dy, Ho, Er, Yb) [40]. The structure of the HCyHQ[6]/Sm^{3+} complex is given in Fig. 3.17 as an example. The Sm^{3+} cations exhibit octacoordination, with each Sm^{3+} cation (Sm1) coordinated to eight oxygen atoms, viz. four carbonyl oxygen atoms from two neighboring HCyHQ[6] molecules (O1, O6, O7, and O8) and four water molecules (O1W, O2W, O3W, and O4W).

Thuéry recently prepared a series of 1D polymers through direct coordination of Q[6] molecules and lanthanides or uranyl cations in presence of a third species. For example, the reaction of lanthanide nitrates with Q[6] under hydrothermal conditions in the presence of perrhenic acid can yield two 1D polymers. These

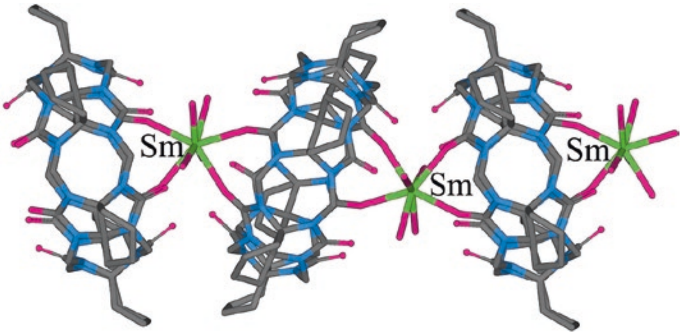

Fig. 3.17 X-ray crystal structures of a 1D polymer formed through direct coordination of HCyHQ[6] molecules and Sm^{3+} cations

polymers have been crystallographically characterized and have been observed to have some unique features. The two Q[6] complexes (Ce and Gd) involve perrhenate encapsulation [14]. In the Q[6]/Ce^{3+} complex, there are two different Q[6]-based molecular capsules that include a perrhenate anion and three different coordinated Ce^{3+} cations (Fig. 3.18a). Each Ce1 and Ce2 cation around the first Q[6] molecule is bound to three carbonyl groups, but two glycoluril units are shared by the cations in this case. Moreover, Ce1 is bound to two carbonyl groups of the second Q[6] molecule. The Ce3 cation is bound to one carbonyl donor from the first Q[6] molecule and to three carbonyl groups of the second Q[6] molecule, with one glycoluril unit in common with Ce1. Both Ce1 and Ce3 are bridging two Q[6] molecules. Considering the Q[6] ligands, one Q[6] molecule is bound to three cations, with Ce2 at one portal, Ce1 and Ce3 at the other portal, and the other Q[6] molecule to the two cations Ce1 and Ce3 on its two sides. This bonding scheme results in the formation of a strongly sinuous coordination polymer (Fig. 3.18a). A monodentate–bidentate bridging of the two Q[6] molecules by two Gd^{3+} cations results in the formation of a 1D coordination polymer. Two independent Gd^{3+} cations, Gd1 and Gd2, are located at 1.630(12) and 1.540(12) Å from the mean carbonyl oxygen plane of the associated bidentate portal. The coordination sphere of both cations is linked by two perrhenate ions, one of which is bound to Gd1 included in the Q[6] cavity (Fig. 3.18b). In the presence of 3-sulfobenzoate, two isomorphous complexes containing Ln (Ln = Ce or Nd) were obtained. These complexes display the 1D feature of coordination by the monodentate sulfonate group only. A columnar assembly is formed by coordination of each metal ion to two Q[6] molecules, with the 3-sulfobenzoate ligand having no role in the 1D polymer formation (Fig. 3.18c) [42].

A complex has been obtained from the hydrothermal reaction of uranyl nitrate with long-chain alkyldicarboxylic acids ($HOOC–(CH_2)_8–COOH$, denoted here as H_2C10) in the presence of Q[6], and dimethylformamide (DMF). This reaction generates dimethylammonium cations and additional Sr^{2+} ions in situ [43]. The complex, $[Sr_2Q[6](H_2O)_8(DMF)_2][(UO_2)_8O_4(C10)_6]$, includes columns built

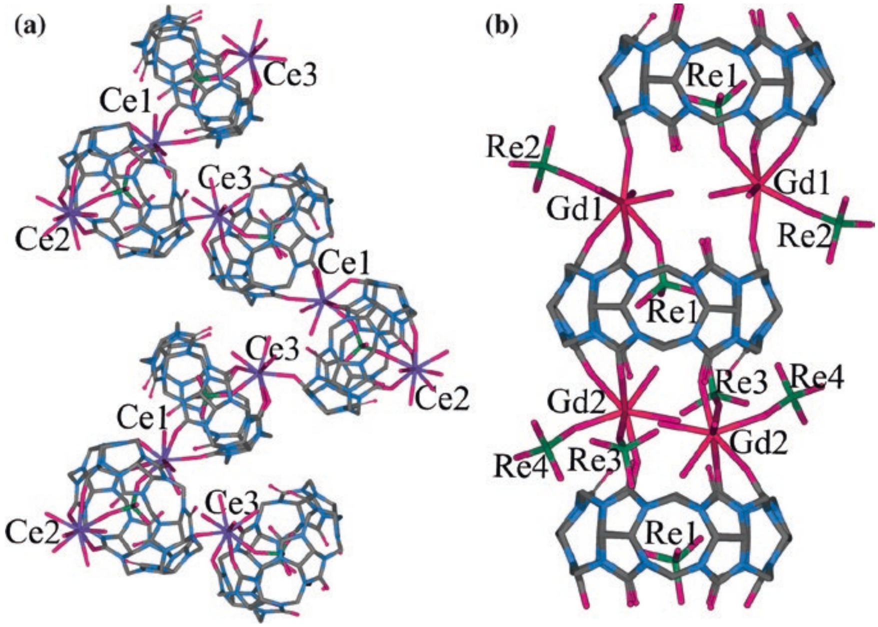

Fig. 3.18 X-ray crystal structures of a 1D polymer synthesized through direct coordination of Q[6] molecules and **a** Ce^{3+} cations in the presence of ReO_4^- anions; **b** Gd^{3+} cations in the presence of ReO_4^- anions; and **c** Nd^{3+} cations in the presence of 3-sulfobenzoate

from Sr^{2+} ions with Q[6]s, which are 1D polymeric. Two independent Sr^{2+} ions are bound to each portal of the Q[6] molecule, one is being bound to two carbonyl groups and the other to only one. Thus, each cation is bound to three carbonyl groups from two Q[6] molecules. The coordination sphere of both Sr^{2+} ions also includes the coordinated DMF molecule (Fig. 3.19a, b). Moreover, these 1D coordination polymers are separated from one another and surrounded by the corrugated 2D uranyl organic networks (Fig. 3.19c–e). In the 2D network, four independent uranyl ions that comprise two centrosymmetric, bis(μ_3-oxo)-centered tetranuclear clusters, are present in the complex; these two clusters can be considered to be isomorphous. Each of the two groups of atoms, U1 and U2 and U3 and U4 is bound to one chelating, one bridging tridentate, and one bridging bidentate carboxylate group (Fig. 3.19f).

In Q[*n*]-based coordination chemistry and Q[*n*]-based host–guest coordination chemistry, there are supramolecular assemblies in which the Q[*n*]s are linked by clusters or coordination units through direct coordination; these assemblies form coordination polymers. In one of Thuery's works, a 1D coordination polymer was obtained by mixing Q[6] and $UO_2(NO_3)_2 \cdot 6H_2O$ with or without formic acid under hydrothermal conditions (Fig. 3.20a) [44]. In the 1D coordination polymer, the uranyl ions form a centrosymmetric, μ_3-oxo-bridged tetranuclear cluster (Fig. 3.20b), and the U1 atom is bound to a Q[6] carbonyl group (O10).

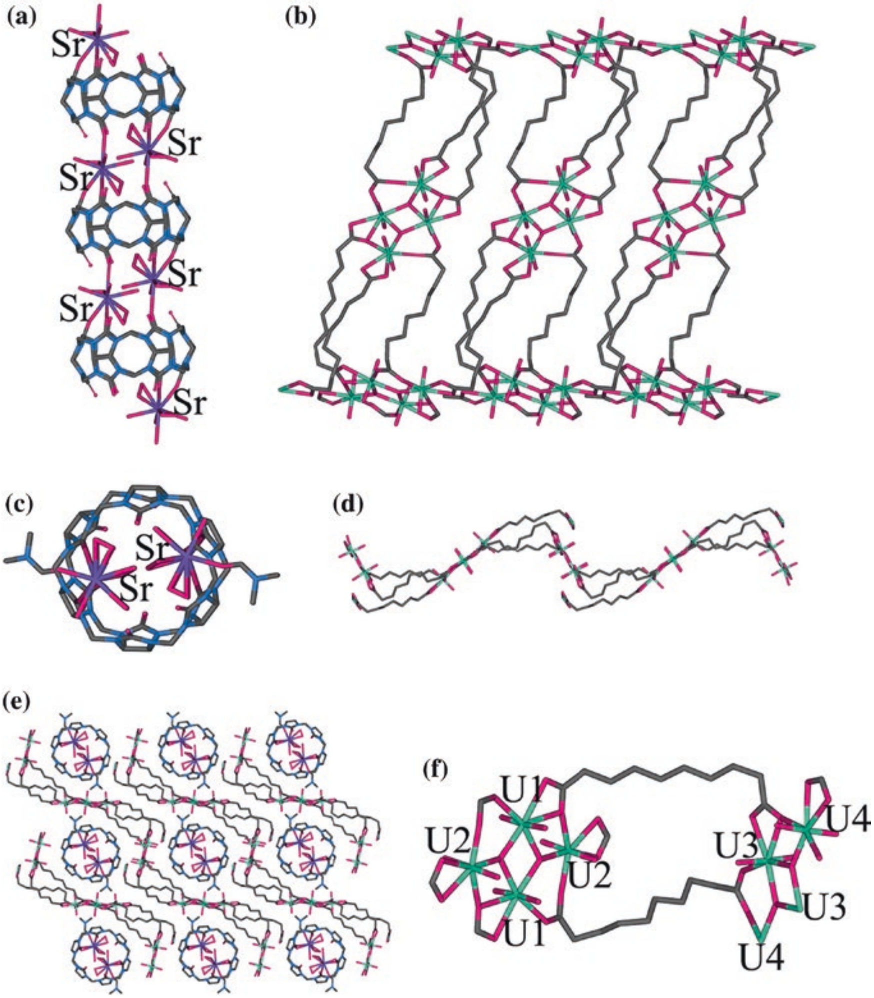

Fig. 3.19 X-ray crystal structures of a 1D polymer through direct coordination of Q[6] molecules and Sr^{2+} cations: **a** side view and **b** top view; **c** top view and **d** side view of a 2D network constructed from UO_2/C10; **e** stacking of 1D polymers and 2D networks; **f** two centrosymmetric, tetranuclear clusters

Another instance of a 1D coordination polymer was observed in the reaction of lanthanide nitrate salts with 2-sulfobenzoic acid in the presence of Q[6] under hydrothermal conditions. This reaction yields a series of Q[6]/Ln^{3+} 1D polymeric complexes of columnar shape, which have been crystallographically characterized. These 1D polymeric complexes are of two isomorphous groups, as shown in Fig. 3.20c (Ln = La, Ce) and Fig. 3.20e (Ln = Eu, Dy, Er, and Yb). These compounds all comprise carboxylate-bridged dinuclear units connecting the Q[6] molecules through lanthanide–carbonyl coordination. The units differ in that sulfonate

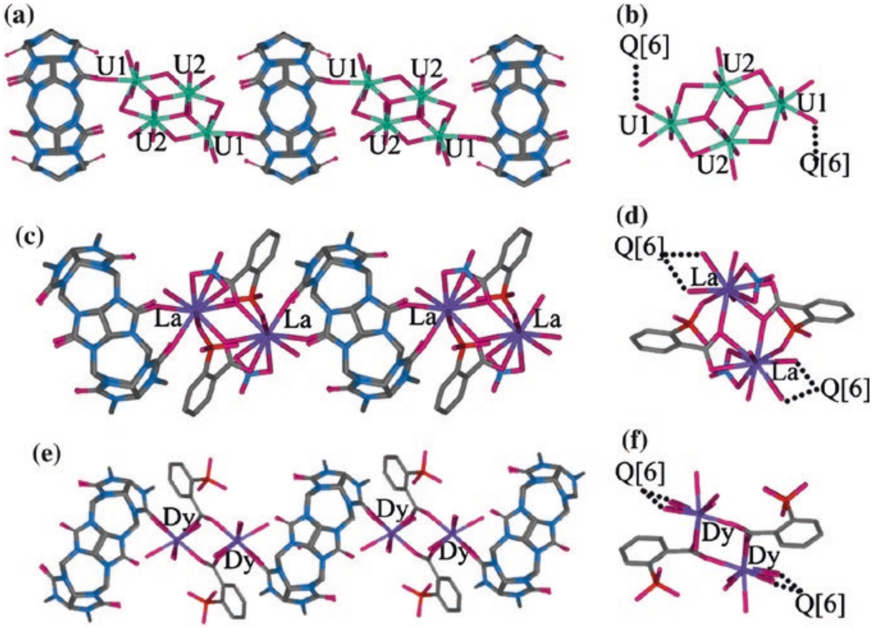

Fig. 3.20 X-ray crystal structures of a 1D polymer through direct coordination of Q[6] molecules; **a** and **b** tetranuclear cluster uranyl clusters; **c** and **d** carboxylate-bridged dinuclear units with a chelate ring; **e** and **f** carboxylate-bridged dinuclear units

bonding and formation of a chelate ring is present in only the first isomorphous group (Fig. 3.20d, f).

On the basis of experiences in the preparation of tubular coordination polymers involving Q[*n*]s other than Q[6], we introduced transition metal salts, such as Cd^{2+} or Zn^{2+} salts, into Q[6]–Ln^{3+}–HCl systems [41]. From this procedure, we obtained a series of supramolecular assemblies of lanthanide cations and Q[6] molecules in the presence of $[CdCl_4]^{2-}$ or $[ZnCl_4]^{2-}$ anions, which were formed in aqueous HCl solution containing the Cd^{2+} or Zn^{2+} salt. The $[MCl_4]^{2-}$ (M = Cd, Zn) anions displayed a "honeycomb effect", forming honeycomb-like hollows that could accommodate the 1D supramolecular chains or tubes constructed from Ln^{3+} cations and Q[6] molecules through direct coordination. Considering the similar chemical properties of the lanthanides due to the poor shielding of nuclear charge by filling of the 4f electron shell, it is reasonable to expect that the interaction of the various lanthanide cations with Q[6] molecules give rise to similar coordination features and supramolecular assemblies. Indeed, the solid-state structures of the obtained complexes, as determined by X-ray crystallography, were all isomorphous in the presence of $[CdCl_4]^{2-}$ anions. Similar results could be observed in the Q[6]–Ln^{3+}–$[ZnCl_4]^{2-}$ systems [41].

An overall view of the coordination features and the supramolecular assembly of the Q[6]/Sm^{3+} complex is given in Fig. 3.21a as a representative example of

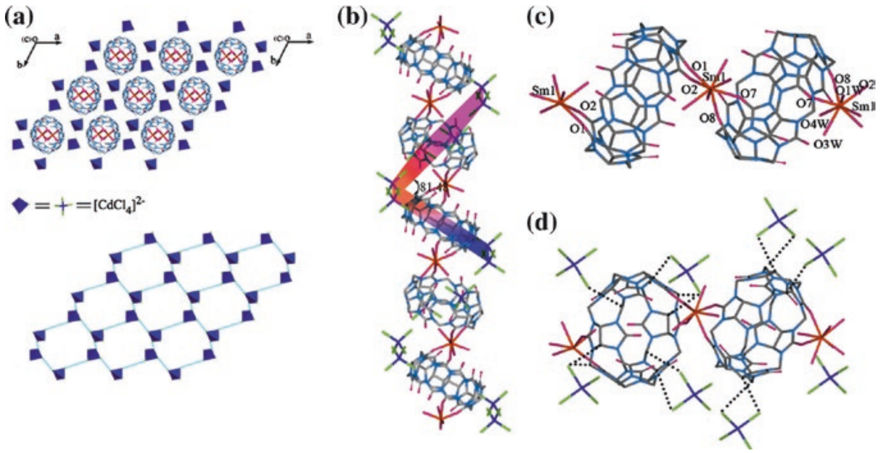

Fig. 3.21 X-ray crystal structure of the Q[6]/Sm^{3+} compound: **a** overall view of the coordination features and supramolecular assembly of the compound and the honeycomb-like framework composed of $[CdCl_4]^{2-}$ anions; **b** a zigzag coordination polymer of Sm^{3+} cations and Q[6] molecules surrounded by the $[CdCl_4]^{2-}$ anions; **c** coordination of the Sm^{3+} cations to the portal carbonyl oxygens of the Q[6] molecules; and **d** interaction of the $[CdCl_4]^{2-}$ anions with the Q[6] molecules

the Ln–Q[6]–$[CdCl_4]^{2-}$ systems. The $[CdCl_4]^{2-}$ anions appear to form a honeycomb structure (Fig. 3.21a), and the Sm^{3+} cations coordinate to neighboring Q[6] molecules to form zigzag coordination polymers that insert into the channels of the honeycomb framework, such that each individual zigzag coordination polymer is surrounded by $[CdCl_4]^{2-}$ anions (Fig. 3.21b). The Sm^{3+} cations are octacoordinated by eight oxygen atoms, namely, four carbonyl oxygen atoms from two neighboring Q[6] molecules (O1, O2, O7, and O8) and four water molecules (O1W, O2W, O3W, and O4W) (Fig. 3.21c). The formation of the $[CdCl_4]^{2-}$ honeycomb is a consequence of ion–dipole interaction between the portal carbonyl carbon atoms of the Q[6] molecules as well as hydrogen bonding between the chlorine atoms of the anions and methine groups on the surface of the Q[6] molecules. Moreover, the formation of the $[CdCl_4]^{2-}$ honeycomb is conducive to the coordination of lanthanide cations to Q[6] molecules (Fig. 3.21) [41]. Our recent studies have revealed that most transition metal ions have similar functions in the construction of polydimensional coordination polymers. Most importantly, we want to note here is that the rapid precipitation of Ln^{3+}-Q[6]-$[CdCl_4]^{2-}$ or $[ZnCl_4]^{2-}$ systems in which the Ln^{3+} are La, Ce, Pr and Nd cations [41]. It is therefore believed that such approaches could offer an opportunity to separate the light lanthanides cations from lanthanides.

Recently, we explored a simple way to isolate *i*Q[6] from normal Q[6] by using a Dowex 50W × 2-400(H) column. The subtle difference in electrostatic properties of the surfaces of *i*Q[6] and Q[6] result in significant differences in physical and chemical properties so that *i*Q[6] can be isolated from major normal Q[6]

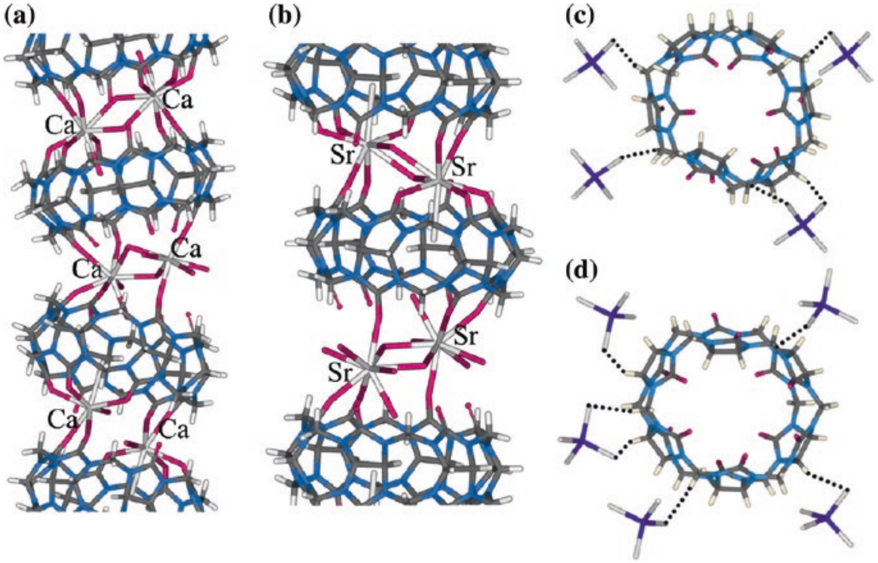

Fig. 3.22 **a** and **b** linear coordination polymers of *i*Q[6] with Ca^{2+} and Sr^{2+}, **c** and **d** detailed interactions between *i*Q[6] and $[ZnCl_4]^{2-}$ anions

[45]. Moreover, we used *i*Q[6] as a ligand, and investigated its interaction with alkaline earth metal ions (AE^{2+}) in the presence of the structure directing agent, $[ZnCl_4]^{2-}$. Single-crystal X-ray diffraction analysis revealed that interaction of *i*Q[6] with AE^{2+} (except Mg^{2+}, which has the smallest ionic radius) forms 1D coordination polymers. Coordination of AE^{2+} to *i*Q[6] and their supramolecular assemblies could be influenced by the interaction of the positively charged outer surface of *i*Q[6] with $[ZnCl_4]^{2-}$ anions, that is, the outer surface interactions of Q[*n*]s [13]. Figure 3.22a, b show linear coordination polymers of *i*Q[6] with Ca^{2+} and Sr^{2+} and Fig. 3.22c, d show the detailed interactions between *i*Q[6] and $[ZnCl_4]^{2-}$ anions.

A series of studies reported by Thuéry reveals that the uranyl ion is a very special species in the construction of Q[*n*]-based polydimensional coordination polymers. This ion may not only directly coordinate to the portal carbonyl oxygens, but also form various uranyl-based clusters and coordinate to the portal carbonyl oxygens, resulting in the formation of a variety of Q[*n*]-based polydimensional coordination polymers. For example, preparation of the polydimensional coordination polymers is carried out in the presence of long-chain alkyldicarboxylic acids ($HOOC–(CH_2)_{n-2}–COOH$, denoted here as H_2C_n), such as H_2C_8 or H_2C_9, DMF (added to enhance solubility of higher diacids), and alkali (Li^+) or alkalineearth metal ions (added in order to promote the dissolution of the cucurbituril). The unsubstituted Q[6] interacts with uranyl (clusters) and form 2D coordination networks [43]. The crystal structures of the resulting complexes, which have stoichiometries of $[H_2NMe_2]_2\{(UO_2)_4O_2(OH)_2(C8)_2Q[6]\} \cdot 8H_2O$ and $[H_2NMe_2]_2$

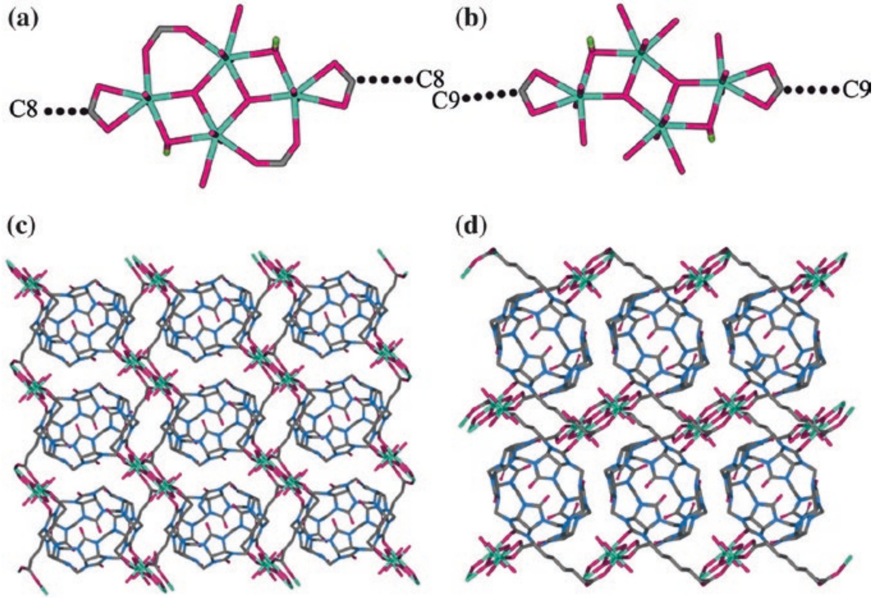

Fig. 3.23 X-ray crystal structure of tetranuclear UO_2 clusters linked by **a** C8 and **b** C9; X-ray crystal structure of a 2D network of Q[6]/UO_2 clusters linked by **c** C8 and **d** C9

$\{(UO_2)_4O_2(OH)_2(C9)_2Q[6]\} \cdot 5H_2O$ are closely related, since both of them contain similar tetranuclear UO_2^{2+} clusters held by two μ_3-oxo and two μ_2-hydroxo ions (Fig. 3.23a, b). In addition, both are attached to Q[6] by uranyl–O–carbonyl bonds to form 2D coordination polymers. Figure 3.23b, c show such Q[6]/$U_{cluster}$ 2D networks linked by C8 and C9, respectively.

An extensive investigation on inorganic molecule-induced Q[*n*]/metal coordination polymers reveals that the Cd cation is also a very special species. It can not only directly coordinate to the portal carbonyl oxygens, but also form various Cd-based complexes or clusters that coordinate to the portal carbonyl oxygens or accompany Q[*n*]/metal complexes. Formation of the Cd-based complexes or clusters result in the formation of a variety of Q[*n*]-based polydimensional coordination polymers. One of our recent works examined such 2D coordination polymer. The crystal structure of the polymer reveals that there are two Cd^{2+} units held by two μ_2-Cl ions in this assembly (Fig. 3.24a, b) and the Q[6] molecules are linked by these two Cd^{2+} units. These linkages result in the formation of the Q[6]/Cd^{2+}-based 2D coordination polymers (Fig. 3.24c). In this assembly, each Cd^{2+} ion is hexacoordinated in three different features, and the ligand Q[6] coordinates with three Cd^{2+} ions (for Q[6]A) or two Cd^{2+} ions (for Q[6]B). The Cd1 ion is coordinated by three carbonyl oxygens (O2 from Q[6]A, and O13 and O14 from Q[6]B), two shared chloride anions (Cl2 and Cl3), and one water molecule (O7W). The Cd2 ion is coordinated by one carbonyl oxygen (O8 from Q[6]A), three chloride anions (Cl4, Cl1, and Cl10, the last two of which are shared), and two water

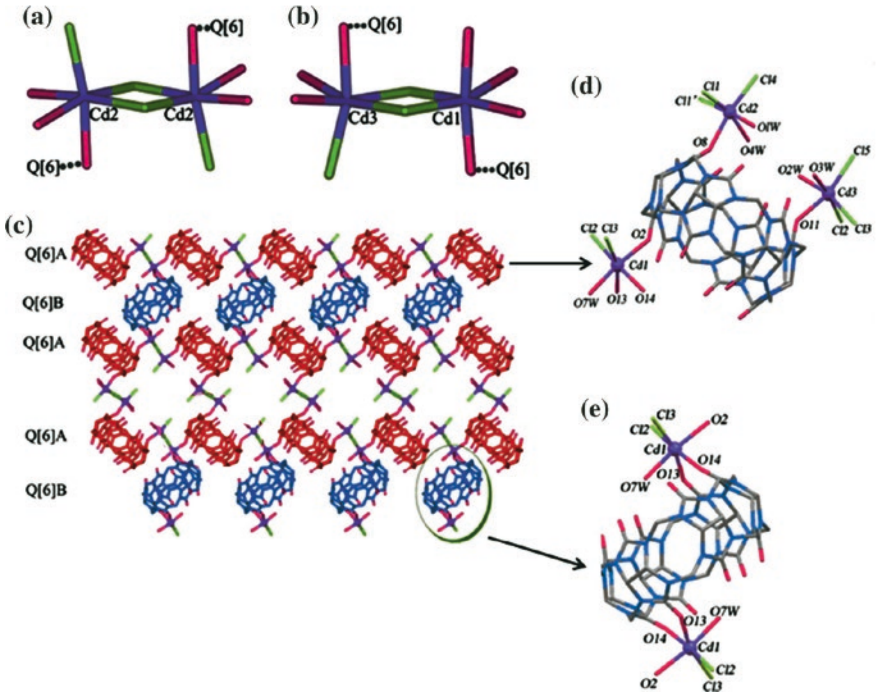

Fig. 3.24 X-ray crystal structures of **a** and **b** two different Cd^{2+} units; **c** the 2D network linked by complexation of Cd^{2+} units. A detailed view of the coordination of **d** $Cd1^{2+}$; $Cd2^{2+}$; and $Cd3^{2+}$ with Q[6]A and **e** $Cd1^{2+}$ with Q[6]B

molecules (O1W and O4W). The Cd3 ion is coordinated by one carbonyl oxygen (O11 from Q[6]A), three chloride anions (Cl5, Cl2, and Cl3, the last two of which are shared) and two water molecules (O2W and O3W). The ligand Q[6]A plays the role of a ternary ligand donor and coordinates with three Cd^{2+} ions (Cd1, Cd2, and Cd3), while the ligand Q[6]B plays the role of a binary ligand donor and coordinates with two Cd^{2+} ions (2 Cd1), (Fig. 3.24d, e) [46].

Very recently, we obtained another Q[6]-based 2D coordination polymer constructed from Q[6]/Na^+-based 1D coordination polymers linked by $[CdCl_4]^{2-}$ anions by introducing NaCl into a Q[6]–$CdCl_2$ system in a HCl solution. In this assembly, the 1D supramolecular chains (Fig. 3.25a) and the neighboring Q[6]s are linked by three sodium units in the tubular coordination polymers. One Na^+ cation (Na2) links two adjacent Na^+ cations (Na1) by sharing water molecules O1W and O1W, and form a unit of three Na^+ cations (Fig. 3.25b) [47]. We found that $[CdCl_4]^{2-}$ or $[ZnCl_4]^{2-}$ may behave as structure inducer that prefers to form honeycomb frameworks in which the linear metal–Q[*n*] coordination polymers fill the channels of the $[CdCl_4]^{2-}$ or $[ZnCl_4]^{2-}$ honeycomb. However, in the present work, the $[CdCl_4]^{2-}$ anions do not arrange within the honeycomb framework; instead, they interact with Na^+ cations in the tubular coordination polymers

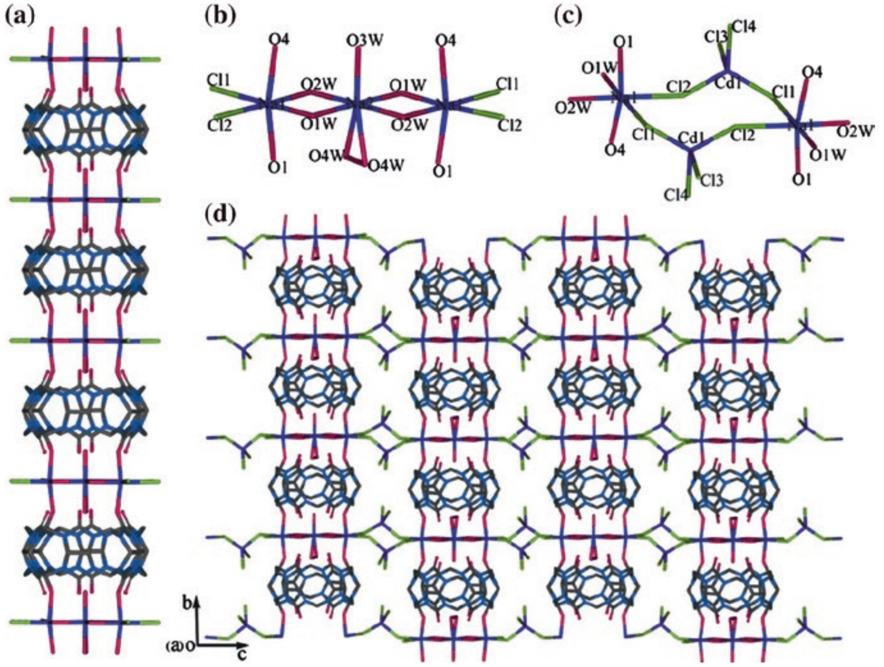

Fig. 3.25 X-ray crystal structures of **a** a tubular coordination polymer constructed from alternating Q[6] and units of three Na^+ cations; **b** a unit of three Na^+ cations; **c** a $[CdCl_4]^{2-}$–Na^+ unit; and **d** the 2D network constructed from Q[6]/Na^+-based 1D coordination polymers and $[CdCl_4]^{2-}$ anions

through electrostatic interactions. Every two $[CdCl_4]^{2-}$ anions interact with two sodium cations (Na1) belonging to the neighboring tubular polymers, as shown in Fig. 3.25c. This interaction results in the formation of a 2D network, as shown in Fig. 3.25d.

Earlier, we mentioned that DMF and $Sr(NO_3)_2$ were added into the Q[6]–UO_2^{2+}–H_2Cn systems in order to enhance the solubility of the higher diacid and Q[6] in the reaction medium and thus obtain the 2D network coordination polymers. Without $Sr(NO_3)_2$, the Q[6]–UO_2^{2+}–H_2C9–DMF system produces a novel 3D framework in which the layers are composed of uranyl clusters and C9 diacids, as shown in Fig. 3.19. These layers are bridged by Q[6] molecules (Fig. 3.26a). Such linkage can also be viewed as resulting from the bridging of the $[(UO_2)_4O_2(OH)_2Q[6]]^{2+}$ chains by C9 dicarboxylate ligands (Fig. 3.26b) [43]. Thus, the tendency for uranyl ions to give planar or gently undulating ribbons or sheets appears to match the propensity of Q[6] to fit between them.

In addition to the previous summary on 1D and 2D uranyl-based coordination polymers, these results provide new examples of the potential of cucurbiturils as uranyl complexants or as structure directing agents. The frameworks, sheets, or columns readily formed by Q[6] appear to be particularly well suited to associate

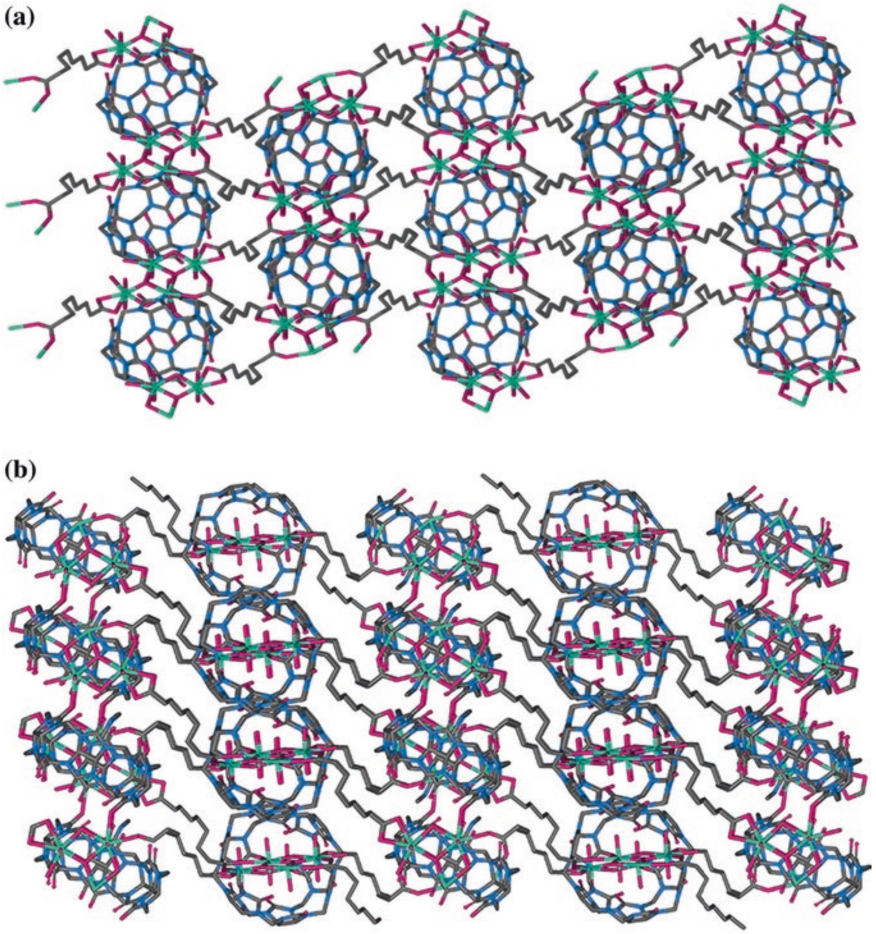

Fig. 3.26 X-ray crystal structures of the 3D framework in which **a** the UO$_{2\text{cluster}}$/C9$_{\text{dicarboxylate}}$ layers are bridged by Q[6] molecules; and **b** the UO$_{2\text{cluster}}$/Q[6] 1D coordination polymer is bridged by C9 dicarboxylate ligands

with the 2D or ribbon-like topologies most common among uranyl organic species, which opens perspectives for the design of hybrid layered materials.

Again, a Q[6]/Cd^{2+}-based 3D framework may readily be obtained by mixing KCl, CdCl$_2$, and Q[6] in a HCl solution [47]. Although no K$^+$ ions seem to be present in the solid compound, they appear to act as structure directing agents, resulting in the formation 3D Q[6]/Cd^{2+}-based 3D framework. The X-ray crystal structure shows the coordination feature of Cd^{2+} cations with Q[6] (Fig. 3.27a, b). A Q[6] molecule appears to coordinate with six Cd^{2+} cations to form Cd$_2$(μ-Cl)$_2$Cl$_2$(H$_2$O)$_3$ complexes (Fig. 3.27c). Each Cd^{2+} cation coordinates to six atoms (with 50 % occupancy), one portal carbonyl oxygen (O3), three water molecules (O1W, O7W, and O9W), and two chloride anions (2Cl1), which are shared by

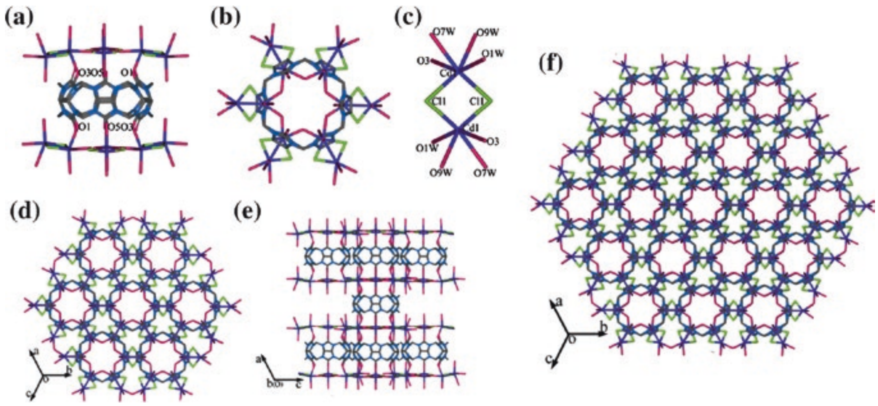

Fig. 3.27 X-ray crystal structures of the Q[6]/Cd^{2+}-based compound: **a** and **b** the coordination feature of Cd^{2+} cations with cucurbituril; **c** the $Cd_2(\mu\text{-}Cl)_2Cl_2(H_2O)_3$ complex; **d** and **e** a coordinated cucurbituril surrounded by six coordinated cucurbiturils through the $Cd_2(\mu\text{-}Cl)_2Cl_2(H_2O)_3$ complexes; **f** an overall view of the arrangement of the coordinated cucurbiturils and $Cd_2(\mu\text{-}Cl)_2Cl_2(H_2O)_3$ complexes

the two Cd^{2+} cations (2Cd1) in the $Cd_2(\mu\text{-}Cl)_2Cl_2(H_2O)_3$ complex. Each $Cd_2(\mu\text{-}Cl)_2Cl_2(H_2O)_3$ complex can link two neighboring cucurbituril molecules. Thus, at each portal of the cucurbituril molecule, three Cd^{2+} cations (Cd1) from three $Cd_2(\mu\text{-}Cl)_2Cl_2(H_2O)_3$ complexes coordinate to three portal carbonyl oxygens alternatively, and each cucurbituril molecule can link six such coordinated cucurbituril molecules (Fig. 3.27d, e). Figure 3.27f shows an overall view of the arrangement of coordinated Q[6] molecules and $Cd_2(\mu\text{-}Cl)_2Cl_2(H_2O)_3$ complexes. Although KCl was added to the synthetic system, K^+ was not observed in the obtained compound. Nevertheless, the presence of potassium cations could influence the coordination and supramolecular assembly of Q[6] molecules and Cd^{2+} ions. In HCl solution, Cd^{2+} produces $[CdCl_4]^{2-}$ anions that form the Cd honeycomb, which are filled with the tubular Cd^{2+}–cucurbituril coordination polymers [47].

3.4 Induced Coordination Polymers of Cucurbit[7]uril with Metal Ions

In cucurbiturils-based coordination chemistry, it seems that the coordination of Q[n, $n \geq 7$]s with metal ions seems to be more difficult than that of Q[5] or Q[6] with metal ions. It is likely that the larger portal size of Q[n, $n \geq 7$]s causes a wider distribution of the carbonyl oxygens, resulting in difficulty in the effective coordination of Q[n, $n \geq 7$] with metal ions. However, recent works reveal that the Q[7] molecule may also readily coordinate to metal ions and form novel polydimensional coordination polymers in the presence of the structure directing agents [35, 48, 49]. In previous studies, there have been numerous attempts to grow single crystals of complexes in which lanthanide cations are coordinated to Q[7] in various acidic media, but all have proved unsuccessful. However, when transition metal ions are introduced into HCl solutions containing Q[7] and Ln^{3+} salts, Q[7]/Ln^{3+}-based linear coordination polymers are readily produced, and the transition metal cations in the form of the tetrachloride ($[MCl_4]^{2-}$) may be arranged into honeycomb-like hollows. These hollows can then accommodate the Q[7]/Ln^{3+}-based linear coordination polymers through ion–dipole and C–H···Cl interactions coupled with metal coordination, as shown in Fig. 3.11f. We first demonstrated the synthesis of a series of Q[7]/Ln^{3+}-based linear coordination polymers in the presence of $[CdCl_4]^{2-}$ anions [47]. Subsequent studies have revealed that a few transition metal ions, such as Zn^{2+}, Cu^{2+}, and Co^{2+}, in the form of tetrachloride anions $[MCl_4]^{2-}$, may also play a similar role in triggering the formation of 1D Ln^{3+}–Q[*n*] coordination polymers [41, 48, 49].

Because of the similar chemical properties of the lanthanides, the interactions of various lanthanide cations with Q[7] molecules give rise to similar coordination features and supramolecular assemblies. Interestingly, the shapes of the 1D Q[7]/Ln^{3+}-based coordination polymers could be finely tuned by the lanthanide metal ions under high concentrations of acid in the presence of $[CdCl_4]^{2-}$ dianions [35]. As shown in Scheme 3.4, lanthanide cations coordinated with Q[7] to form zigzag channels in less acidic media (<3.0 mol/L HCl) (Scheme 3.4b). However, in more acidic media (>3.0 mol/L) tubular channels formed (Scheme 3.4c). Figure 3.28 shows the common structures of Q[7]/Ln^{3+}-based zigzag and tubular structures. The former has alternating Q[7] molecules and Ln^{3+} cations at 1:1 ratio; the latter has alternating Q[7] molecules and Ln^{3+} cations at 1:2 ratio.

The crystal structures in both cases also reveal that the $[CdCl_4]^{2-}$ dianions surround each Q[7] molecule in the coordination polymer via ion–dipole interactions between the portal carbonyl carbon atoms ($O{=}C^{\delta+}\cdots Cl^{-}{-}CdCl_3^{-}$) and the chlorine atoms of the anions, as well as hydrogen bonding between the chlorine

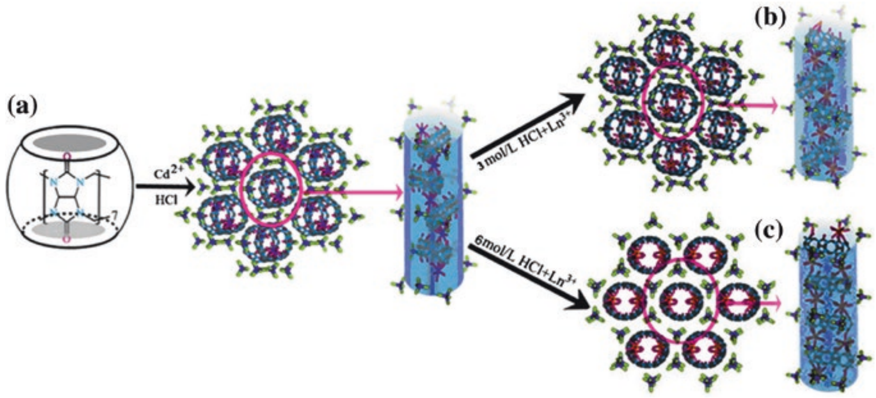

Scheme 3.4 Zigzag and tubular channels construction from Q[7]/Ln^{3+}-based coordination polymers in the presence of $[CdCl_4]^{2-}$ dianions

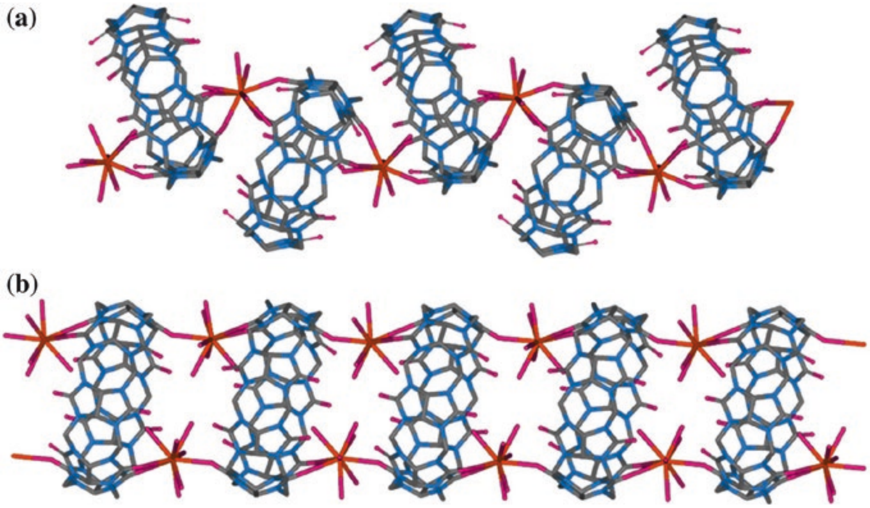

Fig. 3.28 The common X-ray crystal structures of the Q[7]/Ln^{3+}-based 1D coordination polymers with **a** zigzag and **b** tubular structures in the presence of the $[CdCl_4]^{2-}$

atoms of the anions and the methine groups on the surface of the Q[*n*] molecules ($C–H_{methylene}\cdots Cl^{-}–CdCl_3^{-}$). Electrostatic interactions between Ln^{3+} cations and $[CdCl_4]^{2-}$ anions could be another important driving force resulting in the formation of the $[CdCl_4]^{2-}$ honeycomb in both zigzag and tubular structures (Fig. 3.29a–d). Notably, ion–dipole interactions exist between the methine groups of the Q[7] molecules in the zigzag structure (Fig. 3.29a, b), which are inclined on the portals of the neighboring Q[7] molecules (Fig. 3.29b).

Apart from the Q[7]/Ln^{3+}-based 1D coordination polymers, the uranyl ion presents an unusual affinity for Q[*n*], and even Q[7]. By dissolving Q[7] and $UO_2(NO_3)_2 \cdot 6H_2O$ in excess perrhenic acid under hydrothermal conditions, Thuéry synthesized two isomeric 1D zigzag polymers in which the uranyl ion is bound to two carbonyl groups from two neighboring Q[7] ligands. Each Q[7] molecule acts as a bidentate ligand and coordinates with a uranyl cation at each portal (Fig. 3.3a, b) [50, 51]. Moreover, Thuéry first demonstrated a Q[7]/UO_2^{2+}-based 2D coordination network by dissolving Q[7] and $UO_2(NO_3)_2$ st demonstrated $6H_2O$ in excess sulfuric acid under hydrothermal conditions (Fig. 3.31a, b) [44]. The crystal structure of the network shows that each Q[7] molecule coordinates with four UO_2^{2+} cations (Fig. 3.31c), while two sulfate anions coordinate with two uranyl cations and form a pentagonal bipyramidal uranium environment (Fig. 3.31d). The combined coordination of Q[7] molecules and uranyl/sulfate units leads to the formation of novel Q[7]-based coordination networks.

In the presence of $CsNO_3$, which may function as a structure inducer, the Q[7]–$UO_2(NO_3)_2$ system may also yield a 2D coordination network under hydrothermal conditions (Fig. 3.32a) [51]. Similarly, each Q[7] molecule coordinates with four UO_2^{2+} cations, while two uranyl cations form a planar

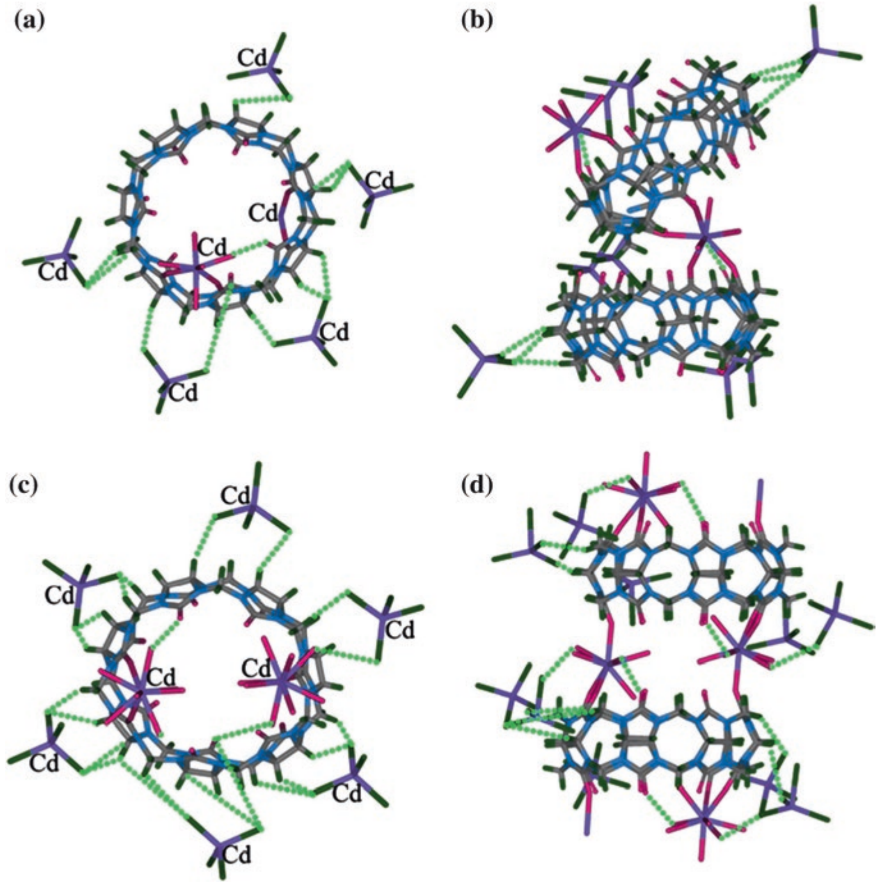

Fig. 3.29 X-ray crystal structures of the isolated Q[7]/Ln^{3+} complex with **a** and **b** the zigzag structures; **c** and **d** the tubular structures in the presence of the $[CdCl_4]^{2-}$ dianions

$[(UO_2)_2(\mu_2\text{-}OH)_2(H_2O)_4]^{2+}$ cation in the 2D coordination network (Fig. 3.32b, c). The 2D coordination network may be viewed as resulting from the bridging of the $[(UO_2)_2(\mu_2\text{-}OH)_2(H_2O)_4]^{2+}$ cations by the Q[7] ligands.

In order to understand the influence of an included guest on the coordination of metal ions to Q[*n*], a series of aromatic molecules known to be suitable guests may be selected [52–54]. We describe in detail a novel 3D framework constructed from Q[7] pairs through Hyq-induced coordination of a rubidium unit to the portal oxygens of Q[7]s [55]. To the best of our knowledge, this is the first observed Q[7]-based 3D framework in Q[*n*] chemistry. Attempts of mixing Q[7] and rubidium salts in aqueous solutions did not result in the formation of the Rb–Q[7] complex through direct coordination, but instead produced Q[7] crystals with free metal ions. However, a compound containing a novel 3D framework was first found when a guest Hyq was introduced into the RbCl–Q[7] solution. Crystals obtained

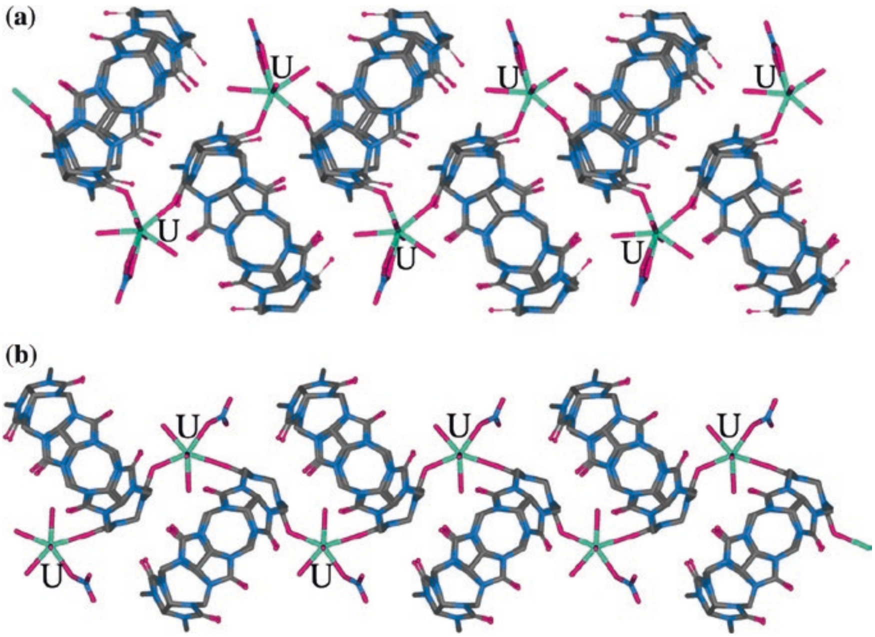

Fig. 3.30 X-ray crystal structure of two isomeric 1D zigzag polymers constructed of Q[7]/UO_2^{2+} complexes

from the RbCl–Q[7]–Hyq mixture had a stoichiometry of $\{Rb_2(\mu\text{-}OH)(H_2O)_2(Hyq@Q[7])_2\}\cdot Cl$. The crystal structure shows that a portal of each Q[7] molecule in the Q[7] pair is covered by a $[Rb_2(\mu\text{-}OH)(H_2O)_2]$ unit containing two rubidium cations (2Rb1), and the other portal of each Q[7] molecule in the Q[7] pair is coordinated to a Rb1 cation belonging to a neighboring rubidium unit. Each of the Q[7] molecules in the Q[7] pair includes a Hyq guest through the combination of the cavity bonding of the host Q[7] and the coordination of a Rb1 cation to a hydroxyl oxygen (O15) of the Hyq guest (Fig. 3.33a). It should be noted that O1 and O1A are shared with the other rubidium cation (Rb1A) in the rubidium unit. In the Q[7] pair, there are additional interactions of the hydroxyl O15–H15A with the portal carbonyl oxygen O3, as well as interactions of O16–H16 with O12 through hydrogen bonding. The interaction between Rb^+ and the hydroxyl oxygen (O15) could play an important role in the formation of the Q[7]–Rb^+ complex through direct coordination of Q[7] to the rubidium unit [55].

Remarkably, the crystal structure of the compound shows a 3D infinite framework constructed from the Q[7] pairs through the coordination of the rubidium unit to the Q[7] molecules (Fig. 3.33b). From different directions, different linear channels in the crystal structure of the compound may be seen. For example, channels with around 7.45 Å diameter extend along the *b* axis (Fig. 3.33c). However, another set of linear channels of around 10.43 × 5.2 Å cross-sectional area (Fig. 3.33d) can be observed. Close inspection reveals that a network can be

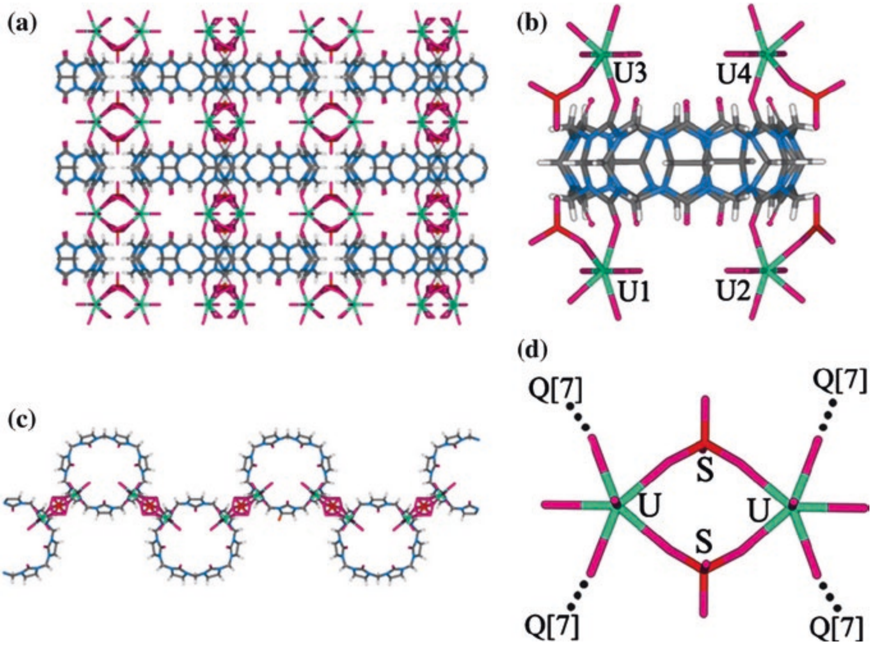

Fig. 3.31 X-ray crystal structure of Q[7]/UO_2^{2+}-based 2D coordination network **a** side view; **b** top view; **c** coordination of a Q[7] molecule with four UO_2^{2+} cations; **d** the UO_2^{2+}/SO_4^{2-} unit

found in the direction shown in Fig. 3.33e; the network consists of fused seven-membered bracelets in which each Q[7] "bead" is linked by directly coordinated rubidium ions (Fig. 3.33f). The size of the bracelet is partly dictated by the size of each Q[7] bead, which has a diameter of ~13 Å. The seven-membered bracelets have a diameter of around 10.43 Å (Fig. 3.33f). Thus, the seven-membered bracelet rings lead to the formation of channel structures with different sizes and shapes in the compound. The channels are filled with water molecules that form a complicated hydrogen bonding network among themselves, as well as with the water molecules coordinated to the metal centers [55].

3.5 Induced Coordination Polymers of Cucurbit[8]uril with Metal Ions

The coordination of metal ions to Q[*n*]s and their coordination polymers in the presence of inorganic structure inducers have been extensively investigated in our laboratory. In particular, we introduced certain transition metal ions into metal–Q[*n*] systems in an HCl solution to prepare various polydimensional coordination

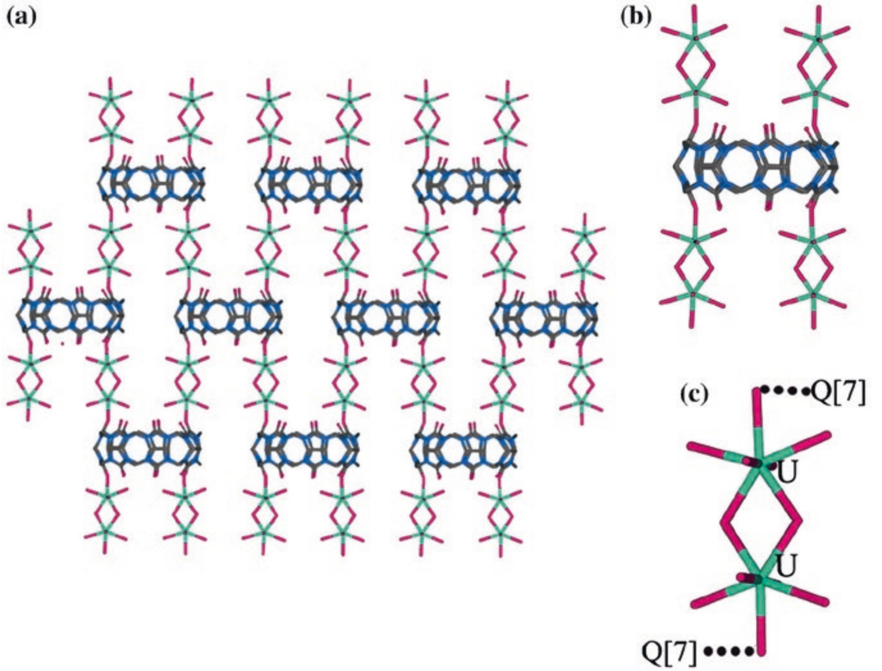

Fig. 3.32 X-ray crystal structure of **a** Q[7]/UO_2^{2+}-based 2D coordination network; **b** coordination of a Q[7] molecule with four UO_2^{2+} cations; **c** the $[(UO_2)_2(\mu_2\text{-}OH)_2(H_2O)_4]^{2+}$ cation unit

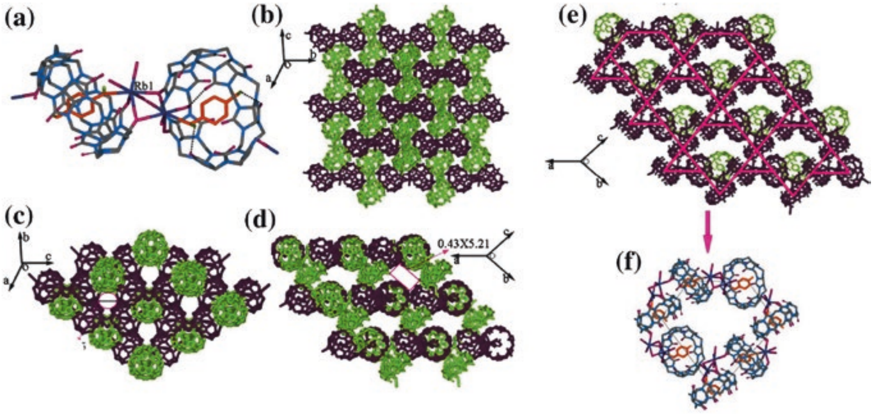

Fig. 3.33 X-ray crystal structure of **a** the Q[7] pair with an included Hyq molecule linked to a rubidium unit; **b** a 3D framework constructed from the Q[7] pairs; **c** and **d** the linear channels in the Q[7]–Rb–Hyq framework, as observed from different directions; **e** a layer composed of the multifused Q[7]-based seven-membered bracelets; and **f** the Q[7]-based seven-membered bracelet

polymers with arrangements that are markedly different from those formed without structure inducers. The most remarkable examples of formation of polydimensional coordination polymers are seen in the coordination of Ln^{3+} cations to Q[6] or Q[7], which lead to the corresponding supramolecular assemblies in the presence of transition metal dications ($M_{trans}{}^{2+}$) in the HCl solution. The $M_{trans}{}^{2+}$ cations form $[M_{trans}Cl_4]^{2-}$ anions and honeycomb-shaped cells via ion–dipole and C–H···Cl interactions, and the tubular Q[n = 6, 7]/Ln^{3+} coordination polymers fill the honeycomb cells [56].

Herein, we introduce a process beginning with tetrachloride transition metal anions ($[M_{trans}Cl_4]^{2-}$, M_{trans} = Cd, Zn, Cu, Co) as the "inducer" to undergoing the "honeycomb" effect. These anions induce Sr^{2+} cations to coordinate to Q[8] molecules, resulting in the formation of 1D coordination polymers [56]. The X-ray crystal structure given in Fig. 3.34 shows an overall view of the coordination features and supramolecular assembly in the compound as a representative example of all four Sr^{2+}–Q[8]–$[M_{trans}Cl_4]^{2-}$ systems. The $[CdCl_4]^{2-}$ anions appear to form the honeycomb structure (Fig. 3.34a), and two Sr^{2+} cations coordinate to the neighboring Q[8] molecules and form zigzag coordination polymers which insert into the channels in the $[CdCl_4]^{2-}$ honeycomb framework. Each coordination polymer is surrounded by the $[CdCl_4]^{2-}$ anions (Fig. 3.34b). Moreover, the coordinated Q[8] molecules in the 1D coordination polymer are alternately surrounded by six $[CdCl_4]^{2-}$ anions (Fig. 3.34d). Part of the back of the inclined Q[8] is close to the portal of the actinic Q[8] (Fig. 3.34c). The distance of the carbonyl oxygen from the carbonyl carbon (C=O···C=O) in the inclined Q[8] is about 3.0 Å, and the distance of the carbonyl oxygen from the methane carbon

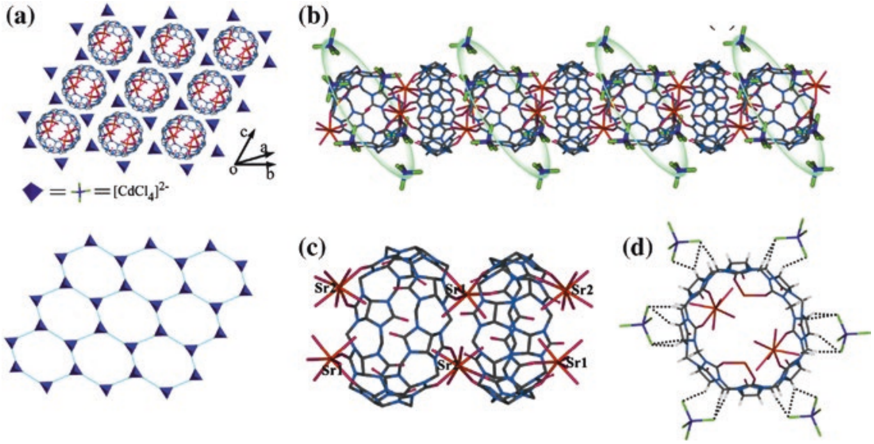

Fig. 3.34 X-ray crystal structure of the compound from the Q[8]–Sr^{2+}–$[CdCl_4]^{2-}$ system: **a** overall view of the coordination features and the supramolecular assembly and the $[CdCl_4]^{2-}$ honeycomb-like frame; **b** a zigzag coordination polymer of Sr^{2+} cations to Q[8] molecules surrounded by the $[CdCl_4]^{2-}$ anions; **c** details of coordination of Sr^{2+} cations to the portal carbonyl oxygens of the Q[8] molecule; and **d** details of the interaction of $[CdCl_4]^{2-}$ with Q[8]

(C–H···O=C, another type of pseudo-hydrogen bonding) is in the range of 3.076–3.242 Å. Using a similar strategy, $ZnCl_2$, $CuCl_2$, and $CoCl_2$ were introduced into the Sr^{2+}–Q[8]–HCl systems to give isomorphous compounds that exhibit similar coordination features and supramolecular assemblies.

We have introduced the honeycomb effect of the $([M_{trans}Cl_4]^{2-}$ anions, which form honeycomb-shaped cells via ion–dipole interactions and C–H···Cl interactions, as well as tubular Q[*n*]/M^{n+} coordination polymers that fill the honeycomb cells. M_{trans} in the $([M_{trans}Cl_4]^{2-}$ anions could be Cd, Zn, Cu, Co, Ni, or others; the Q[*n*]s in the tubular Q[*n*]/M^{n+} coordination polymers include Q[6], Q[7], and Q[8]. The metal in the tubular Q[*n*]/M^{n+} coordination polymers could be a lanthanide or alkaline earth metal. The process is summarized in Scheme 3.5 [56].

We have observed various 2D coordination polymers involving Q[5]s, Q[6]s, and Q[7]. Herein, we introduce the 2D-network coordination polymers involving Q[8]. Thuéry first demonstrated a Q[8]/$UO_{2cluster}$-based 2D network coordination polymer by chance when he simply mixed Q[6] with $UO_2(NO_3)_2 \cdot 6H_2O$ in sulfuric acid in a tightly closed glass vessel under hydrothermal conditions. The obtained product probably includes Q[8] as an impurity in Q[6]. Figure 3.35 shows an overall view of the Q[8]/$UO_{2cluster}$-based 2D-network coordination polymer, which is the third example of metal-coordinated Q[8] after the Bi(III) [57] and Sr(II) [58] complexes, which are the first known Q[8]-based 2D-network coordination polymers. Each Q[8] molecule is thus bound to four uranium atoms through two centrosymmetrically related groups of two adjacent glycoluril units,

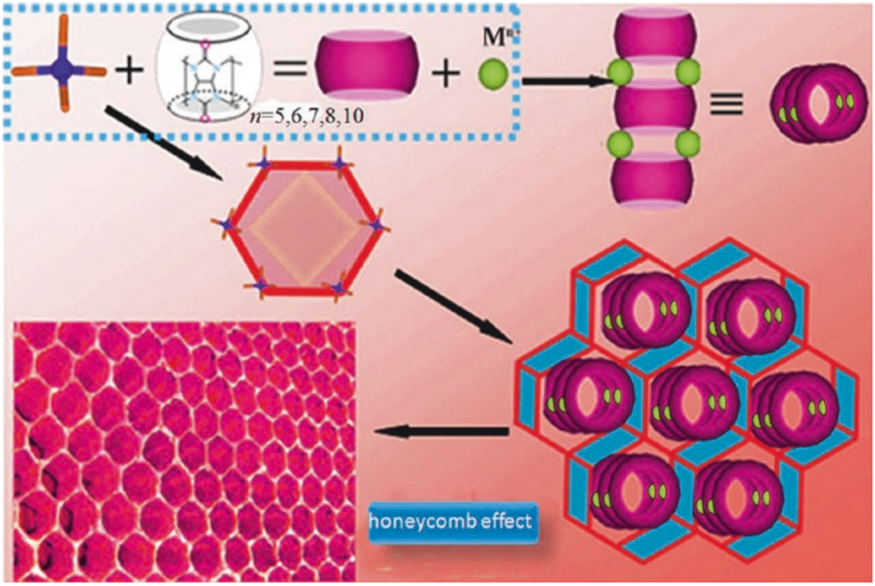

Scheme 3.5 Representation of the honeycomb effect derived from the cucurbit[*n*]urils-based coordination chemistry. Adapted from Ref. [56] with permission from The Royal Society of Chemistry

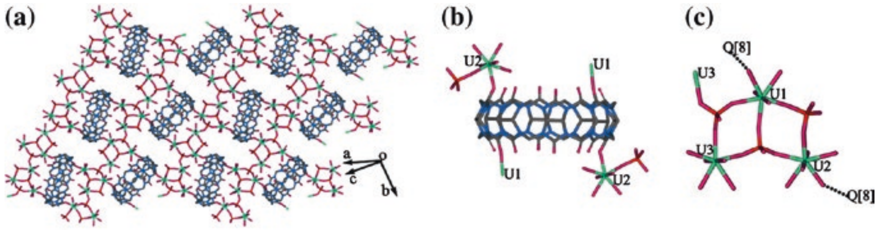

Fig. 3.35 X-ray crystal structure of **a** Q[8]/UO_2^{2+}-based 2D coordination network; **b** Coordination of a Q[8] molecule with four UO_2^{2+} cations and **c** the UO_2/SO_4-based trinuclear motif

which are coordinated on both sides. Q[8] is thus doubly monodentate at each portal, with the two oxygen donors far apart from one another; whereas it is chelating, bidentate, and doubly bidentate at each portal (Fig. 3.35b). The three sulfate ions are bridging, with two of them (S1 and S2) connecting three uranium atoms (U1, U2, and U3 for S2; U1, U2, and U3 in the neighboring unit), and the third (S3) bridging U1 and U3, resulting in the formation of a UO_2/SO_4-based trinuclear motif (Fig. 3.35c). This UO_2/SO_4-based polymeric subunit constructed from these motifs is an undulated ribbon running along the *b* axis. Each of these trinuclear motifs is bound to two Q[8] molecules and, conversely, each portal of Q[8] is bound to two such motifs.

Very recently, we reported a series of Q[8]–M_{alkali} or $M_{\text{alkaline earth}}$-based 2D coordination networks (M_{alkali} and $M_{\text{alkaline earth}}$ are alkali or alkaline earth metal ions, respectively), one of which was first found by chance in 2009. More recently, they have been readily and robustly prepared with the aid of some inorganic structure inducers [59]. Q[8] is the least soluble member in the Q[*n*]-family, but it could made more soluble through host–guest interaction with polar organic molecules or in acidic medium such as HCl. Metal ions do not significantly enhance the solubility of Q[8]. Generally, Q[8] does not readily coordinate to M_{alkali} or $M_{\text{alkaline earth}}$, and upon mixing Q[8] with salts of these metals, metal-free Q[8]-based crystals are easily obtained. However, when a second metal ion, in particular, a transition metal ion, is introduced into the Q[8]–$M_{(\text{alkali or alkaline earth metal})}$ systems, crystals with novel 2D network features are formed through direct coordination of Q[8] with $M_{(\text{alkali or alkaline earth metal})}$ cations. Different metal ions could lead to the formation of Q[8]/M-based networks with different coordination and stacking features.

For example, when transition metal ions, such as Cu^{2+}, Co^{2+}, Ni^{2+}, and Mn^{2+} are introduced into a Q[8]–Rb^+–HCl system [59], novel 2D Q[8]/Rb^+ networks with the same crystal feature are always obtained; the crystals are isomorphous and belong to the $p_{(R\text{-}3)}$ space group. X-ray structural analysis has shown an overall view of the 2D Q[8]/Rb^+ network formed through direct coordination (Fig. 3.36a). A six-Q[8]-membered ring from the 2D network, wherein each of the two Q[8] molecules are linked by a pair of Rb^+ ions at the two portals of each Q[8] molecule, could be observed (Fig. 3.36b). Moreover, a trigonal-planar branch

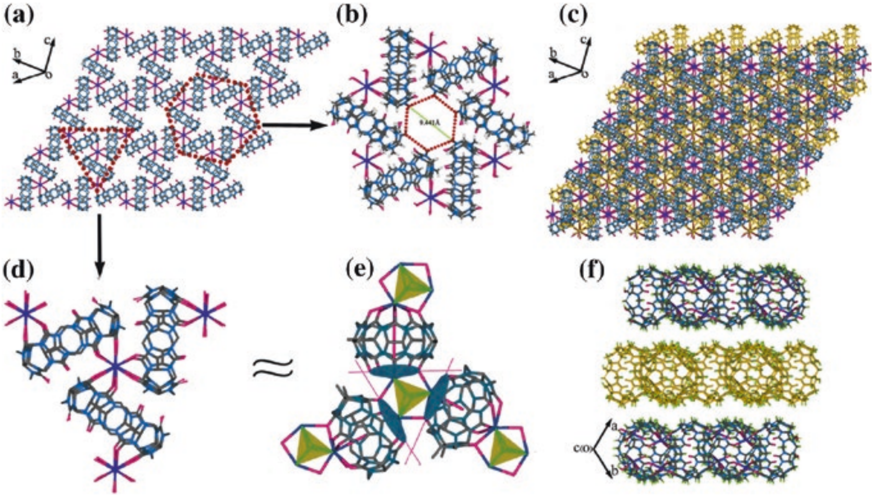

Fig. 3.36 X-ray crystal structure of the 2D Q[8]/Rb^+ network: **a** an overall view; **b** a six-Q[8]-membered ring isolated from the 2D network; **c** a trigonal-planar branch constructed from three Q[8] molecules linked by a Rb^+ pair; **d** a trigonal-planar branch constructed from three dimethyl-substituted Q[5] molecules and K^+ ions, shown for comparison; **e** and **f** the superimposed Rb^+/Q[8]-based networks, top view and side view, respectively

composed of three Q[8] molecules, each of which are linked by a pair of Rb^+ ions, could be observed (Fig. 3.36c). This structure is similar to that discovered in the coordination of SQ[5]s with potassium cations (Fig. 3.36d). When the 2D networks are stacked upon one another, channels filled with the Rb^+ pairs are created. Networks with identical chemical environments alternate with one another, as shown in Fig. 3.36e, f.

When $InCl_3$ was introduced into the Q[8]–Na^+–HCl system, the obtained crystal structure shows similar 2D Q[8]/Na^+ networks accompanying $[In(H_2O)_2Cl_4]^-$ anions. Each trigonal-planar branch is accompanied by six $[In(H_2O)_2Cl_4]^-$ anions, and three Q[8] molecules in the trigonal-planar branch is linked by only one Na^+ cation (Na1) (Fig. 3.37a). The trigonal-planar branch can fuse into a six-Q[8]-membered ring, and both portals of the ring form the rims of the six $[In(H_2O)_2Cl_4]^-$ anions (Fig. 3.37b, c). Thus, the extension of the six-Q[8]-membered ring results in the formation of the 2D Q[8]/Na^+ networks (Fig. 3.37d). Unlike the stacking of the 2D Q[8]/Rb^+ networks, the 2D Q[8]/Na^+ network sheets are repeatedly superimposed upon one another in exact order (Fig. 3.37d). The six-Q[8]-membered rings and the 12 rimmed $[In(H_2O)_2Cl_4]^-$ anions create a nanochannel (Fig. 3.37e).

When the Sr^{2+} cation replaces the Rb^+ cation in the presence of transition metal ions, the Q[8]–Sr^{2+}–HCl system gives crystals with similar features. However, a close inspection revealed that the eight-Q[8]-membered rings, and not six-Q[8]-membered rings, are present in the 2D Q[8]/Sr^{2+} network (Fig. 3.38a, b). Each eight-Q[8]-membered ring is linked by eight Sr^{2+} cations (Fig. 3.38b). The

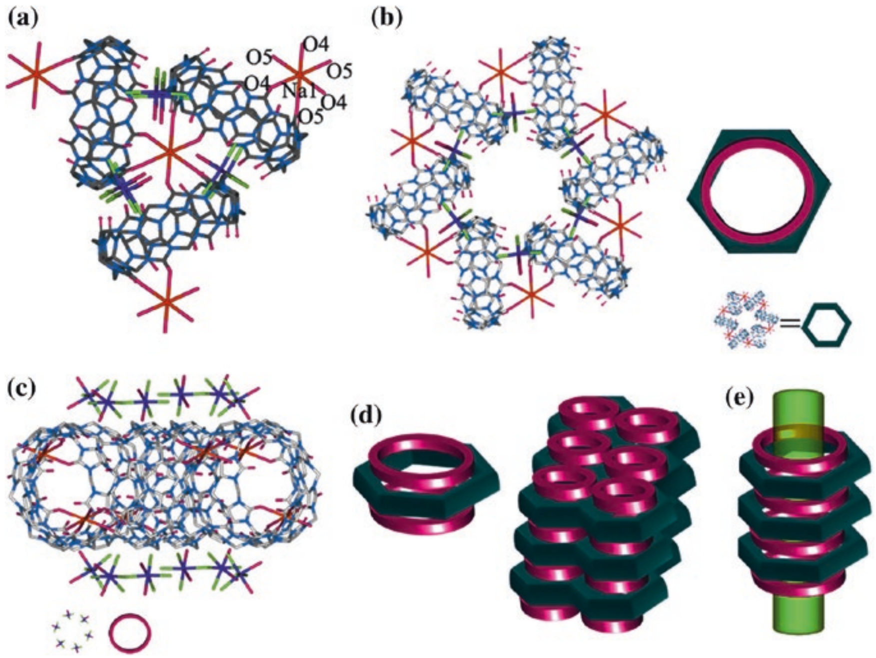

Fig. 3.37 X-ray crystal structure of **a** the trigonal-planar branch constructed from three Q[8] molecules linked by a Na^+ cation and the detailed coordination of Q[8] to the Na^+ cation; **b** the six-Q[8]-membered ring riming of six $[In(H_2O)_2Cl_4]^-$ anions at both portals; **c** *top* view; **d** an overall view of the superimposed 2D Q[8]/Na^+ networks; **e** an isolated tubular channel constructed from the six-Q[8]-membered rings and the rimmed $[In(H_2O)_2Cl_4]^-$ anions. Adapted from Ref. [59] with permission from The Royal Society of Chemistry

stacking of the Q[8]/Sr^{2+} networks repeatedly overlay upon one another in exact order, creating tubular channels (Fig. 3.38c–d).

Above, we mentioned the first novel 3D framework in which a Hyq molecule is included in the cavity of a Q[7] molecule. This inclusion results in the coordination of rubidium cations to the portal carbonyl oxygens of the Q[7] hosts. Formation of a Q[7]-based framework is a consequence of the Q[7]-Rb^+ coordination [55]. Herein, we introduce a novel 3D framework generated by crystallization of a ternary mixture of Q[8], CsCl, and Hyb [60]. The crystal structure shows that there are two different inclusion complexes of $(Hyb)_2$@Q[8] in the unit consisting of four Q[8] molecules (Fig. 3.39a): two parallel Hyb molecules almost vertically insert into the cavity of the host Q[8] (Fig. 3.39b), and two parallel Hyb molecules incline in the cavity of the host Q[8]. In addition, both Hyb molecules coordinate with cesium cations in the $(Hyb)_2$@Q[8] complex (Fig. 3.39c). Coordination of the hydroxyl oxygen atom (O(17)) with the two included Hyb molecules induces further coordination of the Cs1 cation to the portal carbonyl oxygen atoms (O(12) and O(13)) of the host Q[8]. Moreover, there are two **b** complexes and two **c** complexes in the unit of four Q[8]molecules; they are connected by a unit of two cesium cations (Fig. 3.39d). Each cesium Cs1 coordinates directly to three Q[8]

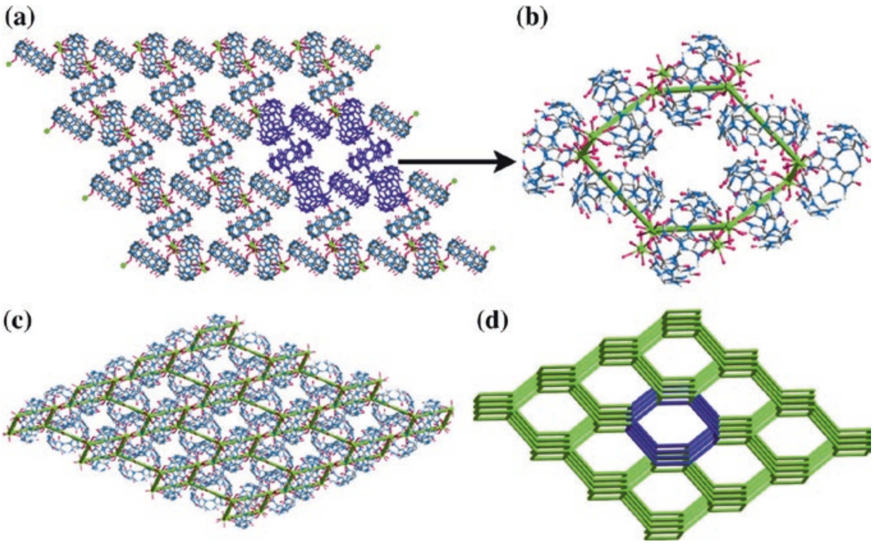

Fig. 3.38 X-ray crystal structure of the 2D Q[8]/Sr^{2+} network: **a** an overall view; **b** an eight-Q[8]-membered ring isolated from the 2D network; and **c** and **d** the superimposed network sheets in exact order with tubular channels constructed from the eight-Q[8]-membered rings. Adapted from Ref. [59] with permission from The Royal Society of Chemistry

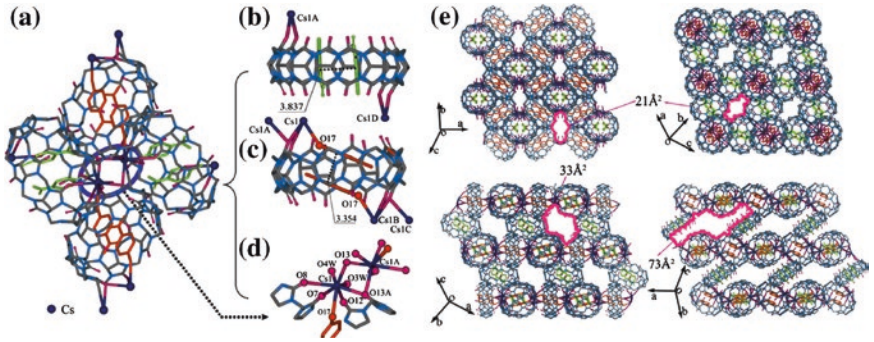

Fig. 3.39 X-ray crystal structures of **a** the unit of four Q[8] molecules with two different host–guest inclusion complexes; **b** the inclusion complex b with vertically parallel included Hyb molecules; **c** the inclusion complex **c** with parallel included Hyb molecules that recline in the cavity of the host Q[8]; **d** the labeled cesium unit; and **e** the 3D framework with different nanochannels

molecules in the four-Q[8]-molecule unit, one **b** complex, and two **c** complexes. In turn, both opening portals of the host Q[8] coordinate with cesium cations; each portal coordinates with one cesium cation in the **b** complex and each portal coordinates with two cesium cations in the **c** complex. Thus, the crystal structure of this compound has a novel 3D framework with different nanochannels constructed from the Q[8]-based inclusion complexes (Fig. 3.39e).

3.6 Induced Coordination Polymers of Cucurbit[*n* > 8]uril with Metal Ions

The largest Q[n] family member, tQ[14], with 14 glycoluril units linked by 28 methylene bridges [61], has recently been reported by the authors' Quizhou group. This molecule has a twisted figure-eight structure and thus does not contain a bowl-shaped cavity of the type present in the other Q[*n*] molecules discussed so far. Reaction of a selection of Ln^{3+} ions with tQ[14] in 6 mol/L HCl in the presence of $[CdCl_4]^{2-}$, interestingly only afforded isolated tQ[14] complexes with Eu^{3+}. The X-ray structure of $[Eu_2(H_2O)_7Cl(tQ[14])]Cl_5 \cdot 66H_2O$ showed the presence of enantiomeric pairs in the crystal (Fig. 3.40a, b). In addition, a pair of 1D coordination polymers in which each tQ[14] is coordinated to three Eu^{3+} cations was also obtained (Fig. 3.40c). These experimental results suggest that the novel tQ[14] could selectively coordinate certain lanthanide cations and yield crystals with novel supramolecular assemblies.

Although, there is only one example of polydimensional coordination polymers of cucurbit[*n* > 8]uril (Q[*n* > 8]) with metal ions at this stage, it could mainly be because of the difficulties in synthesis or isolation sufficient amounts of Q[*n* > 8], such as Q[10] and tQ[14]. However, we believe that their coordination chemistry will gradually develop in the future.

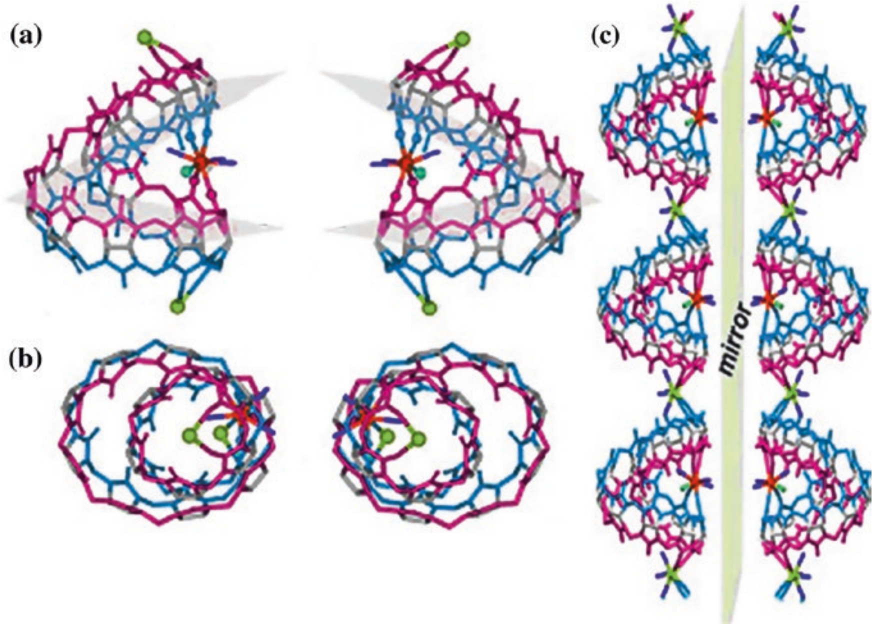

Fig. 3.40 X-ray crystal structure of the two enantiomers of the Eu^{3+}-tQ[14] complex: **a** side view, **b** top view; and **c** a pair of 1D coordination polymers incorporating tQ[14] molecules and Eu^{3+} cations

The solid-state structures mentioned in this book include examples of simple Q[n]/metal complexes to polydimensional polymers prepared through direct coordination of Q[n]s with metal ions. There appears to be no limit to the direct coordination of various kinds of Q[n]s with various metal ions. The concept of structure “inducer” for their structural design are hold promise in the formation of Q[n]/metal-based simple complexes to polydimensional polymers. Although we do not fully understand the driving forces arising from the structure inducer that result in the formation of supramolecular assemblies and coordination polymers with the properties, structural novelties, and functionalities exceeding those obtained by using normal methods, some interactions could be elucidated to explain the formation of unusual Q[n]/metal complexes to exquisite polydimensional polymers. For example, construct coordination networks or frameworks from alkyl-substituted Q[5] could be attributed to the increased electron density as a consequence of the electrondonating effect of the alkyl substituents, which enhances the affinity of portal carbonyl oxygens for the metal ions. Among various methods of synthesizing these polymers is introducing a third species into a Q[n]–metal salt system, which results in the formation of novel polydimensional coordination polymers. For example, when an aromatic organic molecule is introduced into a Q[n]–metal salt system and functions as a structure inducer, the presence of π–π stacking between the aromatic ring of the added organic molecule and portal carbonyl bonds may be observed. In addition, there are C–H$\cdots\pi$ interactions between the aromatic ring of the added organic molecule and methylene on the back of the Q[n] molecule. An inorganic molecule, such as tetrachloride transition metal anions $[\mathrm{M_{trans}Cl}_x]_n^-$ anions, may interact with methenyl or methylene on the back of the Q[n] molecules via ion–dipole interaction with the carbonyl carbon atom of the Q[n] molecules. Moreover, special components, such as uranyl species, may be used as building blocks to create unusual Q[n]/metal-based architectures. In summary, this book aims at (1) identification of all uncovered Q[n]/metal complexes and polydimensional polymers through direct coordination; (2) overall assessment of approaches that have proved to be successful in the construction of Q[n]/metal complexes and polydimensional polymers through direct coordination; and (3) expansion of Q[n]-based coordination chemistry and Q[n]-based host–guest coordination chemistry, which are major parts of the Q[n] chemistry. It is more important that more novel Q[n]/metal-based polydimensional coordination polymers that have potential applications in nanotechnology, molecular sieves, sensors, gas absorption and separation, ions or molecules transportation, and heterogeneous catalysis are expected to be discovered.

References

1. J.X. Liu, L.S. Long, R.B. Huang, L.S. Zheng, Cryst. Growth Des. **6**, 2611 (2006)
2. W.A. Freeman, W.L. Mock, N.-Y. Shih, J. Am. Chem. Soc. **103**, 7367 (1981)
3. W.A. Freeman, Acta Cryst. **B40**, 382 (1984)
4. M.R. Ghadiri, J.R. Granja, R.A. Milligan, D.E. McRee, N. Khazanovich, Nature **366**, 324 (1993)

5. S. Iijima, Nature **354**, 56 (1991)
6. N. Sakai, J. Mareda, S. Matile, Acc. Chem. Res. **38**, 79 (2005)
7. F. Zhang, T. Yajima, Y.Z. Li, G.Z. Xu, H.L. Chen, Q.T. Liu, O. Yamauchi, Angew. Chem. Int. Ed. **44**, 3402 (2005)
8. J. Heo, J. Kim, D. Whang, K. Kim, Inorg. Chim. Acta **297**, 307 (2000)
9. J. Heo, S.Y. Kim, D. Whang, K. Kim, Angew. Chem. Int. Ed. **38**, 641 (1999)
10. J. Lü, J.X. Lin, M.N. Cao, R. Cao, Coord. Chem. Rev. **257**, 1334 (2013)
11. J.X. Liu, C.H. Dong, L.S. Long, R.B. Huang, L.S. Zheng, Dalton Trans. **36**, 7344 (2009)
12. E.A. Mainicheva, A.A. Tripolskaya, O.A. Gerasko, D.Y. Naumov, V.P. Fedin, Russ. Chem. Bull. **55**, 1566 (2006)
13. X.L. Ni, X. Xiao, H. Cong, Q.J. Zhu, S.F. Xue, Z. Tao, Acc. Chem. Res. **47**, 1386 (2014)
14. P. Thuéry, Inorg. Chem. **48**, 4497 (2009)
15. J.X. Hu, Y.F. Hu, X. Xiao, Y.Q. Zhang, Z. Tao, S.F. Xue, J.X. Liu, Q.J. Zhu, Eur. J. Inorg. Chem. **2013**, 3632 (2013)
16. Y.F. Hu, K. Chen, R.L. Lin, W.Q. Sun, J. Zhu, J.X. Liu, S.F. Xue, Q.J. Zhu, Z. Tao, RSC Adv. **2**, 5663 (2012)
17. J.X. Liu, Y.F. Hu, R.L. Lin, W.Q. Sun, X.F. Chu, S.F. Xue, Q.J. Zhu, Z. Tao, Cryst. Eng. Commun. **14**, 6983 (2012)
18. X.L. Ni, J.X. Lin, Y.Y. Zheng, W.S. Wu, Y.Q. Zhang, S.F. Xue, Q.J. Zhu, Z. Tao, A.I. Day, Cryst. Growth Des. **8**, 3446 (2008)
19. Z.F. Li, L.L. Liang, F. Wu, F.G. Zhou, X.L. Ni, X. Feng, X. Xiao, Y.Q. Zhang, S.F. Xue, Q.J. Zhu, J.K. Clegg, Z. Tao, L.F. Lindoy, G. Wei, Cryst. Eng. Commun. **15**, 1994 (2013)
20. Z.F. Li, F. Wu, F.G. Zhou, X.L. Ni, X. Feng, X. Xiao, Y.Q. Zhang, S.F. Xue, Q.J. Zhu, L.F. Lindoy, J.K. Clegg, Z. Tao, G. Wei, Cryst. Growth Des. **10**, 5113 (2010)
21. J.E. Green, J.W. Choi, A. Boukai, Y. Bunimovich, E. Johnston-Halperin, E. Delonno, Y. Luo, B.A. Sheriff, K. Xu, Y.S. Shin, H.R. Tseng, J.F. Stoddart, J.R. Heath, Nature **445**, 414 (2007)
22. K.E. Griffiths, J.F. Stoddart, Pure Appl. Chem. **80**, 48 (2008)
23. P. Passaniti, P. Ceroni, V. Balzani, O. Lukin, A. Yoneva, F. Vogtle, Chem. Eur. J. **12**, 5685 (2006)
24. S. Sun, R. Zhang, S. Anderson, J. Pan, B. Akermark, L. Sun, Chem. Commun. **2006**, 4195 (2006)
25. K. Kim, Chem. Soc. Rev. **31**, 96 (2002)
26. Y.H. Ko, K. Kim, J.K. Kang, H. Chun, J.W. Lee, S. Sakamoto, K. Yamaguchi, J.C. Fettinger, K. Kim, J. Am. Chem. Soc. **126**, 1932 (2004)
27. K. Chen, L.L. Liang, H.J. Liu, Z. Tao, S.F. Xue, Y.Q. Zhang, Q.J. Zhu, Cryst. Eng. Commun. **14**, 8049 (2012)
28. K. Chen, L.L. Liang, H.J. Liu, Y.Q. Zhang, S.F. Xue, Z. Tao, X. Xiao, Q.J. Zhu, L.F. Lindoy, G. Wei, Cryst. Eng. Commun. **14**, 7994 (2012)
29. J.X. Hu, Y.F. Hu, X. Xiao, Y.Q. Zhang, Z. Tao, S.F. Xue, J.X. Liu, Q.J. Zhu, Eur. J. Inorg. Chem. **2013**, 3632 (2013)
30. K. Chen, L.L. Liang, Y.Q. Zhang, Q.J. Zhu, S.F. Xue, Z. Tao, Inorg. Chem. **50**, 7754 (2011)
31. Z.W. Gao, X. Feng, L. Mu, X.L. Ni, L.L. Liang, S.F. Xue, Z. Tao, X. Zeng, B.E. Chapman, P.W. Kuchel, L.F. Lindoy, G. Wei, Dalton Trans. **42**, 2608 (2013)
32. F. Zhang, T. Yajima, Y.Z. Li, G.Z. Xu, H.L. Chen, Q.T. Liu, O. Yamauchi, Angew. Chem. Int. Ed. **44**, 3402 (2005)
33. K. Chen, X. Feng, L.L. Liang, Y.Q. Zhang, Q.J. Zhu, S.F. Xue, Z. Tao, Cryst. Growth Des. **11**, 5712 (2011)
34. X.K. Fang, P. Kogerler, L. Isaacs, S. Uchida, N. Mizuno, J. Am. Chem. Soc. **131**, 432 (2009)
35. L.L. Liang, X.L. Ni, Y. Zhao, K. Chen, X. Xiao, Y.Q. Zhang, C. Redshaw, Q.J. Zhu, S.F. Xue, Z. Tao, Inorg. Chem. **52**, 1909 (2013)
36. X. Feng, K. Chen, Y.-Q. Zhang, S.-F. Xue, Q.-J. Zhu, Z. Tao, A.I. Day, Cryst. Eng. Commun. **13**, 5049 (2011)

37. H. Cong, K. Chen, C.-Z. Wang, L.-L. Liang, S.-F. Xue, Y.-Q. Zhang, Z. Tao, Q.-J. Zhu, Chin. J. Inorg. Chem. **30**, 2839 (2014)
38. X. Xiao, Z. Tao, S.F. Xue, Q.J. Zhu, J.X. Liu, G. Wei, Cryst. Eng. Commun. **13**, 3794 (2011)
39. W.J. Chen, J.P. Zeng, J.M. Yi, Y.Q. Zhang, Q.J. Zhu, S.F. Xue, Z. Tao, G. Wei, Chin. J. Inorg. Chem. **26**, 2018 (2010)
40. X. Qin, X.L. Ni, J.X. Hu, K. Chen, Y.Q. Zhang, C. Redshaw, Q.J. Zhu, S.F. Xue, Z. Tao, Cryst. Eng. Commun. **15**, 738 (2013)
41. Y. Zhao, L.L. Liang, T. Zhang, K. Chen, X. Xiao, Y.Q. Zhang, Z. Tao, S.F. Xue, Q.J. Zhu, Cryst. Eng. Commun. **15**, 7987 (2013)
42. P. Thuery, Cryst. Growth Des. **12**, 1632 (2012)
43. P. Thuery, Cryst. Growth Des. **11**, 2606 (2011)
44. P. Thuery, Cryst. Growth Des. **8**, 4132 (2008)
45. D.-Q. Zhang, T. Sun, Y.-Q. Zhang, S.-F. Xue, Q.-J. Zhu, J.-X. Zhang, Z. Tao, Eur. J. Inorg. Chem. **2015**, 318 (2015)
46. X. Feng, X.J. Lu, S.F. Xue, Y.Q. Zhang, Z. Tao, Q.J. Zhu, Inorg. Chem. Commun. **12**, 849 (2009)
47. H. Cong, Y. Zhao, L.-L. Liang, K. Chen, X.-J. Chen, X. Xiao, Y.-Q. Zhang, Q.-J. Zhu, S.-F. Xue, Z. Tao, Eur. J. Inorg. Chem. **2014**, 2262 (2014)
48. L.L. Liang, Y. Zhao, Y.Q. Zhang, Z. Tao, S.F. Xue, Q.J. Zhu, J.X. Liu, Cryst. Eng. Commun. **15**, 3943 (2013)
49. L.L. Liang, Y. Zhao, K. Chen, X.J. Cheng, N.N. Ji, X. Xiao, Y.Q. Zhang, Z. Tao, S.F. Xue, Q.J. Zhu, G. Wei, Polymers **5**, 418 (2013)
50. P. Thuery, Cryst. Growth Des. **10**, 716 (2010)
51. P. Thuery, Cryst. Eng. Commun. **11**, 1150 (2009)
52. Y.J. Zhao, S.F. Xue, Q.J. Zhu, Z. Tao, J.X. Zhang, Z.B. Wei, L.S. Long, M.L. Hu, H.P. Xiao, A.I. Day, Chin. Sci. Bull. **49**, 1111 (2004)
53. H.Y. Fu, S.F. Xue, Q.J. Zhu, Z. Tao, J.X. Zhang, A.I. Day, Incl. Phenom. Macrocycl. Chem. **52**, 101 (2005)
54. Y.J. Zhao, S.F. Xue, Q.J. Zhu, Z. Tao, Y.Q. Zhang, J.X. Zhang, Z.B. Wei, L.S. Long, Acta Chim. Sinica **63**, 913 (2005)
55. K. Chen, H. Cong, X. Xiao, Y.Q. Zhang, S.F. Xue, Z. Tao, Q.J. Zhu, G. Wei, Cryst. Eng. Commun. **13**, 5105 (2011)
56. L.L. Liang, K. Chen, N.N. Ji, X.J. Cheng, Y. Zhao, X. Xiao, Y.Q. Zhang, Q.J. Zhu, S.F. Xue, Z. Tao, Cryst. Eng. Commun. **15**, 2416 (2013)
57. M.N. Sokolova, T.V. Mitkinaa, O.A. Geraskoa, V.P. Fedina, A.V. Virovetsa, R. Llusar, Z. Anorg, Allg. Chem. **629**, 2440 (2003)
58. O.A. Gerasko, A.V. Virovets, D.G. Samsonenko, A.A. Tripolskaya, V.P. Fedin, D. Fenske, Russ. Chem. Bull. **52**, 585 (2003)
59. N.N. Ji, X.J. Cheng, L.L. Liang, X. Xiao, Y.Q. Zhang, S.F. Xue, Z. Tao, Q.J. Zhu, Cryst. Eng. Commun. **15**, 7709 (2013)
60. K. Chen, L.L. Liang, H. Cong, X. Xiao, Y.Q. Zhang, S.F. Xue, Q.J. Zhu, Z. Tao, Cryst. Eng. Commun. **14**, 3862 (2012)
61. X.J. Cheng, L.L. Liang, K. Chen, N.N. Ji, X. Xiao, J.X. Zhang, Y.Q. Zhang, S.F. Xue, Q.J. Zhu, X.L. Ni, Z. Tao, Angew. Chem. Int. Ed. **52**, 7252 (2013)

Chapter 4
Potential Applications of Q[*n*]-Based Coordination Complexes and Polymers

Abstract This chapter represents a comprehensive overview of the potential applications of Q[*n*]-based coordination complexes and polymers in recent years. In part, the behavior reflects the inherent affinity of the hard carbonyl oxygen atoms for the hard trivalent lanthanide ions, the different portal sizes of the respective available Q[*n*] macrocycles, the nature of the anion employed, and the small but progressive contraction of ionic radii along the lanthanide series. Also, the presence or absence of a structure inducer can be of crucial importance. The present discussion also highlights several examples of particular Q[*n*]/Ln^{3+}/anion systems that exhibit selective coordination behavior toward light or heavy lanthanide ions that point the way for the use of such processes in new lanthanide separation applications.

Keywords Lanthanide separation · Coordination polymers · Lanthanide ions · Structure inducer · Q[*n*] macrocycles

There is much interest in developing stable materials that possess cavities, channels, or holes that have an affinity for volatile and gaseous molecules. These materials have the potential to stabilize reactive molecules; allow safer storage; provide the means for the purification of mixtures or of waste streams; and act as catalysts [1–3]. Along with the development of Q[*n*]-based coordination chemistry, not only were more and more novel Q[*n*]-based coordination complexes, coordination polymers, and supramolecular assemblies found [4], but also various synthesis and construction strategies of Q[*n*]-based coordination complexes, coordination polymers, and supramolecular assemblies were established [5]. More importantly, there is a trend to focus on the unique properties and applications of these novel Q[*n*]-based architectures.

A previous mentioned work showed that when Hyb was introduced into the Q[5]–KI system as a structure directing agent, a stable 2D network-like coordination polymer with accessible channels was obtained (see Fig. 3.12) [6]. Moreover, this Q[5]-based supramolecular assembly was not only stable, easily prepared, and from relatively inexpensive starting compounds, but also demonstrated significant absorption selectivity to a group of polar volatile organic molecules, presenting an absorption material.

X.-L. Ni et al., *Supramolecular Assemblies of Cucurbit[*n*]urils with Metal Ions*,
SpringerBriefs in Molecular Science, DOI 10.1007/978-3-662-46629-2_4

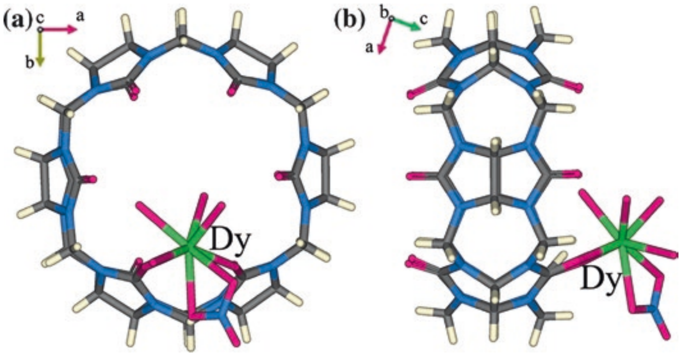

Fig. 4.1 Top and side views of the molecular structure of the complex of Q[6]/Dy^{3+}

In a recent study a simple 1:1 (Dy:Q[6]) complex, $[Dy\{Q[6](NO_3)(H_2O)_4\}](NO_3)_2 \cdot nH_2O$ ($n = 6$ or 7) (Fig. 4.1), was prepared and its magnetic properties were investigated [7]. This complex displays single-ion magnet behavior with two slow magnetic relaxation processes. The latter is sensitive to the degree of solvation present. Changes in solvation can induce the slow magnetic relaxation of this compound to switch between the temperature-independent and the temperature-dependent regimes.

More recently, we used the strategy to synthesize Q[7]-based coordination polymers by introducing $[M_{trans}Cl_4]^{2-}$ anions as structure directing agents into the Q[7]-$M_{alkaline\ earth}$ systems. The structure directing effect of the $[M_{trans}Cl_4]^{2-}$ anions not only appears in the construction of novel Q[*n*]/metal ions-based coordination polymers but can also result in the formation of Q[*n*]-based novel supramolecular assemblies, such as the mentioned honeycomb-like frameworks [4, 5]. The proposed driving forces of the structure directing effect of the $[M_{trans}Cl_4]^{2-}$ anions are ion-dipole interactions and hydrogen bonding between the $[M_{trans}Cl_4]^{2-}$ anions and ≡CH or $=CH_2$ groups on the back of the Q[8] molecules. The solid state structures, as determined by X-ray crystallography, show that compounds $\{Ca_2(H_2O)_4(Q[7])\}2[CdCl_4]22H_2O$ and $\{Sr_3(H_2O)_{16}(Q[7])_2\}4[CdCl_4](H_3O)_236H_2O$ exhibit similar coordination features and supramolecular assemblies, in which $[CdCl_4]^{2-}$ anions surround a Q[7] molecule through: (1) the dipole interaction between portal carbonyl carbons with Cl from $[CdCl_4]^{2-}$ anions, and (2) the unusual hydrogen bonding of Cl from $[CdCl_4]^{2-}$ anions with methine or methylene on the back of the Q[7] molecules. Generally, Q[7] molecules rarely coordinate with common metal ions to form stable Q[7]/Metal complexes, in particularly, the coordination polymers. However, with a negative $[CdCl_4]^{2-}$ anion ring, which attracts positively charged species, Q[7] molecules are ready to coordinate with metal ions. The "honeycomb effect" of $[CdCl_4]^{2-}$ anions result in the formation of one-dimensional coordination polymers (Fig. 4.2a–c) [8]. Moreover, These Q[7]-based coordination polymers present remarkable selective sorption properties for separation. The $M_{alkaline}$-Q[7]-based coordination polymers were used as an extraction coating on solid-phase microextraction (SPME) fibers to examine their usefulness for separation. The SPME

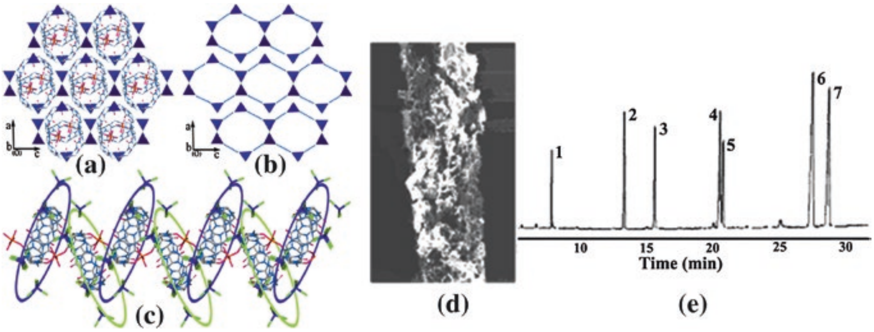

Fig. 4.2 X-ray crystal structures of Q[7]/$\mathrm{M}_{\text{Alkaline earth}}$-based coordination polymers in the presence of $[\mathrm{CdCl_4}]^{2-}$ anions: **a** representation of an overall view of the coordination feature and the supramolecular assembly; **b** the $[\mathrm{CdCl_4}]^{2-}$ anions honeycomb-like framework; **c** a zigzag coordination polymer of Alkaline earth^{2+} cations to Q[7] molecules surrounded by the $[\mathrm{CdCl_4}]^{2-}$ anions; **d** magnified SME image of the crystal-coated SPME fiber at 300 °C; **e** GC-FID chromatograms of seven PAHs extracted by the novel fiber coated with crystal. Peaks: naphth alene (*1*); acenaphthene (*2*); fluorene (*3*); phenanthrene (*4*); anthracene (*5*); fluoranthene (*6*); and pyrene (*7*). Adapted from Ref. [8] with permission from The Royal Society of Chemistry

fiber consists of a supporting substrate and a thin layer of sorbent material. Fused-silica fiber was used as the supporting substrate and the Q[7]-based porous crystals were fixed to the surface of the fused-silica fiber using high-temperature epoxy. The surface structure of the SPME was investigated by SEM, as shown in Fig. 4.2d. The micro-structured coating is rough, porous, roughly uniform, and about 32 μm thick. The fiber was coupled to a gas chromatography unit and its separation effectiveness was investigated using seven polycyclic aromatic hydrocarbons (PAHs) in wastewater samples, in head-space mode (Fig. 4.2e). The novel fiber with its crystalline extraction coating exhibited excellent extraction efficiency and stability. These experimental results suggest that such Q[7]-based coordination polymers could be applied to the analysis of trace PAHs in real water samples.

In fact, our laboratory is interested in studying the cucurbit[*n*]urils (Q[*n*]s) coordination chemistry [4], among which Q[*n*]-Ln^{3+} interaction chemistry is an important part. Professor Zhu's group in our laboratory has focused on the Q[*n*]-Ln^{3+}-based interaction chemistry and potential applications, and we have found that almost all Q[*n*]s and their derivates can interact with lanthanide cations, in particular, Q[*n*]s can easily coordinate with Ln^{3+} cations and form novel different coordination polymers and supramolecular assemblies in the presence of third species as structure directing agents; the outer-surface interactions of Q[*n*]s are considered as the driving forces [5]. More recently, we expanded the Q[*n*]-Ln^{3+}-based interaction chemistry from construction of novel coordination polymers and supramolecular assemblies to the isolation or separation of lanthanide cations based on the discovery of ability of Q[*n*]s to identify lanthanide cations, and plan to systematically investigate the interactions of each of Q[*n*]s and their derivates with series of lanthanide cations, and the potential applications of these Q[*n*]s in isolation or separation of lanthanide. For example, the interactions between a series of lanthanide cations (Ln^{3+}) and a

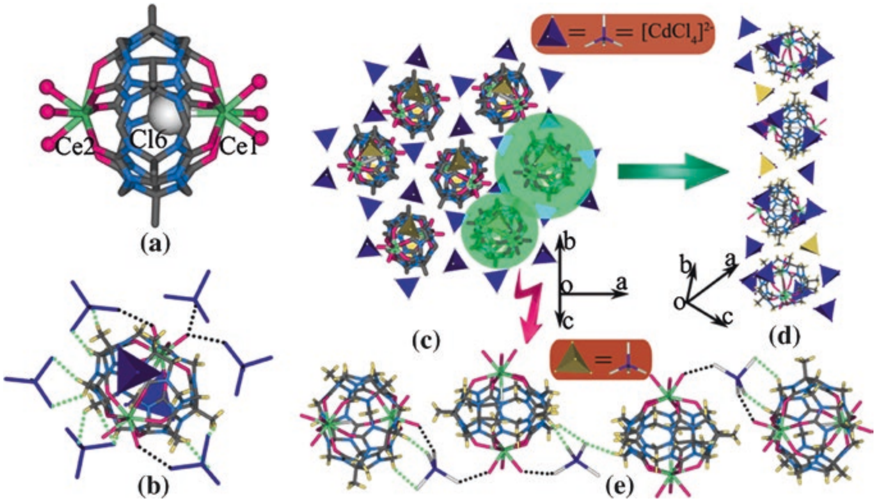

Fig. 4.3 X-ray crystal structure of a representative compound: **a** a Ce^{3+}/SPMeQ[5] complex with an included chloride anion and cerium cations; **b** detailed interactions between a Ce^{3+}/SPMeQ[5] complex and the surrounding eight $[CdCl_4]^{2-}$ anions; **c** an overall view of the honeycomb-like supramolecular assembly constructed of Ce^{3+}/SPMeQ[5] complexes and $[CdCl_4]^{2-}$ anions; **d** a channel in the assembly containing a Ce^{3+}/SPMeQ[5] complex chain; **e** detailed interactions between Ce^{3+}/SPMeQ[5] complexes and $[CdCl_4]^{2-}$ anions in the chain

methyl-substituted cucurbit[5]uril (SPMeQ[5]) derived from a 3α-methyl-glycoluril have been investigated. Single-crystal X-ray diffraction analysis revealed that the SPMeQ[5] selectively interacts with certain lanthanide ions and forms a coordination capsule where a chloride anion is included in the cavity of the SPMeQ[5] molecule in the presence of $[CdCl_4]^{2-}$ (Fig. 4.3). The Ln^{3+} cations which interact with SPMeQ[5] are the four light lanthanides, La^{3+}, Ce^{3+}, Pr^{3+}, Nd^{3+}, while the remaining lanthanide cations stay in solution under the same interaction conditions. These results suggest that SPMeQ[5]–$Ln(NO_3)_3$–$CdCl_2$–HCl systems could be useful for the selective isolation of these light lanthanide cations from mixtures also containing heavier lanthanide cations. In order to confirm this suggestion, representative $Ln^{3+}_{light}-Ln^{3+}_{heavy}-$SPMeQ[5]$-CdCl_2-$HCl systems with 1:1 ratios were selected for isolating lighter lanthanides, namely Pr^{3+}–Sm^{3+}, Pr^{3+}–Eu^{3+}, Pr^{3+}–Tb^{3+}, and Pr^{3+}–Lu^{3+} systems. Energy dispersive spectrometry (EDS) showed that the crystals obtained from these systems contained a high proportion of the lighter lanthanides (almost 100 %) for the group with 1:1 of Ln^{3+}_{light}: Ln^{3+}_{heavy} ratios (Fig. 4.4). These experimental results suggest that this strategy could be really useful, and SPMeQ[5] could be used for isolating lighter lanthanides from their heavier counterparts [9].

Similar properties can be found in various Q[6]s-Ln^{3+} interaction systems. As previously mentioned, linear coordination polymers have been assembled from lanthanide cations (Ln^{3+}) and cucurbituril (Q[6]) in the presence of $[CdCl_4]^{2-}$ or $[ZnCl_4]^{2-}$ anions as inorganic structure directing agents in HCl solution [10]. X-ray diffraction analysis has revealed honeycomb-patterned supramolecular assemblies, in which $[CdCl_4]^{2-}$ or $[ZnCl_4]^{2-}$ anions form the honeycomb and the hexagonal cells

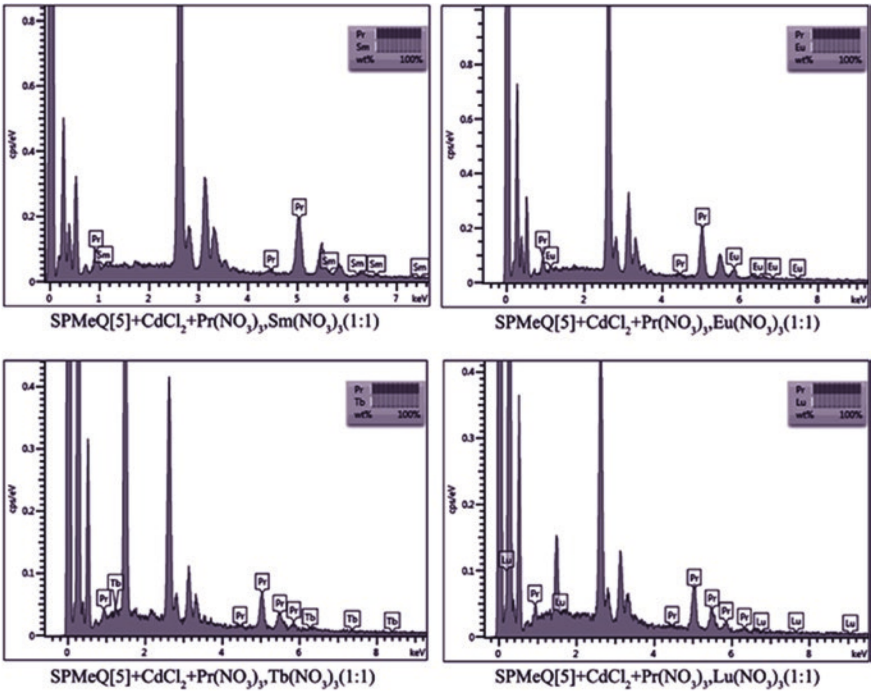

SPMeQ[5]+CdCl$_2$+Pr(NO$_3$)$_3$,Sm(NO$_3$)$_3$(1:1)

SPMeQ[5]+CdCl$_2$+Pr(NO$_3$)$_3$,Eu(NO$_3$)$_3$(1:1)

SPMeQ[5]+CdCl$_2$+Pr(NO$_3$)$_3$,Tb(NO$_3$)$_3$(1:1)

SPMeQ[5]+CdCl$_2$+Pr(NO$_3$)$_3$,Lu(NO$_3$)$_3$(1:1)

Fig. 4.4 EDS of the representative products isolated from $\mathrm{Ln}^{3+}_{\mathrm{light}}-\mathrm{Ln}^{3+}_{\mathrm{heavy}}-$SPMeQ[5] $-\mathrm{CdCl}_2-\mathrm{HCl}$ systems mixtures with 1:1 $\mathrm{Ln}^{3+}_{\mathrm{light}}:\mathrm{Ln}^{3+}_{\mathrm{heavy}}$ ratios (unpublished)

are occupied by Ln^{3+}-Q[6] linear coordination polymers (Figs. 3.21 and 4.5). The most remarkable phenomenon was the rapid precipitation of Ln^{3+}-Q[6]-$[\mathrm{CdCl}_4]^{2-}$ or -$[\mathrm{ZnCl}_4]^{2-}$ systems when the Ln^{3+} cations were La, Ce, Pr, or Nd. This may offer a means to separate the light lanthanides cations from their heavier counterparts. When a solution of Q[6] in aqueous HCl was added to mixtures of light and heavy lanthanides in a 1:1 ratio, for example La:Eu, in aqueous HCl solution, a large amount of white precipitate was again deposited. EDS showed that in terms of cations the white precipitate contained ~90 % La and ~10 % Eu, suggesting a strategy for the separation of light lanthanides from their heavier counterparts (Fig. 4.5) [10].

We have recently investigated the coordination of $(\mathrm{HO})_{10}$Q[5] molecules with a series of Ln^{3+} cations in the presence of potassium salt of $[\mathrm{PMo}_{12}\mathrm{O}_{40}]^{3-}$ anion. The results, mainly based on X-ray diffraction analysis, have revealed that the $\mathrm{K}^+/\mathrm{Ln}^{3+}/(\mathrm{HO})_{10}$Q[5]/$[\mathrm{PMo}_{12}\mathrm{O}_{40}]^{3-}$ systems result in the formation of three different supramolecular assembly isomorphous groups with increasing atomic number of lanthanides, in particular, the complexes and corresponding supramolecular assemblies contain lighter lanthanide cations which coordinate to $(\mathrm{HO})_{10}$Q[5] molecules in solid state for the first two isomorphous groups, while the solid crystals involving heavy lanthanide systems show no heavier lanthanide cations, which still stay in the solution state. Such difference offers a possible means to separate the lighter lanthanide cations from their heavier counterparts. Figure 4.6 shows these representative

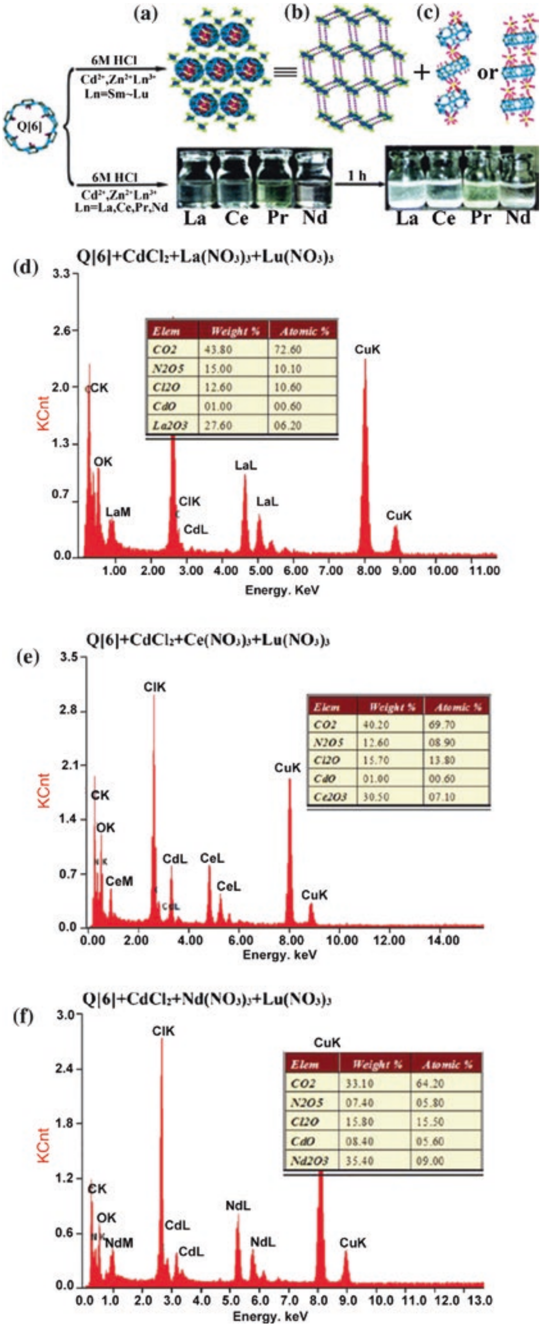

Elem	Weight %	Atomic %
CO2	43.80	72.60
N2O5	15.00	10.10
Cl2O	12.60	10.60
CdO	01.00	00.60
La2O3	27.60	06.20

Elem	Weight %	Atomic %
CO2	40.20	69.70
N2O5	12.60	08.90
Cl2O	15.70	13.80
CdO	01.00	00.60
Ce2O3	30.50	07.10

Elem	Weight %	Atomic %
CO2	33.10	64.20
N2O5	07.40	05.80
Cl2O	15.80	15.50
CdO	08.40	05.60
Nd2O3	35.40	09.00

Fig. 4.5 X-ray crystal structure of Q[6]/M_{Ln}-based coordination polymers in the presence of $[MCl_4]^{2-}$ anions: (*top*) **a** representation of an overall view of the coordination features and supramolecular assembly; **b** the honeycomb-like framework composed of $[MCl_4]^{2-}$ anions and **c** linear coordination polymers of Ln^{3+} cations and Q[6] molecules; (*middle*) the progress of precipitation in the Ln–Q[6]–$[CdCl_4]^{2-}$ systems (Ln = La, Ce, Pr, Nd), and **d**–**f** representatives of EDS of the white precipitate from the Ln_{light}–Ln_{heavy}–Q[6]–$[CdCl_4]^{2-}$ system. Adapted from Ref. [10] with permission from The Royal Society of Chemistry

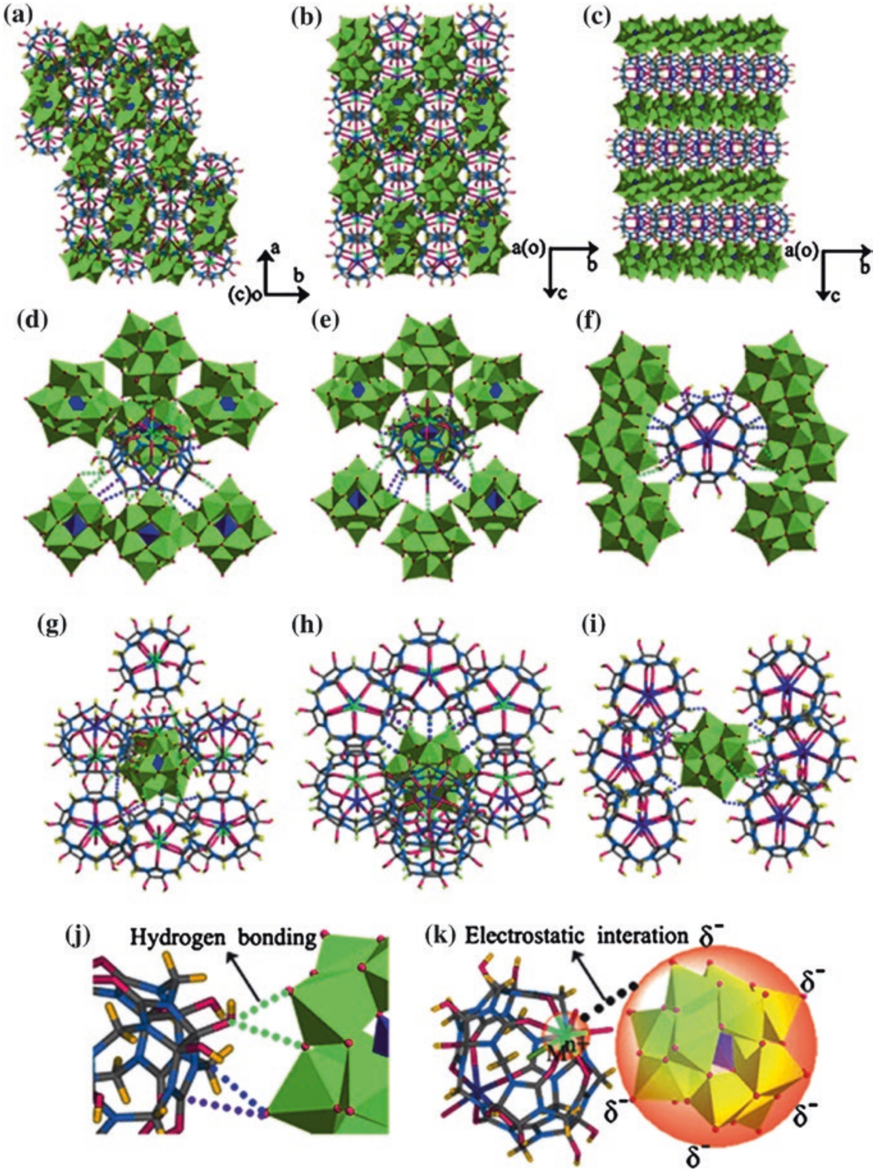

Fig. 4.6 X-ray crystal structures of **a**–**c** three representative supramolecular assemblies; **d**–**f** the detailed interactions of an $(HO)_{10}Q[5]$ molecule with $[PMo_{12}O_{40}]^{3-}$ anions; in turn, **g**–**i** the detailed interactions of a $[PMo_{12}O_{40}]^{3-}$ anion with $(HO)_{10}Q[5]$ complexes corresponding to the compounds in the three isomorphous groups, respectively, **j**, **k** the detailed interactions between an $(HO)_{10}Q[5]$ molecule and a $[PMo_{12}O_{40}]^{3-}$anion [11]

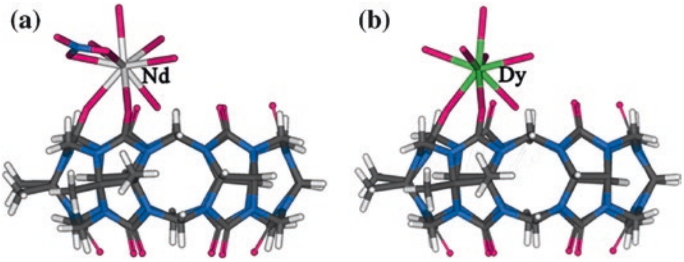

Fig. 4.7 **a**, **b** X-ray crystal structures of two representative complexes of *o*-TMeQ[6] with Nd^{3+} and Dy^{3+} cations, respectively; EDS of *o*-TMeQ[6] with 1:1 ratios of light: heavy lanthanides

supramolecular architectures and detailed interactions between the components, such as a $[PMo_{12}O_{40}]^{3-}$ anion surrounded by $(HO)_{10}Q[5]$ molecules, and a $(HO)_{10}Q[5]$ molecule surrounded by $[PMo_{12}O_{40}]^{3-}$ anions, in the $K^+/Ln^{3+}/(HO)_{10}Q[5]/[PMo_{12}O_{40}]^{3-}$ systems. Nine typical systems were selected as the representative examples, such as Ce/Tb, Ce/Er, Ce/Yb, Nd/Tb, Nd/Er, Nd/Yb, Sm/Tb, Sm/Er, and Sm/Yb, in aqueous HCl solution (1.0 mol/L), respectively, then the $K^+/(HO)_{10}Q[5]/[PMo_{12}O_{40}]^{3-}$ system in aqueous HCl 1.0 mol/L was added to the mixtures of light and heavy lanthanide nitrate salts with ratios of 1:1, respectively; energy dispersive spectroscopy (EDS) data showed that the obtained crystals from the above systems contained only or dominated light lanthanide [11].

Our another recent work showed the coordination in supramolecular assemblies by reacting a series of lanthanide cations (Ln^{3+}) and a new alkyl-substituted cucurbituril, the ortho-tetramethyl substituted cucurbituril (*o*-TMeQ[6]), in the presence of cadmium nitrate as an inorganic structure directing agent in neutral solution. X-ray diffraction analysis revealed that the coordination of lanthanide cations gives rise to simple *o*-TMeQ[6]/Ln^{3+} complexes ($Ln^{3+} = Gd^{3+}$, Tb^{3+}, Dy^{3+}, Ho^{3+}, Er^{3+}, Tm3+, Yb^{3+} and Lu^{3+}). Figure 4.7a, b shows two representative *o*-TMeQ[6]/Ln^{3+} complexes, TMeQ[6]/Nd^{3+} and TMeQ[6]/Dy^{3+}. Most interestingly, no solid crystals were obtained for any compounds containing La, Ce, or Pr, suggesting that these compounds may be suitable for the separation of heavier lanthanide cations from their lighter counterparts [8]. In order to investigate this further, nine typical $Ln^{3+}_{light}-Ln^{3+}_{heavy}-o-TMeQ[6]-Cd(NO_3)_3$ systems were selected as representative examples ($Ln^{3+}_{light} - Ln^{3+}_{heavy}$ and $La^{3+}-Ho^{3+}$, $La^{3+}-Tm^{3+}$, $La^{3+}-Yb^{3+}$, $Ce^{3+}-Ho^{3+}$, $Ce^{3+}-Tm^{3+}$, $Ce^{3+}-Yb^{3+}$, $Pr^{3+}-Ho^{3+}$, $Pr^{3+}-Tm^{3+}$ and $Pr^{3+}-Yb^{3+}$), all in 1:1 ratios. EDS showed that the crystals obtained only heavy lanthanides, while the Ln^{3+}_{light} lanthanides remained in the mother liquor [12].

Not only smaller Q[*n*]s, such as Q[5]s and Q[6]s, but also larger Q[n]s, such as Q[8], can present the potential application for isolation of lanthanide cations. X-ray diffraction analysis has revealed that the coordination of lanthanide ions to Q[8] and corresponding supramolecular assemblies can be cataloged into two isomorphous groups [13]. One group is characteristic of coordination of Q[8] molecules with the light lanthanide cations, such as Ce^{3+}, Nd^{3+}, Sm^{3+},

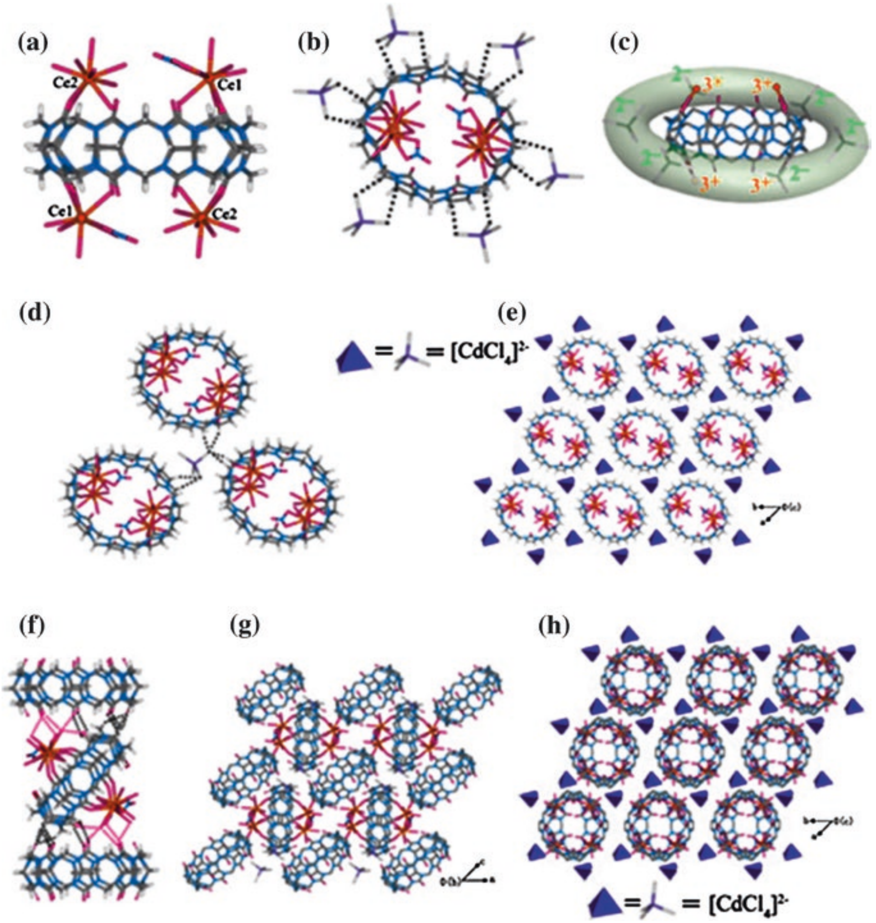

Fig. 4.8 X-ray crystal structure of two compounds for the two isomorphous groups: **a** a complex of Q[8] with cerium cations; **b**, **c** a Ce^{3+}/Q[8] complex surrounded by six $[CdCl_4]^{2-}$ anions; **d** a $[CdCl_4]^{2-}$ anion surrounded by three Ce^{3+}/Q[8] complexes; **e** 2D network constructed of Ce^{3+}/Q[8] complexes and $[CdCl_4]^{2-}$ anions; **f** a sandwich constructed from two metal free Q[8] molecules and a Ce^{3+}/Q[8] complex which is surrounded by six $[CdCl_4]^{2-}$ anions; **g**, **h** an overall view of the stacking of Ce^{3+}/Q[8] complexes and $[CdCl_4]^{2-}$ anions [13]

and Eu^{3+} respectively, while the other group is characteristic of coordination of Q[8] molecules with the heavy lanthanide cations, such as Gd^{3+}, Tb^{3+}, Ho^{3+}, Er^{3+}, Tm^{3+}, Yb^{3+}, and Lu^{3+} respectively. A complex consisting of a Q[8] molecule with Ce^{3+}, is given in Fig. 4.8 as a representative example of the Ln^{3+}_{light}–Q[8]–$[CdCl_4]^{2-}$ group. The crystal structure of the Ce^{3+}/Q[8] complex shows that the Q[8] molecule coordinates to four Ce^{3+} cation ions. An unusual interaction between the $[CdCl_4]^{2-}$ anions and methine or methylene on the outer surface of the Q[8] molecule can be also observed. Each Ce^{3+}/Q[8] complex is

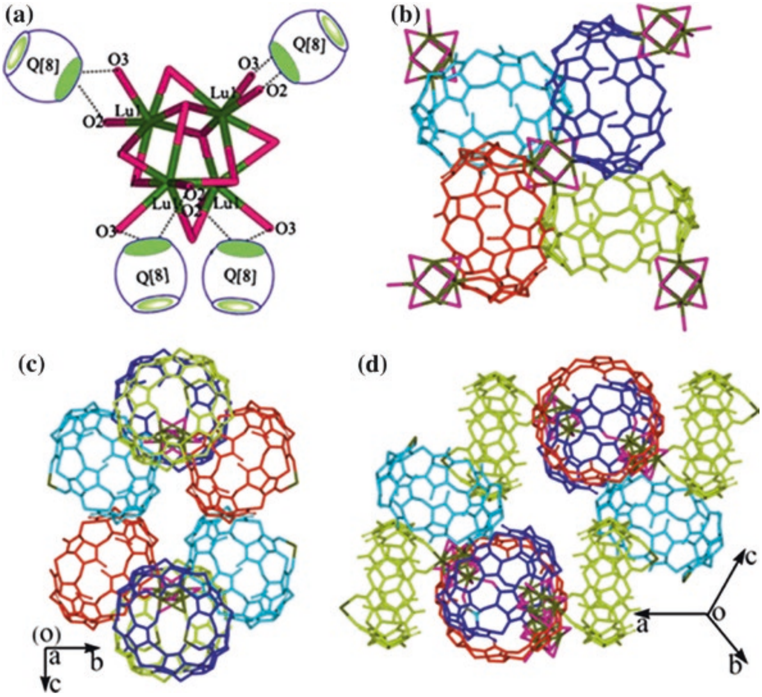

Fig. 4.9 **a** A Lu^{3+}-unit; **b** a basic four-Q[8] building block; **c–d** 3D frameworks based on the direct coordination of Lu^{3+} cations to Q[8] molecules along different directions [13]

surrounded by six $[CdCl_4]^{2-}$ anions through the so-called outer-surface interaction of Q[*n*]s. The coordination of Lu^{3+} with Q[8] molecules in the presence of $[CdCl_4]^{2-}$ anions served as a representative isomorphous complex of the $Ln^{3+}_{heavy}-Q[8]-[CdCl_4]^{2-}$ group, showed an unexpected experimental result. An Lu^{3+}-unit containing four Lu^{3+} cations with a 50 % occupancy links four Q[8] molecules as a basic building block (Fig. 4.9a, b) and each Lu^{3+}-unit links four Q[8] molecules and forms the basic four-Q[8] building block. In turn, each Q[8] molecule in the block coordinates with two Lu^{3+}-units. Moreover, the extra hydrogen bonding of $\equiv$CH or $=CH_2$ groups on the back of a Q[8] molecule with portal carbonyl oxygens of Q[8] exist between every two adjacent Q[8] molecules in the block (Fig. 4.9b). Thus, extending the basic building block results in the formation of a novel 3D framework with various channels, through the direct coordination of Lu^{3+} cations to Q[8] molecules (Fig. 4.9c, d).

Most interestingly, systems containing the light lanthanides and Q[8] in 6 mol aqueous HCl have been found to give crystals more rapidly than systems containing the heavy lanthanides. This suggests that the difference could be used to separate the lighter lanthanides cations from their heavier counterparts. When a solution of Q[8] in aqueous HCl was added to mixtures of light and heavy lanthanides in a 1:1 ratio, for example Ce:Lu, in aqueous HCl solution, stick-like

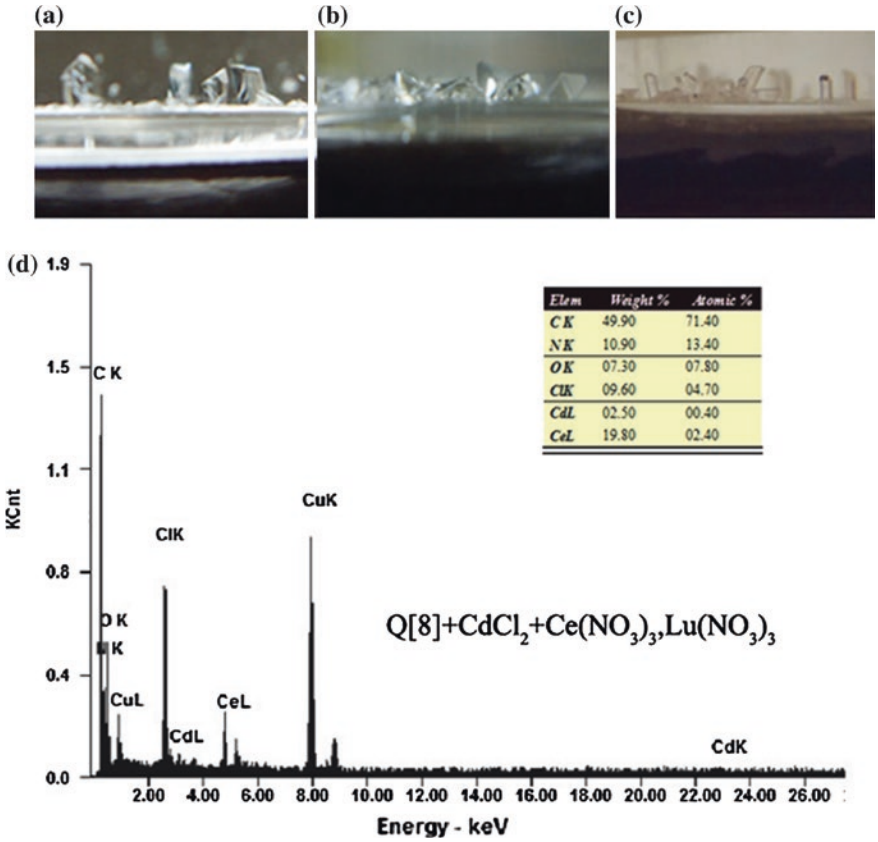

Fig. 4.10 Crystals grown from **a** Ce^{3+}–Q[6]–$[CdCl_4]^{2-}$ system; **b** Lu^{3+}–Q[6]–$[CdCl_4]^{2-}$ system; **c** Ce^{3+}–Lu^{3+}–Q[6]–$[CdCl_4]^{2-}$ system; and **d** electron spectroscopy data of the stick-like crystals from the Ce–Lu–Q[8]–$[CdCl_4]^{2-}$ system. Adapted from Ref. [13] with permission from The Royal Society of Chemistry

crystals were first obtained (Fig. 4.10a–c). EDS showed that the stick-like crystals contained only Ce cations and no Lu (Fig. 4.10d). Several other typical $Ln^{3+}_{light}-Ln^{3+}_{heavy}-Q[8]-[CdCl_4]^{2-}$ systems were selected and EDS of the crystals show high ratios $Ln^{3+}_{light}/Ln^{3+}_{heavy}$ [13]. We continue to carry out further detailed investigations aimed at developing a practically useful technique.

References

1. J.R. Long, O.M. Yaghi, Chem. Soc. Rev. **38**, 1213 (2009)
2. S.M. Cohen, Chem. Sci. **1**, 32 (2010)
3. H. Kim, Y. Kim, M. Yoon, S. Lim, S.M. Park, G. Seo, K. Kim, J. Amer. Chem. Soc. **132**, 12200 (2010)

4. X.L. Ni, X. Xiao, H. Cong, L.L. Liang, K. Chen, X.J. Cheng, N.N. Ji, Q.J. Zhu, S.F. Xue, Z. Tao, Chem. Soc. Rev. **42**, 9480 (2013)
5. X.L. Ni, X. Xiao, H. Cong, Q.J. Zhu, S.F. Xue, Z. Tao, Acc. Chem. Res. **47**, 1386 (2014)
6. X. Feng, K. Chen, Y.-Q. Zhang, S.-F. Xue, Q.-J. Zhu, Z. Tao, A.I. Day, CrystEngComm **13**, 5049 (2011)
7. M. Ren, D. Pinkowicz, M. Yoon, K. Kim, L.-M. Zheng, B.K. Breedlove, M. Yamashita, Inorg. Chem. **52**, 8342 (2013)
8. Y. Zhao, L.L. Liang, K. Chen, N.N. Ji, X.J. Cheng, X. Xiao, Y.Q. Zhang, S.F. Xue, Q.J. Zhu, N. Dong, Z. Tao, Dalton Trans. **43**, 929 (2014)
9. C.Z. Wang, W.X. Zhao, Y.Q. Zhang, S.F. Xue, Zhu Tao, Q.J. Zhu, ChemPlusChem (2015). doi: 10.1002/cplu.201500045R1
10. Y. Zhao, L.-L. Liang, K. Chen, T. Zhang, X. Xiao, Y.-Q. Zhang, Z. Tao, S.-F. Xue, Q.-J. Zhu, CrystEngComm **15**, 7987 (2013)
11. B.-X. Han, C.-Z. Wang, K. Chen, X. Xiao, Z. Tao, S.-F. Xue, Y.-Q. Zhang, Q.-J. Zhu, CrystEngComm **16**, 1615 (2014)
12. J.-J. Zhou, X. Yu, Y.-C. Zhao, X. Xiao, Y.-Q. Zhang, S.-F. Xue, Z. Tao, J.-X. Liu, Q.-J. Zhu, CrystEngComm **16**, 10674 (2014)
13. X.-J. Cheng, N.-N. Ji, Y. Zhao, L.-L. Liang, X. Xiao, Y.-Q. Zhang, S.-F. Xue, Q.-J. Zhu, Z. Tao, CrystEngComm **16**, 144 (2014)